ISSN 1820-8665

Vol. 12 · No1 · MAY 2011

Serbian Journal of Experimental and Clinical Research

2000

Serbian Journal of Experimental and Clinical Research

2000

Print
Medical Faculty, Kragujevac

Indexed in
EMBASE/Excerpta Medica, Index Copernicus, BioMedWorld, KoBSON, SCIndeks

Address:
Serbian Journal of Experimental and Clinical Research, Medical Faculty, University of Kragujevac
Svetozara Markovića 69, 34000 Kragujevac, PO Box 124
Serbia
e-mail: sjecr@medf.kg.ac.rs
www.medf.kg.ac.rs/sjecr

SJECR is a member of WAME and COPE. SJECR is published at least twice yearly, circulation 300 issues The Journal is financially supported by Ministry of Science and Technological Development, Republic of Serbia
ISSN 1820 – 8665

Table Of Contents

HOMOCYSTEINE: NEUROTOXICITY AND MECHANISMS OF INDUCED HYPEREXCITABILITY

Stanojlovic Olivera, Hrncic Dragan, Rasic-Markovic Aleksandra and Djuric Dragan
Institute of Medical Physiology "Richard Burian", School of Medicine, University of Belgrade, Belgrade, Serbia

HOMOCISTEIN: NEUROTOKSIČNOST I MEHANIZMI INDUKOVANE HIPEREKSCITABILNOSTI

Stanojlović Olivera, Hrnčić Dragan, Rašić-Marković Aleksandra i Đurić Dragan
Institut za Medicinsku fiziologiju "Rihard Burijan", Medicinski fakultet, Univerzitet u Beogradu, Beograd, Srbija

Received / Primljen: 09. 02. 2011.

ABSTRACT

Within the past four decades, investigators worldwide have established that the amino acid homocysteine (Hcy) is a potent, independent, novel and emerging risk factor for arteriosclerosis. In addition, Hcy is considered a vasotoxic and neurotoxic agent that interferes with fundamental biological processes common to all living cells. The aim of this article is to present data addressing central nervous system hyperexcitability in experimental models of homocysteine-induced seizures. These results demonstrate that acute administration of homocysteine and homocysteine-related compounds significantly affects neuronal activity, electroencephalographic (EEG) recordings and behavioural responses in adult Wistar male rats. It is suggested that hyperhomocysteinemia may generate similar effects on human brain activity. Homocysteine and D,L-homocysteine thiolactone are excitotoxic and elicit seizures through stimulation of NMDA receptors. In addition, they inhibit Na^+/K^+-ATPase activity in the cortex, hippocampus and brain stem. Nitric oxide (NO) acts as an anticonvulsant in D,L-homocysteine thiolactone-induced seizures and prevents D,L-homocysteine thiolactone-induced inhibition of Na^+/K^+-ATPase activity. EEG monitoring for the effects of ethanol on homocysteine-induced epilepsy support the idea that ethanol intake could represent one of the exogenous factors influencing brain excitability. Finally, it was found that homocysteine thiolactone significantly inhibits acetylcholinesterase (AChE) activity in rat brain tissue.

Keywords: *homocysteine, CNS, hyperexcitability, rat*

Abbreviations used:
AchE - *acetylcholinesterase*
BHMT - *betaine-Hcy S-methyltransferase*
CNS - *central nervous system*
EEG - *electroencephalography*
Hcy - *homocysteine*
NO - *nitric oxide*
SWDs - *spike-wave discharges*
tHcy - *total plasma homocysteine*

SAŽETAK

Četiri decenije istraživačkog rada širom sveta dovele su do ustanovljavanja semi-esencijalne sulfihidrilne aminokiseline homocisteina (Hcy) kao novog potentnog i nezavisnog faktora rizika za arteriosklerozu, kao i vazotoksične i neurotoksične supstance koja učestvuje u fundamentalnim biološkim procesima svojstvenim svim živim ćelijama. Cilj ovog rada je da prikaže dostupna saznanja na temu hiperekscitabilnosti centralnog nervnog sistema u eksperimentalnom modelu homocisteinom indukovene epilepsije. Rezultati pokazuju da akutna administracija homocisteina i homocisteinu-srodnih supstanci značajno utiče na nervnu aktivnost, elektroencefalografske (EEG) zapise i ponašanje odraslih mužjaka soja Wistar pacova, a smatra se da hiperhomocisteinemija može imati slične efekte i na aktivnost ljudskog mozga. Homocistein i D,L-homocistein tiolakton su ekscitotoksični i izazivaju epileptične napade stimulacijom NMDA receptora; oni indukuju značajnu inhibiciju aktivnosti Na^+/K^+-ATPaze u korteksu, hipokampusu i moždanom stablu. Azot monoksid (NO) deluje kao antikonvulzant u D,L-homocistein tiolakton indukovanim epileptičnim napadima i vrši prevenciju D,L-homocistein tiolakton indukovane inhibicije aktivnosti Na^+/K^+-ATPaze. EEG monitoring efekata etanola na homocisteinom indukovanu epilepsiju podržava ideju da akutni unos etanola može predstavljati jedan od faktora egzogenog uticaja na moždanu ekscitabilnost. Takođe je utvrđeno da D, L-homocistein tiolakton u značajnom procentu inhibira aktivnost acetilholinesteraze u mozgu pacova.

Ključne reči: *homocistein, CNS, hiperekscitabilnost, pacov*

Korišćene skraćenice:
AchE – *acetilholin esteraza*
BHMT - *betain-homocistein S-metiltransferaza*
CNS – *centralni nervni sistem*
EEG - *elektroencefalografija*
Hcy - *homocistein*
NO – *azot monoksid*
SWDs – *"šiljak pražnjenja"*
tHcy – *ukupni plazma homocistein*

UDK 612.8:577.112.34 ; 616.853 / Ser J Exp Clin Res 2011; 12 (1): 3-9

Correspondence to: Dragan M. Djurić, M.D. Ph.D. Institute of Medical Physiology "Richard Burian", School of Medicine, University of Belgrade, Višegradska 26/II, 11000 Belgrade, Serbia, Tel: +381-11-3607-112, Fax: +381-11-36 11 261, e-mail: drdjuric@eunet.rs

BACKGROUND

Within the past four decades, investigators worldwide have established that the amino acid homocysteine (Hcy) is a novel and independent risk factor for arteriosclerosis. In addition, Hcy is a vasotoxic and neurotoxic agent that interferes with the fundamental biological processes common to all living cells. Therefore, it has also been termed the "cholesterol of the 21st century."

Metabolism of homocysteine is coordinately regulated to maintain a balance between remethylation and transsulfuration pathways, which are critical to maintaining low levels of this potentially cytotoxic sulphur containing amino acid (1). Homocysteine belongs to a group of molecules known as cellular thiols and is considered a "bad" thiol. Glutathione and cysteine, the most abundant cellular thiols, are considered to be "good" thiols (2). In the methylation pathway that occurs in all tissues, homocysteine acquires a methyl group to form methionine in a vitamin B12 dependent reaction, which is catalysed by methionine synthase. The second substrate required by methionine synthase is 5-methyltetrahydrofolate, which is formed by the reduction of 5,10-methylenetetrahydrofolate. This reaction is catalysed by the enzyme methylenetetrahydrofolate reductase (MTHFR). The TT genotype of this enzyme causes thermolability and reduces enzyme activity, which impairs the formation of 5-methyltetrahydrofolate. This reduced enzyme activity explains why this genotype is associated with increased Hcy levels when the folate status is relatively low. However, liver, kidney and the lens of the eye have the ability to convert Hcy to L-methionine through a vitamin B12-independent reaction catalysed by betaine-Hcy S-methyltransferase (BHMT). The CNS lacks BHMT and it is completely dependent on the folate and vitamin B12 pathway for the conversion of Hcy to L-methionine.

Homocysteine condenses with serine to form cystathionine in an irreversible reaction catalysed by the B6 containing enzyme cystathionine beta-synthase, which is known as the transsulfuration pathway. Hcy catabolism requires vitamin B6 and as a consequence, alterations in folic acid and B vitamin status impairs Hcy biotransformation. These alterations result in the synthesis of cysteine, taurine and inorganic sulphates that are excreted in urine.

Elevation of homocysteine levels is known to lead to the metabolic conversion and inadvertent elevation of homocysteine thiolactone, which is a reactive thioester representing less than 1% of total plasma homocysteine. In all cell types, from bacteria to human, homocysteine is metabolised to homocysteine thiolactone by methionyl-tRNA synthetase (3). Homocysteine thiolactone causes lethality, growth retardation, blisters and abnormalities in somite development by oxidative stress, which is one of important mechanisms for its toxicity to neuronal cells (4). The highly reactive and toxic homocysteine metabolite, homocysteine thiolactone, can be produced in two steps by enzymatic and/or non-enzymatic reactions in blood serum. The ability to detoxify or eliminate homocysteine thiolactone is essential for biological integrity (3, 4).

Total plasma Hcy (tHcy) consists of a pool of free homocysteine, homocystine, Hcy-S-S-Cys disulphide, protein bound N- and S-linked Hcy as well as their oxidised forms and Hcy-thiolactone (5-7). Under physiological conditions, less than 1% of the total Hcy is present in a free reduced form. Approximately 10–20% of total Hcy is present in different oxidised forms, such as Hcy-Cys and homocystine, which is a Hcy dimer. Plasma tHcy levels are affected by genetic, physiologic (age and sex) and lifestyle factors as well as various pathologic conditions (5, 6, 8). Hyperhomocysteinemia is defined as an elevated plasma total homocysteine (tHcy) concentration (>15 μM).

Elevated tHcy is a recognised risk factor for cardiovascular disease (9) and has been linked to neurological diseases during aging, such as cognitive declines, cerebrovascular disease and stroke, vascular dementia and Alzheimer's disease. In addition, elevated tHcy levels are linked with pathological brain functioning, such as mental retardation, depression, schizophrenia and memory impairment. Hcy is also a pro-thrombotic and pro-inflammatory factor, vasodilatation impairing substance and an endoplasmatic reticulum stress inducer (10, 11).

Mitrovic et al. (12) evaluated total plasma homocysteine in patients with angiographically confirmed coronary artery disease. In addition, they investigated the effects of homocysteine lowering therapy on endothelial function, carotid wall thickness and myocardial perfusion. Their study found that homocysteine levels decreased significantly (34%) with folic acid therapy and that endothelium function improved by 27% with this treatment. However, carotid structure and myocardial perfusion did not show any significant improvement in patients with confirmed coronary artery disease (13). Djuric et al. (14, 15) also investigated the link between homocysteine and folic acid, demonstrated folic acid induced coronary vasodilation and decreased oxidative stress in the isolated rat heart.

HOMOCYSTEINE AND NEUROTOXICITY

Despite several theories, a complete understanding of Hcy toxicity remains unclear. In particular, the hypothesis that relates homocysteine to CNS dysfunction by way of overt neurotoxicity is based on the neuroactive properties of homocysteine. Elucidating the link between homocysteine and CNS dysfunction is vital for improving the treatment of homocysteine related CNS disorders. Hcy adversely affects brain functioning (i.e., mental retardation, dementia and memory impairment) and high tissue concentrations cause oxidative stress and excitotoxicity in neurons (16). When these symptoms are combined with homocystinuria, patients often present with convulsions (17). These studies provide evidence for a complex and multifaced relationship between homocysteinemia and CNS disorders. Hcy is an endogenous compound that is neurotoxic at supraphysiological concentrations and induces neuronal damage and cell loss through excitotoxicity and apoptosis. These CNS

pathologies could be a direct consequence of the inability of cerebral tissue to metabolise Hcy through the betaine and transsulfuration pathways, thereby favouring Hcy accumulation in the nervous system (18). High brain concentrations of either Hcy or its oxidised derivatives have been shown to alter neurotransmission (19). The accumulation of homocysteine (at synapses or in the extracellular space) increases intracellular S-adenosylhomocysteine (SAH), which is a potent inhibitor of many methylation reactions that are vital for neurological function including the O-methylation of biogenic amines. Methylation of myelin basic protein and reducing the synthesis of phosphatidyl choline, which can lead to blood-brain barrier (BBB) disruption, are a few pathological processes that are possible in the absence of normal methylation patterns (20).

It has been recently suggested that Hcy toxicity is a consequence of its covalent binding to proteins, which interferes with protein biosynthesis and decreases the normal physiological activity of proteins. This modification of protein function is a process called homocysteinylation. Transthyretin is a plasma protein that is modified through homocysteinylation (3, 21). Other reports suggest that Hcy exerts its toxicity through the induction of endoplasmic reticulum (ER) stress. Increased intracellular Hcy concentrations are associated with both the alteration of redox balance and post-translational protein modifications through N- and S-homocysteinylation (22). Other studies suggest that Hcy induces the expression of superoxide dismutase in endothelial cells, which leads to the consumption of NO and impairs endothelial vasorelaxation (23).

HOMOCYSTEINE AND SEIZURES

Experimental models of generalised clonic-tonic seizures induced by metaphit (1-[1(3-isothiocyanatophenyl)-cyclohexyl] piperidine) (24, 25) and lindane (γ-1,2,3,4,5,6-hexachlorocyclohexane) (26, 27) are widely used for the study of epilepsy and the preclinical evaluation of potential antiepileptic treatments. In contrast to audiogenic epilepsy induced by metaphit with its typical and characteristic three degrees of intensity, the lindane model is similar to Hcy-induced epilepsy with a wide spectra of behavioural manifestations (e.g., hot plate reaction and Kangaroo position) incorporated into the rating scale from grades 0 - 4. Almost four decades ago, Sprince et al. (28) described that elevated levels of homocysteine arising from excess dietary methionine may induce epilepsy and lethality. The fact that increased homocysteine concentrations damage endothelial structures and the blood coagulation system during aging and in patients on antiepileptic drugs (29) justifies the attention directed toward the examination of homocysteine's neural effects.

Furthermore, experimental models of epilepsy may be induced by manipulations of γ-aminobuturic acid (e.g., bicuculline, corasol, picrotoxin and benzylpenicillin sodium) (30). In contrast, epilepsy can be induced by an opposite mechanism such as by increasing cerebral excitatory neurotransmission. There are several proposed mechanisms by which exposure to excess D,L-homocysteine or D,L-homocysteine thiolactone induce seizures. The most reactive natural amino acid is homocysteic monocarboxylic, which is sulphur-containing and its homocysteic sulphinic acid derivatives are excitatory amino acids that have been proposed as candidates for brain excitatory neurotransmitters (31). However, answering the question as to whether D,L-homocysteine thiolactone should be included in the list of epileptogenic factors according to behavioural and electrographic responses will require additional studies and future human therapeutic trials. Increased levels of Hcy and its oxidised forms can provoke seizures by increasing activation of certain neuronal receptors such as N-methyl d-aspartate (NMDA), α-amino-3-hydroxy-5-methyl-4-isoxazolepropionate (AMPA)/kainate ionotropic glutamate receptors or group I and group III metabotropic glutamate receptors (5). All of these glutamate receptors are expressed in hippocampal pyramidal cells and may directly induce or drive these cells over the threshold for excitotoxic cell death. Overstimulation of these receptors triggers cytoplasmic calcium pulses, $Ca2^{+}$ influx and intraneuronal calcium mobilisation in the presence of glycine (32). Increased cytosolic $Ca2^{+}$ concentrations affect enzyme activities and the synthesis of nitric oxide, which is a retrograde messenger that overstimulates excitatory amino acid receptors including glutamate, thereby lowering the convulsive threshold (33). However, expression of the NMDA receptor is not confined to neurons. Other cell types, including endothelial cells from cerebral tissue, can express this receptor. Free radicals induce the up-regulation of the NR1 subunit of the NMDA receptor, thereby increasing the susceptibility of cerebral endothelial cells to excitatory amino acids, which can lead to blood brain barrier disruption (34). Microglia are also subject to the toxic effects of Hcy (35). Hcy can induce convulsions in adults and in immature experimental animals through modulating the activity of metabotropic glutamate receptors (mGluRs) (36). Kubova et al. (37) stated that the main epileptic phenomenon in homocysteine thiolactone treated rats was emprosthotonic, flexion seizures, which are observed in young animals but never seen in rats older than 25 days. Homocysteine was shown to elicit minor (predominantly clonic) and major (generalised tonic-clonic) seizures during ontogenesis in immature Wistar rats (36, 37). It seems that Hcy exerts a direct excitatory effect comparable to the action of glutamate (17). In addition, Hcy has been shown to enhance either the release or uptake of other endogenous excitatory amino acids (36).

Classical anticonvulsants such as phenytoin, carbamazepine and valproic acid lower plasma folate levels and significantly increase homocysteine levels, which induces epileptogenesis and reduces the control of seizures in patients with epilepsy (38). On the other hand, increasing excitability with this native amino acid further contributes to epileptogenesis and disturbs the balance between excitation and inhibition in

the brain. Following the work of Djuric's study, Stanojlovic et al. administered homocysteine (i.p.) to adult rats, and for the first time, convulsive and non-convulsive seizures were recorded (39). This form of epilepsy was followed by two-wave patterns of seizures with one replacing the other. It has been suggested that D,L-homocysteine thiolactone may be considered as an excitatory metabolite, which is capable of becoming a natural convulsant if accumulated to a great extent in the brain (39). Hyperhomocysteinemia in awake adult male Wistar rats induced a generalised seizure disorder characterised by recurrent unprovoked clonic-tonic convulsions and absence-like seizures as well as epileptic electrical discharges. In addition to a prolonged median latency to the first seizure, the seizure incidence, median seizure episode severity and median number of seizure episodes per rat were significantly higher in all Hcy treated groups (39). Non-convulsive status epilepticus can occur from a variety of causes, including primarily generalised absence epilepsy, genetic origins (Wakayama or tremor epileptic rats) or pharmacologically (penicillin, pentylenetetrazole or γ-hydroxy-butyric acid) induced models (40). Behavioural immobility during motor cortex activation and the occurrence of generalised spike-wave activity are among the most puzzling phenomena in absence epilepsy. According to one of numerous hypotheses addressing the development of spike-wave discharges (SWDs), these electrographic discharges may belong to the same class of phenomena such as sleep spindles. Sleep spindals are normally generated sleep rhythms that transformation one, two or more spindle waves into the spike component of the SWD (41). Cortico-thalamo-cortical oscillatory network connections may play a pacemaker role in the electrogenesis of oscillations and primarily represent the neurophysiological basis underling the initiation and propagation of SWD (40).

In keeping with the well-known fact that rhythmic bursts of spikes represent an electrophysiological marker of a hyperexcitability, Folbergrova et al. (42) found a very poor electroclinical correlation between electroencephalographic (EEG) patterns and motor phenomena in immature rats. The epileptogenic process is closely associated with the changes in neuronal synchronisation, and non-convulsive, generalised epilepsy is characterised by brief episodes of unpredictable and unresponsive behaviours with a sudden arrest accompanied by SWDs. However, the spike-wave complexes of SWDs have a unique shape. Bilateral, high-voltage, synchronous, spindle-like electrical oscillations, which are common phenomenon during paroxysmal EEG attacks, are termed SWDs. These are associated with sudden motor immobility and minor clinical signs, such as the loss of responsiveness with rhythmic twitches of vibrissae or cervicofacial musculature and are seen after i.p. administration of D,L-homocysteine thiolactone in adult rats. Interestingly, absence-like animals showed no reaction to these different stimuli (e.g., audiogenic, tactile).

Stanojlović et al. (39) found poor electro-clinical correlations in Hcy treated rats. It is worth mentioning that electrographic seizure discharges were absent even during motor convulsions of grade 3 or 4. On the contrary, EEG seizures without motor symptoms were regularly observed. These aforementioned EEG signatures were distinguishable from sleep spindles (10-16 Hz) in regard to their frequency, duration, morphology (sleep spindles are more stereotyped than SWD waves) and moment of occurrence. For example, SWDs occur during passive wakefulness, while sleep spindle-like oscillations occur during high amplitude delta activity (43). The poor prognosis for the Hcy group of animals appears to be a result of the combined systemic damage caused by continuous seizure activity as well as the excitotoxic and neurotoxic effects of homocysteine accompanied by the action of free radicals, including oxidative brain damage (42, 44). In most of the related studies, it is not quite clear whether the observed effects are due to homocysteine itself or to homocysteine metabolites. Notably, all of the above mentioned mechanisms induce cell death (45) and result in a high mortality rate (100%).

The basic function of the Na^+/K^+-ATPase is to maintain the high Na^+ and K^+ gradients across the plasma membrane of animal cells and it is essential for the generation of the membrane potential and maintenance of neuronal excitability (2). In addition, it has been demonstrated that there is a moderate inhibition of rat hippocampal Na^+/K^+-ATPase activity by D,L-homocysteine, which is not observed in the cortex and brain stem (46). In contrast, D,L-homocysteine thiolactone strongly inhibits Na^+/K^+-ATPase activity in cortex, hippocampus and the brain stem of rats, thereby affecting the membrane potential with deleterious effects for neurons. Considering that hyperhomocysteinemia increases formation of superoxide and hydrogen peroxide and that excitotoxicity indirectly provokes increased intracellular free radicals production, it is feasible that oxidative stress may also be associated with the CNS injury caused by homocysteine and D,L-homocysteine thiolactone (47).

Otherwise, nitric oxide (NO) is a highly reactive second messenger molecule synthesised in a number of tissues. It serves a key role in interneuronal communications via modulating release of classical neurotransmitters and influencing the excitability status of neurons (33). It is produced from L-arginine by the action of a family of enzymes known as NO synthases (NOS). Neural (nNOS) and endothelial NOS (eNOS) are Ca^{2+}/calmodulin-dependent enzymes, while inducible NOS (iNOS) shows Ca^{2+}-independent properties. N-nitro-L-arginine methyl ester (L-NAME) is a non-selective NOS inhibitor commonly used to decrease NO levels. Recently, it has been determined that NO serves a role in the mechanisms underlying D,L homocysteine thiolactone induced seizures. This was demonstrated by testing the action of L- arginine (NO precursor) and L-NAME (NOS inhibitor) on behavioural and EEG manifestations of D,L homocysteine thiolactone induced seizures (48). Following Djuric's study, Hrncic et al. (48) showed functional involvement of NO in the convulsive activity of D,L-homocysteine thiolactone induced seizures in adult rats. Pretreatment with L-NAME in a dose–dependent manner increased seizure incidence and severity and shortened latency time to the first seizure following injection with a subthreshold dose of D,L-homo-

cysteine thiolactone (5.5 mmol/kg, i.p.). Nitro indazole is an inhibitor of neuronal nitric oxide synthase that attenuates pilocarpine-induced seizures (49). NO has been shown to modulate NMDA receptor activity by interacting with the –SH group of its redox modulatory site via S-nitrosylation. This modification results in the downregulation of this receptor complex (19) and prevents the neurotoxic effects of an excessive Ca^{2+} influx during homocysteine induced overstimulation of NMDA and mGluRs I receptors. In addition, Kim et al. (50) demonstrated that NO ameliorates homocysteine's adverse effects of S-nitrosylation in cultured rat cortical neurons. Moreover, NO induces a reduction of glutamate by activation of glial cells. Many experimental studies have demonstrated co-localisation of NOS and GABA and have suggested that basal NO levels induce a depression of inhibition, while high concentrations of NO increase GABA release. In contrast to homocysteine, which increases oxidative stress by the production of reactive oxygen species, NO can act as a neural protector. This neuroprotective property is due to the formation of S-nitroso-L-glutathione, which is an antioxidant and NO scavenging molecule (51). However, the role of NO in epileptogenesis has been studied in different experimental models and reported results are highly contradictory. Namely, the proconvulsive role of NO has been demonstrated in the lindane model of convulsions and several others (52). Thus, it seems that the activity of NO depends on the animal strain, the seizure model employed and the type and dose of drugs used in order to modify cerebral NO levels.

Furthermore, it has been demonstrated that when L-arginine is applied alone, it significantly increases the activity of Na^+/K^+-ATPase activity in the hippocampus, the cortex and the brain stem. However, when L-arginine is applied prior to D,L homocysteine thiolactone (8 mmol/kg), this completely reverses its inhibitory effect (48). The same holds true for its effects on Mg^{2+}-ATPase activity in the rat cortex and the brain stem. L-NAME increases Na^+/K^+-ATPase activity in the cortex and the brain stem but not in the hippocampus. When L-NAME was administered prior to homocysteine thiolactone (5.5 mmol/kg), it increased the activity of both Na^+/K^+-ATPase and Mg^{2+}-ATPase in the rat cortex and the hippocampus.

Changes in total spectral power density after ethanol alone and together with D,L-homocysteine thiolactone in adult rats were examined (53). Recording electrical activity from the brain represents a measure of both brain function and dysfunction. Ethanol is used as a social substance and is the second most widely used psychoactive substance in the world after caffeine. The influence of ethanol on the central nervous system depends on the dose, drinking pattern, tolerance and other factors. While chronic ethanol consumption is followed by a series of seizures during the withdrawal period, acute ethanol intake exerts mainly inhibitory effects on the CNS and is usually associated with an increase of seizure threshold (54). Rasic-Markovic et al. (53) found that ethanol's action on electrographic pattern is biphasic, which is characterised by potentiation of epileptiform activity in one dose range and depression in another one. Low ethanol doses causing euphoria and behavioural arousal are associated with desynchronisation of the EEG, decreases in the mean amplitude and increases in theta and alpha activity. In addition, ethanol increases mean total spectral power density 15 min and 30 min after administration. Ethanol affects voltage-gated ion channels, second messenger systems and a variety of different neurotransmitter systems such as glycine, acetylcholine as well as monoamines and neuropeptides systems (55). Two major amino acid neurotransmitter systems, GABA and glutamate, as well as aspartate are affected by ethanol. Acute administration of ethanol inhibits NMDA-induced Ca2+ influx, cyclic GMP production, neurotransmitter release and reduces NMDA-evoked neurotoxicity (56, 57).

Pre-treatment with MK-801, which is a NMDA receptor antagonist, showed a tendency to reduced the incidence of convulsions, latency to the first seizure onset and the severity of seizure episodes; however, there was no statistical significance when compared to the D,L-homocysteine thiolactone treated group. Nevertheless, the median number of seizure episodes was significantly decreased by MK-801 when compared to the D,L-homocysteine thiolactone treated group. On the other hand, ifenprodil, which is another type of NMDA receptor antagonist, decreased the latency to the first seizure onset and increased the median number of seizure episodes. The majority of seizure episodes in the ifenprodil (72.1%) and MK-801 (73.1%) groups were significantly different compared to the D,L-homocysteine thiolactone treated group (36.0%). Our findings suggest that D,L-homocysteine thiolactone induces seizures through the stimulation of NMDA receptors in the central nervous system but other mechanisms (i.e., NO signalling) may also be involved (58).

Finally, limited data exist in the literature regarding the effects of homocysteine and D,L-homocysteine thiolactone on the activity of the acetylcholinesterase (AChE) enzyme in the blood, but practically no data exist regarding the influence of these compounds on this enzyme in the brain and heart. Recent results showed a significant reduction in AChE activity in all tissues obtained from rats treated with D,L-homocysteine thiolactone compared to the enzyme activity of the control group. In addition, these results also showed that the blood enzyme activity was the lowest (12%) after treatment, while the enzyme activity was slightly higher in the brain (27.8%) and heart samples (86.3%). Therefore, it was concluded that D,L-homocysteine thiolactone significantly inhibited AChE activity in the heart and brain tissue but not in the blood of the rat (59).

Overall, these studies clearly demonstrate that acute administration of homocysteine and especially D,L-homocysteine thiolactone elicit seizures in adult rats, affect neuronal activity, EEG recordings and behavioural responses. These effects have been linked to the stimulation of NMDA receptors, inhibition of the Na^+/K^+-ATPase, inhibition of AChE activity and the functional involvement of NO during D,L-homocysteine thiolactone induced seizures in adult rats.

ACKNOWLEDGEMENTS

This work was supported by the Ministry for Science and Technological Development of Serbia, Grant No. 175032 and Grant No. 175043.

REFERENCES

1. Miller JW, Nadeau MR, Smith D, Selhub J. Vitamin B-6 deficiency vs. folate deficiency: comparison of responses to methionine loading in rats. Am J Clin Nutr 1994; 59: 1033–39.
2. Mato JM, Lu SC. Homocysteine, the bad thiol. Hepatology 2005; 41: 976-79.
3. Chwatko G, Jakubowski H. The determination of homocysteine thiolactone in human plasma. Anal Biochem 2005; 15: 271-7.
4. Obeid R, Herrmann W. Mechanisms of homocysteine neurotoxicity in neurodegenerative diseases with special reference to dementia. FEBS Lett 2006; 580: 2994-05.
5. Jakubowski H. Homocysteine is a protein amino acid in humans.Implications for homocysteine-linked disease. J Biol Chem 2002; 277: 30425–28.
6. Jakubowski H. The pathophysiological hypothesis of homocysteine thiolactone-mediated vascular disease. J Physiol Pharmacol 2008; 59: 155–67.
7. Syardal A, Refsum H, Ueland PM. Determination of in vivo protein binding of homocysteine and its relation to free homocysteine in the liver and other tissues of the rat. J Biol Chem 1986; 261: 3156–63.
8. De Bree A, Verschuren WMM, Kromhout D, Kluijtmans LAJ, Blom HJ. Homocysteine determinants and the evidence to what extent homocysteine determines the risk of coronary heart disease. Pharmacol Rev 2002; 54: 599–18.
9. Clarke R, Daly L, Robinson K, et al. Hyperhomocysteinemia: an independent risk factor for vascular disease. N Engl J Med 1991; 324: 1149– 55.
10. Troen AM. The central nervous system in animal models of hyperhomocysteinemia. Prog Neuropsychopharm Biol Psych 2005; 29: 1140-51.
11. Zou CG, Banerjee R. Homocysteine and redox signaling. Antioxid Redox Signal 2005; 7: 547-559.
12. Mitrovic V, Djuric D, Petkovic D, Hamm C. Evaluation of plasma total homocysteine in patients with angiographically confirmed coronary atherosclerosis: possible impact on therapy and prognosis. Perfusion 2002; 15: 10-19.
13. Rieth A, Dill T, Deetjen A, Djuric D, Mitrovic V. Effects of homocysteine-lowering therapy on endothelial function, carotid wall thickness and myocardial perfusion. Acta Facultatis Medicae Naissensis 2006; 23: 179-184.
14. Djuric D, Vusanovic A, Jakovljevic V. The effects of folic acid and nitric oxide synthase inhibition on coronary flow and oxidative stress markers in isolated rat heart. Molecular and Cellular Biochemistry 2007; 300(1-2): 177-183.
15. Djuric D, Jakovljevic V, Rasic-Markovic A, Djuric A, Stanojlovic O. Homocysteine, folic acid and coronary artery disease: possible impact on prognosis and therapy. Indian J Chest Dis Allied Sci 2008; 50: 39-48.
16. Reis EA, Zugno AI, Zugno AI, et al. Pretreatment with vitamins E and C prevents the impairment of memory caused by homocysteine administration in rats. Metab Brain Disease 2002; 17: 211-17.
17. Wuerthele SE, Yasuda RP, Freed WJ, Hoffer BJ. The effect of local application of homocysteine on neuronal activity in the central nervous system of the rat. Life Sci 1982; 31: 2683-91.
18. Finkelstein JD. The metabolism of homocysteine: pathways and regulation. Eur J Pediatr 1998; 157: S40–Z44
19. Lipton SA, Rosenberg PA. Excitatory amino acids as a final common pathway for neurological disorders. N Engl J Med 1994; 330: 613– 22.
20. Kamath AF, Chauhan AK, Kisucka J, et al. Elevated levels of homocysteine compromise blood-brain barrier integrity in mice. Blood 2006; 107: 591–93.
21. Hanyu N, Shimizu T, Yamauchi K, Okumura N, Hidaka H. Characterization of cysteine and homocysteine bound to human serum transthyretin. Clin Chim Acta 2009; 403: 70–75.
22. Chigurupati S, Wei Z, Belal C, et al. The homocysteine-inducible endoplasmic reticulum stress protein counteracts calcium store depletion and induction of CCAAT enhancer-binding protein homologous protein in a neurotoxin model of Parkinson disease. J Biol Chem 2009; 284: 18323–33.
23. Hucks D, Thuraisingham RC, Raftery MJ, Yagoob MM. Homocysteine induced impairement of nitric oxide-dependent vasorelaxation is reversible by the superoxide dismutase mimetic TEMPOL. Nephrol Dial Transpl 2004; 19: 1999–05.
24. Stanojlovic O, Zivanovic D, Susic V. N-methyl-D-aspartic acid and metaphit-induced audiogenic seizures in rat model of seizure. Pharmacol Res 2000 42: 247–53.
25. Stanojlovic O, Hrncic D, Racic A, Loncar–Stevanovic H, Djuric D, Susis V. Interaction of delta sleep-inducing peptide and valproate on metaphit audiogenic seizure model in rats. Cell Mol Neurobiol 2007; 27: 923- 32.
26. Vucevic D, Hrncic D, Radosavljevic T, et al. Correlation between electroencephalographic and motor phenomena in lindane – induced experimental epilepsy in rats. Canad J Physiol Pharmacol 2008; 286: 173-179
27. Mladenovic D, Hrncic D, Vucevic D, et al. Ethanol suppressed seizures in lindane-treated rats. Electroencephalographic and behavioral studies. J Physiol Pharmacol 2007; 58:641-54.
28. Sprince H, Parker CM, Josephs JA. Homocysteine-induced convulsions in the rat: Protection by homoserine, serine, betaine, glycine and glucose. Agents Actions 1969; 1: 9-13.
29. Perla-Kajan J, Twardowski T, Jakubowski H. Mechanisms of homocysteine toxicity in humans. Amino Acids 2007; 32:561-72.

30. Shandra AA, Godlevskii LS, Brusentsov AI, Karlyuga VA. Effect of delta-sleep- inducing peptide on NMDA-induced convulsive activity in rats. Neurosci Behav Physiol 1998; 28: 694-97.
31. Thompson GA, Kilpatrick IC. The neurotransmitter candidature of sulphur-containing excitatory amino acids in the mammalian central nervous system. Pharmacol Ther 1996; 72: 25– 36.
32. Zieminska E, Stafiej A, Lazarewicz J. Role of group I metabotropic glutamate receptors and NMDA receptors in homocysteine-evoked acute neurodegeneration of cultured cerebellar granule neurons. Neurochem Int 2003; 43, 481-92.
33. Meldrum BS. The role of glutamate in epilepsy and other CNS disorders. Neurology 1994; 44: 4-23.
34. Betzen C, White R, Zehendner CM, et al. Oxidative stress upregulates the NMDA receptor on cardiovascular endothelium. Free Radical Biol Med 2009; 47: 1212–20.
35. Zou CG, Zhao YS, Gao SY, et al. Homocysteine promotes proliferation and activation of microglia. Neurobiol Aging 2010; 31: 2069–79.
36. Folbergrova J. Anticonvulsant action of both NMDA and non-NMDA receptor antagonists against seizures induced by homocysteine in immature rats. Exp Neurol 1997; 145: 442-50.
37. Kubova H, Folbergova J, Mares P. Seizures induced by homocysteine in rats during ontogenesis. Epilepsia 1995, 36: 750-56.
38. Sener U, Zorlu Y, Karaguzel O, Ozdamar O, Coker I, Topbas M. Effects of common anti-epileptic drug monotherapy on serum levels of homocysteine, vitamin B12, folic acid and vitamin B6. Seizure 2006; 15: 79-85.
39. Stanojlovic O, Rasic-Markovic A, Hrncic D, et al. Two types of seizures in homocysteine thiolactone-treated adult rats, behavioral and electroencephalographic study. Cell Mol Neurobiol 2009; 29: 329-39.
40. Coenen AML, Van Luijtelaar, ELJM. Genetic animal models for absence epilepsy: a review of the WAG/Rij strain of rats. Behav Genet 2003; 33: 635-55.
41. Kostopoulos GK. Spike-and-wave discharges of absence seizures as a transformation of sleep spindles: the continuing development of a hypothesis. Clin Neurophysiol 2000; 111: S27-38.
42. Folbergrova J, Haugvicova R, Mares P. Seizures induced by homocysteinic acid in immature rats are prevented by group III metabotropic glutamate receptor agonist (R,S)-4-phosphonophenylglycine. Exp Neurol 2002; 180: 46-54.
43. Pinault D, Vergnes M, Marescaux C. Medium-voltage 5-9 Hz oscillations give rise to spike-and-wave discharges in a genetic model of absence epilepsy: in vivo dual extracellular recording of thalamic relay and reticular neurons. Neurosci 2001; 105: 181-201.
44. Sachdev PS. Homocysteine and brain atrophy. Prog Neuropsychopharmacol Biol Psychiatry 2005; 29:1152-1161.
45. Undas A, Perla J, Lacinski M, Trzeciak W, Kazmierski R, Jakubowski H. Autoantibodies against N-homocysteinylated proteins in humans: implications for atherosclerosis. Stroke 2004; 35: 1299-304.
46. Rasic-Markovic A, Stanojlovic O, Hrncic D, et al. The activity of erythrocyte and brain Na+/K+ and Mg2+-ATPases in rats subjected to acute homocysteine and homocysteine thiolactone administration. Mol Cell Biochem 2009; 327: 39–45.
47. Streck EL, Zugno AI, Tagliari B, Wannmacher C, Wajner M, Wyse AT. Inhibition of Na+,K+-ATPase activity by the metabolites accumulating in homocystinuria. Metabol Brain Dis 2002; 17: 83-91.
48. Hrncic D, Rasic-Markovic A, Krstic D, Macut D, Djuric D, Stanojlović O. The role of nitric oxide in homocysteine thiolactone-induced seizures in adult rats. Cel Mol Neurobiol 2010; 30: 219-31
49. Van Leeuwen R, De Vries R, Dzoljic MR. 7-Nitro indazole, an inhibitor of
neuronal nitric oxide synthase, attenuates pilocarpine- induced seizures. Eur J Pharmacol 1995; 28:7211—7213
50. Kim JM, Lee H, Chang N. Hyperhomocysteinemia due to shortterm folate deprivation is related to electron microscopic changes in the rat brain. J Nutr 2002; 132: 3418-21.
51. Rauhala P, Khaldi A, Mohanakumar KP, Chiueh CC. Apparent role of hydroxyl radicals in oxidative brain injury induced by sodium nitroprusside. Free Radic Biol Med 1998; 24: 1065-73.
52. Hrncic D, Rasic-Markovic A, Djuric D, Susic V, Stanojlovic O. The role of nitric oxide in convulsions induced by lindane in rats. Food Chem Toxicol 2011; In press.
53. Rasic-Markovic A, Djuric D, Hrncic D, et al. High dose of ethanol decreases total spectral power density in seizures induced by D,L- homocysteine thiolactone in adult rats. Gen Physiol Biophys 2009; S28: 25–32.
54. Hillbom M, Pieninkeroinen I, Leone M. Seizures in alcohol-dependent patients: epidemiology, pathophysiology and management. CNS Drugs 2003; 17: 1013-30.
55. Wang H, Jiang XH, Yang F, et al. Cyclin A transcriptional suppression is the major mechanism mediating homocysteine-induced endothelial cell growth inhibition. Blood 2002; 99: 939–45.
56. Simson PE, Criswell HE, Johnson KB, Hicks RE, Breese GR. Ethanol inhibits NMDA-evoked electrophysiological activity in vivo. J Pharmacol Exp Ther 1991; 257: 225-31.
57. Chandler LJ, Newsom H, Sumners C, Crews F. Chronic ethanol exposure potentiates NMDA excitotoxicity in cerebral cortical neurons. J Neurochem 1993; 60: 1578-81.
58. Rašić-Marković A, Hrnčić D, Djurić D, Macut D, Lončar-Stevanović H, Stanojlović O. The effect of N-methyl-D-aspartate receptor antagonists on D,L-homocysteine thiolactone induced seizures in adult rats. Acta Physiologica Hungarica 2011: 98 (1), 17–26.
59. Petrovic M, Fufanovic I, Elezovic I, Colovic M, Krstic D, Jakovljevic V, Djuric D. The effect of homocysteine thiolactone on acetylcholinesterase activity in rat brain, blood and heart. Ser J Exp Clin Res 2010; 11 (1): 19-22.

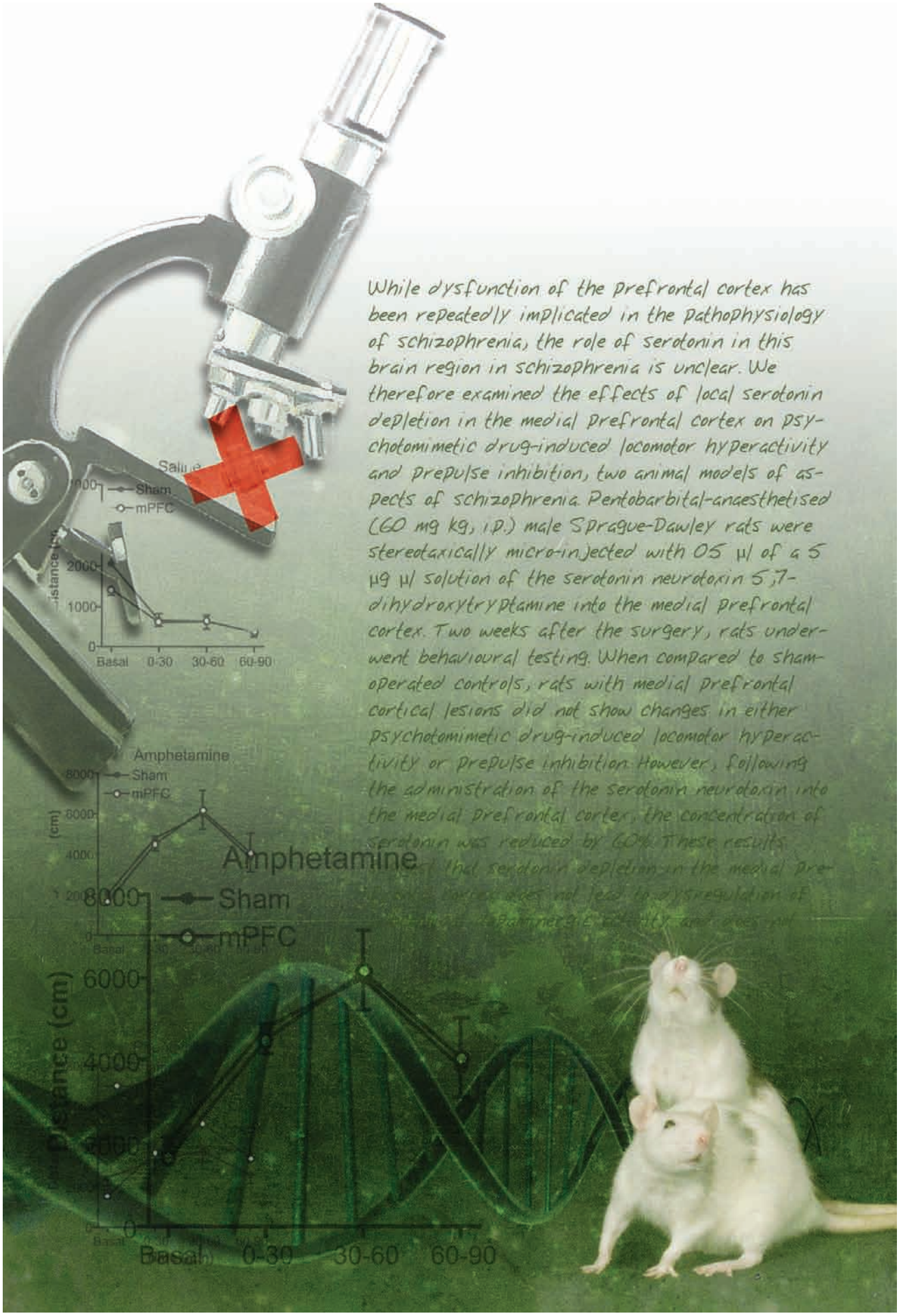
While dysfunction of the prefrontal cortex has been repeatedly implicated in the pathophysiology of schizophrenia, the role of serotonin in this brain region in schizophrenia is unclear. We therefore examined the effects of local serotonin depletion in the medial prefrontal cortex on psychotomimetic drug-induced locomotor hyperactivity and prepulse inhibition, two animal models of aspects of schizophrenia. Pentobarbital-anaesthetised (60 mg kg, i.p.) male Sprague-Dawley rats were stereotaxically micro-injected with 05 µl of a 5 µg µl solution of the serotonin neurotoxin 5,7-dihydroxytryptamine into the medial prefrontal cortex. Two weeks after the surgery, rats underwent behavioural testing. When compared to sham-operated controls, rats with medial prefrontal cortical lesions did not show changes in either psychotomimetic drug-induced locomotor hyperactivity or prepulse inhibition. However, following the administration of the serotonin neurotoxin into the medial prefrontal cortex, the concentration of serotonin was reduced by 60%. These results
Sham
mPFC
Basal
0-30
30-60
60-90
Amphetamine
Sham
mPFC
(cm)
6000
4000
2000
0
Basal
0-30
30-60
60-90

THE EFFECT OF SEROTONERGIC LESIONS IN THE MEDIAL PREFRONTAL CORTEX ON PSYCHOTOMIMETIC DRUG-INDUCED LOCOMOTOR HYPERACTIVITY AND PREPULSE INHIBITION IN RATS

Snezana Kusljic[1,2] and Maarten van den Buuse[2,3]
[1]Department of Nursing, University of Melbourne, Carlton, Victoria, Australia
[2]Behavioural Neuroscience Laboratory, Mental Health Research Institute, Parkville, Victoria, Australia
[3]Department of Pharmacology, University of Melbourne, Carlton, Victoria, Australia

Received / Primljen: 18. 01. 2011. Accepted / Prihvaćen: 03. 03. 2011.

ABSTRACT:

While dysfunction of the prefrontal cortex has been repeatedly implicated in the pathophysiology of schizophrenia, the role of serotonin in this brain region in schizophrenia is unclear. We therefore examined the effects of local serotonin depletion in the medial prefrontal cortex on psychotomimetic drug-induced locomotor hyperactivity and prepulse inhibition, two animal models of aspects of schizophrenia. Pentobarbital-anaesthetised (60 mg/kg, i.p.) male Sprague-Dawley rats were stereotaxically micro-injected with 0.5 µl of a 5 µg/µl solution of the serotonin neurotoxin 5,7-dihydroxytryptamine into the medial prefrontal cortex. Two weeks after the surgery, rats underwent behavioural testing. When compared to sham-operated controls, rats with medial prefrontal cortical lesions did not show changes in either psychotomimetic drug-induced locomotor hyperactivity or prepulse inhibition. However, following the administration of the serotonin neurotoxin into the medial prefrontal cortex, the concentration of serotonin was reduced by 60%. These results suggest that serotonin depletion in the medial prefrontal cortex does not lead to dysregulation of subcortical dopaminergic activity and does not cause aberrant responses to environmental stimuli.

Keywords: *schizophrenia, serotonin, medial prefrontal cortex, prepulse inhibition*

Running title: *Serotonin, the medial prefrontal cortex and behaviour*

Abbreviations used:

5,7-DHT- *5,7-dihydroxytryptamine*
5-HT- *5-hydroxytryptamine, serotonin*
$5\text{-HT}_{1\text{-}7,\ A\text{-}F}$- *serotonin receptor subtypes*
ANOVA- *analysis of variance*
$D_{1\text{-}5}$- *dopamine receptors 1-5*
DRN- *dorsal raphe nucleus*
GABA- *γ-aminobutyric acid*
HPLC- *high pressure liquid chromatography*
i.p.- *intraperitoneal*
MRN: *median raphe nucleus*
mPFC- *medial prefrontal cortex*
NMDA- *N-methyl-D-aspartate*
PPI- *prepulse inhibition*
PP- *prepulse intensity*
PP8- *prepulse of 8 dB*
s.c.- *subcutaneous*
SEM- *standard error of the mean*
VTA- *ventral tegmental area*

UDK 612.8:577.175.8 ; 616.895.8 / Ser J Exp Clin Res 2011; 12 (1): 11-19

Correspondence to: Dr. Snezana Kusljic, Department of Nursing, Melbourne School of Health Sciences, Level 5, 234 Queensberry Street, Carlton VIC 3010 Melbourne Australia, Tel: +613 8344 9428, Fax: +613 9347 4375 , Email: skusljic@unimelb.edu.au

INTRODUCTION

Schizophrenia is a chronic and severe psychiatric disorder that generally occurs in late adolescence or early adulthood. Approximately 1% of the population worldwide is affected by schizophrenia, placing a heavy burden on society, both in terms of emotional suffering and economic loss [1]. Schizophrenia is the classic example of a disorder that always has psychosis as one of its features [2]. As psychotic episodes are extremely debilitating, management and treatment aim to reduce and eliminate these dramatic personality changes, consisting of irritability, confusion and paranoia associated with hallucinations and delusions. Antipsychotic drugs are used to treat nearly all forms of psychosis, including schizophrenia. It has been generally accepted that the mechanism by which antipsychotic drugs decrease hallucinations and delusions is mediated at least in part by dopamine D_2 receptor blockade [3-5]. Moreover, atypical antipsychotic drugs, such as olanzapine, display a unique neuropharmacological profile; they minimise psychoses by interacting with a number of neurotransmitter and receptor systems through binding at multiple receptor sites. Olanzapine has a high affinity for serotonin 5 HT_{2A}, dopamine, cholinergic, histamine and α1-adrenergic receptors [6]. However, the most important mechanisms underlying the clinical properties of atypical antipsychotic drugs appear to be mediated by interactions with the serotonin 5-HT_{2A} receptor subtype [7, 8].

Serotonin is one of the major neurotransmitters in the human brain and plays a central role in the regulation of a wide range of behaviours, such as mood, eating and the stress response [9-11]. The serotonergic projections arising from the brainstem raphe nuclei form the largest and most complex efferent system in the human brain [12, 13]. The axons of dorsal raphe nucleus (DRN) neurons contribute to the majority of the serotonergic innervation in the frontal cortex, ventral hippocampus and striatal regions [14, 15], while the axons of median raphe nucleus (MRN) serotonergic neurons are more abundant in the dorsal hippocampus and the cingulate cortex [16, 17]. The hypothalamus, the substantia nigra and the nucleus accumbens receive serotonergic innervation from both nuclei [18, 19]. This organisation of the serotonergic neuronal population suggests that serotonin is involved in the regulation of different functional systems, such as the motor, limbic and somatosensory systems [13]. Thus, it is not surprising that atypical antipsychotic medications target multiple brain serotonin receptor subtypes. As it is very difficult to assess alterations of serotonergic transmission in the pathophysiology of psychiatric disorders in the living human brain, animal models are needed.

Animal models of psychiatric disorders, including schizophrenia, rely on mimicking specific aspects or symptoms associated with the disease [20-22]. The two most widely used models are locomotor hyperactivity induced by psychotomimetic drugs and prepulse inhibition. Psychotomimetic drugs, such as amphetamine and phencyclidine, can induce abnormal behaviours in animals and mimic certain aspects of psychotic disorders in humans [20, 23-25]. Amphetamine, an indirectly acting sympathomimetic, causes increased dopamine release from presynaptic terminals [26], and hyperlocomotion induced by amphetamine is dependent upon intact subcortical dopamine activity in the nucleus accumbens [27]. In contrast, phencyclidine interferes with multiple neurotransmitter systems [28]. Phencyclidine acts as a non-competitive antagonist at the ion channel associated with the N-methyl-D-aspartate (NMDA) glutamate receptor and also indirectly facilitates dopaminergic and serotonergic transmission [29]. Similar mechanisms are also activated in humans by phencyclidine [30]. Prepulse inhibition of the acoustic startle response is an operational measure of sensorimotor gating that is disrupted in patients with schizophrenia [31, 32] and in rats treated with drugs that facilitate dopaminergic activity [33-35]. Furthermore, prepulse inhibition is reduced in rats treated systemically with serotonin releasers, such as fenfluramine, direct 5 HT_{1A} receptor agonists [36-38] and glutamate receptor antagonists, such as phencyclidine [39]. The prepulse inhibition-acoustic startle reflex model in rats offers a unique opportunity to asses attentional and information processing deficits in schizophrenia, as modulation of the startle responses is similar among mammalian species [40]. In animals, usually the whole body startle response is measured after exposure to acoustic or tactile stimuli, while in humans the eyeblink component of the startle response is measured [40].

There is a growing body of evidence that suggests that the hippocampus, amygdala and prefrontal cortex play an important role in the pathogenesis of schizophrenia. The activity of these brain regions may cause changes in subcortical dopaminergic activity and therefore lead to the inappropriate initiation of behavioural responses to external stimuli. We have previously reported that serotonergic projections into the hippocampus and amygdala are differentially involved in the regulation of psychotomimetic drug-induced locomotor hyperactivity and prepulse inhibition [41, 42]. As serotonergic projections from both raphe nuclei innervate the prefrontal cortex, in addition to the hippocampus and amygdala, the aim of the present study was to determine whether serotonergic lesions of the prefrontal cortex caused behavioural changes similar to those produced by lesions of the hippocampus and/or amygdala.

In humans, dysfunction of the prefrontal cortical areas, with which the medial prefrontal cortex of the rat is comparable, is related to psychopathology of schizophrenia and other psychiatric disorders (for a review, see [43]). A wealth of evidence from studies in animals and humans indicates that the medial prefrontal cortex (mPFC) is a key component of the cortico-limbic-striatal circuits that generate pathological emotional behaviour [44, 45]. The various subdivisions of the mPFC appear to serve separate and distinct functions. For example, ven-

tral regions of the mPFC (the prelimbic and the infralimbic cortices) have been associated with diverse emotional and cognitive processes [43, 46, 47]. The ventral mPFC is also of interest, as it has been strongly implicated in the expression of behavioural and autonomic responses to emotionally relevant stimuli [48]. As dysfunction of the prefrontal cortex has been repeatedly implicated in the pathophysiology of schizophrenia [49-52], studies in the rat have focused on elucidating the role of this region in paradigms such as locomotor activity and prepulse inhibition. Dopaminergic lesions and intra-mPFC infusion of selective dopamine receptor antagonists have been reported to disrupt prepulse inhibition [53, 54], whereas the intra-mPFC infusion of amphetamine has been shown to decrease systemic amphetamine-induced increases in locomotor activity in the open field test [55]. However, none of these studies have addressed the importance of serotonergic innervation of the mPFC in neural circuitry involved in the regulation of motor behaviour and prepulse inhibition. Therefore, the present study investigated the effects of local lesions of serotonergic projections into the mPFC on psychotomimetic drug-induced locomotor hyperactivity and prepulse inhibition.

MATERIALS AND METHODS

Experimental animals

A total of 25 male Sprague-Dawley rats (Department of Pathology, University of Melbourne), weighing 250-300 g at the time of surgery, were used in this study. The animals were housed under standard conditions in groups of two or three with free access to food and water. They were maintained on a 12 h light/dark cycle (lights on at 0700 h) at a constant temperature of 21°C. One week prior to the surgical procedure, the animals were handled each day over a five-day period. The experimental protocol and surgical procedures were approved by the Animal Experimentation Ethics Committee of the University of Melbourne, Australia.

Drugs and solutions

D-amphetamine sulphate (Sigma Chemical Co., St. Louis, MO, USA) and phencyclidine HCl (PCP, Sigma) were dissolved in a 0.9% saline solution and injected subcutaneously (s.c.) into the nape of the neck. Desipramine HCl (Sigma) was dissolved in distilled water and injected intraperitoneally (i.p) 30 min prior to the neurotoxin microinjection. All doses are expressed as the weight of the salt and were administered in an injection volume of 1 ml/kg body weight. The serotonergic neurotoxin, 5,7-dihydroxytryptamine (5,7-DHT) (Sigma), was dissolved in 0.1% ascorbic acid (BDH Chemicals, Kilsyth, VIC, Australia) in saline to prevent oxidation of the neurotoxin. Carprofen (50 mg/ml, Heriot AgVet, Rowille, VIC, Australia) was diluted in 0.9% saline to a dose of 5 mg/kg and injected s.c. immediately after the surgical procedure.

Surgical procedure

The rats were pretreated with 20 mg/kg desipramine, 30 min prior to surgery, to prevent the destruction of noradrenergic neurons by 5,7-DHT [56]. The rats were subsequently anaesthetised with sodium pentobarbitone (60 mg/kg i.p., Rhone Merieux, QLD, Australia). The rats were mounted in a Kopf stereotaxic frame (David Kopf Instruments, Tujunga, CA, USA) with the incisor bar set at –3.3 mm [57]. The skull surface was exposed, and a small hole was drilled. A 25 gauge stainless-steel cannula, which was attached to a 10 µl glass syringe and connected via polyethylene tubing mounted in an infusion pump (UltraMicroPump, World Precision Instruments, Sarasota, FL, USA), was lowered into the mPFC. With bregma set to zero and the stereotaxic arm at 0°, the coordinates were as follows: mPFC lesions (n=13 for behavioural experiments, n=2 for histology): 3.2 mm anterior, 0.7 mm lateral and 4.5 mm ventral to bregma. A volume of 0.5 µl of 5,7-DHT (5 µg/µl) was infused over a period of 2 min on each side. Sham-operated controls (n=10) underwent the same surgical procedure and received an equal volume of vehicle solution. The injection volumes and rate of infusion were selected to minimise non-specific damage at the site of injection. Movement of the meniscus in the cannula was monitored to ensure successful infusion. After infusion, the cannula was left in place for a further 2 min to avoid backflow of the solution up the injection path. After lesioning, the skin was closed with silk-2 sutures (Cynamid, Baulkham Hills, NSW, Australia), and the animals were administered 5 mg/kg of carprofen, a non-steroidal, anti-inflammatory analgesic, to reduce post-operative inflammation and discomfort. The rats were placed on a heated pad until they recovered from the anaesthesia. After the surgery, the rats were allowed to recover for two weeks, during which they were handled regularly and health checks were made two to three times a week.

Experimental design and apparatus

Behavioural tests were performed starting two weeks after the surgery, and each session included random numbers of 5,7-DHT-lesioned rats and sham-operated rats. Locomotor activity was monitored using eight automated photocell cages (31 x 43 x 43 cm, h x w x 1, ENV-520, MED Associates, St. Albans, VT, USA). The position of the rat at any time was detected with sixteen evenly spaced infrared sources and sensors on each of the four sides of the monitor. The addition of a photobeam array above the subject added a second plane of detection to the system to detect rearing and vertical counts. This infrared beam array thus defined an X, Y and Z coordinate map for the system. The sensors detected the presence or absence of the infrared beam at these coordinates. Every 50 msec, the software checked for the presence or absence of the infrared beam at each sensor, allowing for the very precise tracking of the movement of a subject. Several types of behavioural responses were recorded, including distance moved, ambulation, stereotypy and rearing. Ambulatory counts con-

sisted of consecutive interruptions of at least four beams within a period of 500 ms. Small, repetitive beam breaks within a virtual box of 4 x 4 beams around the rat were recorded as stereotypic counts. Recordings of photocell beam interruptions by the rat were taken every 5 min and stored by the computer software. Three locomotor activity tests were done after treatment with saline, 0.5 mg/kg of amphetamine or 2.5 mg/kg of phencyclidine administered in a random order. These locomotor activity tests were done with three to four day intervals to prevent habituation due to repeated testing and to allow for clearance of the drugs. Prior to any drug manipulation, the rats were placed in the locomotor photocell cages for 30 min to establish baseline locomotor activity and allow for habituation to the test environment. After 30 min of spontaneous baseline activity, the rats were injected and locomotor activity was recorded over a further 90 min, generating a total session time of two hours. For the purpose of this paper, locomotor activity data were expressed as cumulative data from 30 min periods and presented as a time course of distance moved during the 30 min before injection and 90 min after injection.

After locomotor activity experiments, rats were tested for prepulse inhibition. This was done using six automated startle chambers (SR-LAB, San Diego Instruments, San Diego, CA, USA) consisting of clear Plexiglas cylinders, 9 cm in diameter, resting on a platform inside a ventilated, sound-attenuated and illuminated chamber. A speaker mounted 24 cm above the cylinder produced both continuous background noise at 70 dB and the various acoustic stimuli. Whole-body startle responses of the animal in response to acoustic stimuli caused vibrations of the Plexiglas cylinder, which were then converted into quantitative responses by a piezoelectric accelerometer unit attached beneath the platform. The percent prepulse inhibition was calculated as 100 x {[pulse-alone trials – (prepulse + pulse trials)] /(pulse-alone trials)} [31]. At least one day before the prepulse inhibition testing, rats underwent a pretest session where they were exposed to the testing cylinders and the testing protocol for the first time. This session was conducted to allow rats to habituate to the testing environment. Each rat was placed into the chamber for a 5 min acclimation period with a 70 dB background noise level that continued throughout the session. A single prepulse inhibition session lasted for about 45 min and consisted of high- and low-intensity stimulus combinations with a continuous background noise of 70 dB. The session started and ended with a block of ten pulse-alone trials of 115 dB. These blocks, together with twenty pseudo-randomly presented pulse-alone trials during the prepulse inhibition protocol, were used to calculate the basal startle reactivity and startle habituation. Prepulses were presented for 20 ms and differed in intensity. Prepulse inhibition was assessed by the random presentation of 115 dB pulses, ten each of prepulse-2, -4, -8, 12 and –16 and ten 'no-stimulus' trials. For example, prepulse-8 (PP8) is a 20-ms prepulse of 8 dB above the background noise, i.e., 78 dB, followed 100 ms later by a 40-ms 115 dB pulse [58]. The interval between trials varied (10 - 37 s) to prevent conditioning of the responses. A microcomputer and an interface assembly that controlled the delivery of acoustic stimuli digitised and recorded the readings.

Tissue preparation for histology and high pressure liquid chromatography (HPLC)

At the end of the experiments, rats were killed by decapitation and the brains were removed from the skull. The brains were placed on a cold plate. First, the frontal cortex was dissected bilaterally [59], and then the mPFC was dissected out. For the histological assessment of the location of the injection sites, 20-µm-thick sections of the medial prefrontal cortex of two mPFC-lesioned rats were cut on a cryostat and mounted onto gelatin-coated glass slides. The sections were then stained with cresyl violet (ProSciTech, Thuringowa, QLD, Australia) and examined microscopically to verify the location of the tips of the infusion cannulas.

The HPLC measurements of the tissue serotonin (5-HT) concentration were carried out in 23 animals. The dissected structures were weighed and stored in Eppendorf tubes at –80°C until the biochemical assays were performed. The tissue samples were homogenised in 500 µl of 0.1 M perchloric acid by ultrasonication and centrifuged at 15,500 g for 5 min. A 50 µl aliquot of the supernatant was injected into a high pressure liquid chromatography (HPLC) system to determine the content of 5-HT (ng/mg tissue of wet weight). The HPLC system consisted of a Waters Model 510 Solvent delivery system, a Waters U6K injector, an Alphabond C18 125A 10 U 150* 3.9 mm column and a Column & Spectra-Physics 970 D-A1 fluorescence spectrometer. The output signal from the fluorescence detector was analysed with the chromatography software package, 810 Baseline, version 3.31. The mobile phase used consisted of 9.8 g/l KH_2PO_4, 1.0 g/l Na_2EDTA, 5% acetonitrile and 1 ml/l triethylamine. The pH of the mobile phase solution was adjusted to 3.0 with 1 M HCl. Subsequently, the solution was filtered and degassed and delivered to the HPLC at a flow rate of 1 ml/min. Prior to sample testing, the following standards for 5-HT were run through the system: 12.5 ng/ml, 25 ng/ml, 50 ng/ml, 100 ng/ml and 200 ng/ml. Calibration curves were constructed, and the level of 5-HT in tissue samples was calculated relative to these standards. Each run lasted 8 min and the retention time for serotonin was 2.6 min.

Statistical analysis

Data were expressed as the mean ± the standard error of the mean (SEM). All of the statistical analyses were performed using the statistical software package SYSTAT 9.0 (SPSS Inc., Chicago, IL, USA). All of the data were analysed using an analysis of variance (ANOVA) with repeated measures where appropriate. In the locomotor activity experiments, data were summed in 30-min blocks, and these blocks were used to assess the main effects of the lesion type (group), the treatment with amphetamine or phency-

clidine (time) and the interactions between these factors. In this analysis, the time effect was a repeated-measures factor. The baseline and the drug-induced locomotor activity were part of the data set analysed. In the prepulse inhibition experiments, the factors were group and habituation (four blocks of ten startle responses) or group and prepulse (five different prepulse intensities), where habituation and prepulse were repeated-measures factors. After calculating ANOVAs for all of the surgery groups, subsequent pairwise ANOVAs were performed where needed. A 'p-value' of $p<0.05$ was considered to be statistically significant. For HPLC measurements, a one-way ANOVA was used, followed by the Bonferroni-corrected t-test comparison.

RESULTS

Histology: injection sites

Inspection of cresyl violet-stained brain sections from two animals revealed that the tip of the infusion cannula was situated within the boundaries of the mPFC, as delineated by the Paxinos and Watson rat brain atlas [57].

HPLC: 5-HT depletion

The behavioural data of four mPFC-lesioned rats with partial depletions of 5-HT (<50%), as measured by HPLC, were excluded from the study. The final group size for the analysis was n=10 for the sham-operated group and n=9 for the mPFC-lesioned group. In the mPFC-lesioned rats, the local injection of 5,7 DHT caused a marked reduction of the 5-HT concentration in the mPFC. After the microinjection of 5,7-DHT into the mPFC, the concentration of 5-HT was reduced by 60% (Figure 1). An ANOVA revealed a significant reduction of the 5-HT concentration in the mPFC-lesioned rats compared to the controls ($F_{1,17}=92.3$, $p<0.001$).

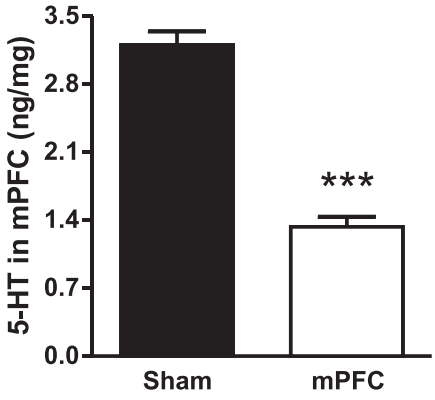

Figure 1
5-HT content in the mPFC after sham surgery or 5,7 DHT microinjection into the mPFC. The data are expressed as the average 5-HT concentration (ng/mg of tissue wet weight) ± SEM. ***p<0.001 for the difference in the 5-HT concentration between the mPFC-lesioned rats and the sham-operated control rats as indicated by ANOVA.

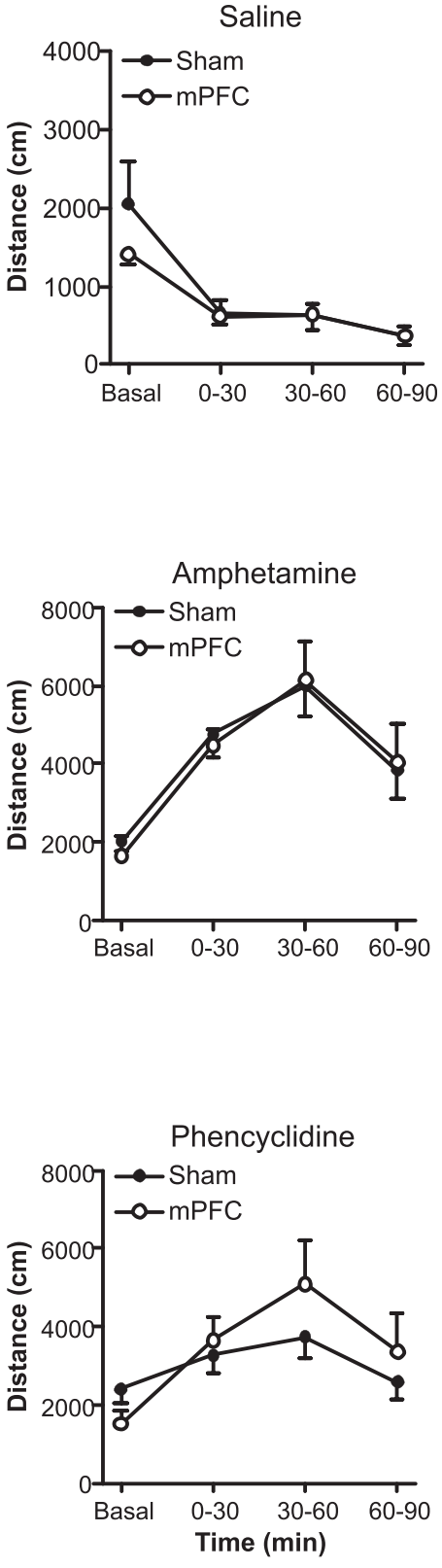

Figure 2
Time course of the effects of a subcutaneous injection of saline, 0.5 mg/kg of amphetamine or 2.5 mg/kg of phencyclidine on locomotor activity in sham-operated rats and rats with 5,7 DHT-induced mPFC lesions. Locomotor hyperactivity is expressed as the distance moved (cm) ± SEM for sham-operated (n=10, ●) and mPFC-lesioned rats (n=9, ○). There were no significant differences between the groups.

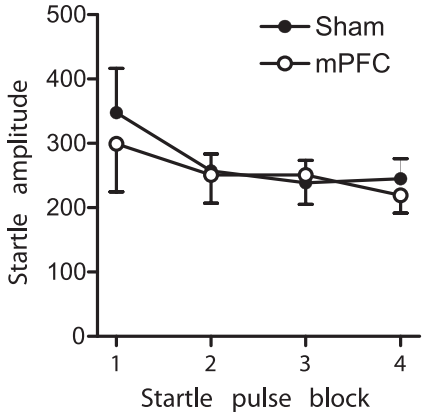

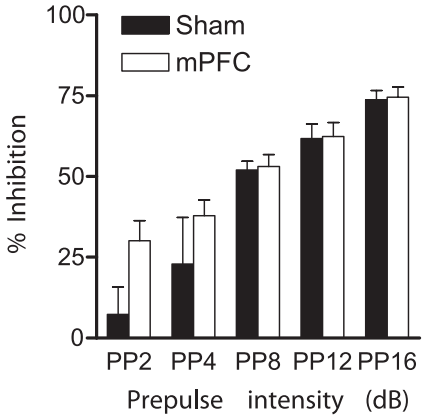

Figure 3
Effect of sham surgery (n=10) or 5,7-DHT lesions of the mPFC (n=9) on startle amplitude, startle habituation and prepulse inhibition. The top panel illustrates the basal startle reactivity and the startle habituation. The data are expressed as mean startle amplitudes ± SEM for each of the four blocks of ten 115 dB pulses. The bottom panel illustrates the prepulse inhibition of the acoustic startle response. The prepulse inhibition is expressed as the % inhibition ± SEM at different prepulse intensities. There were no significant differences between the groups as indicated by ANOVA.

The effects of the microinjection of 5,7-DHT on amphetamine- and phencyclidine-induced locomotor hyperactivity

The locomotor hyperactivity caused by treatment with amphetamine or phencyclidine was not significantly different between sham-operated rats and mPFC-lesioned rats (Figure 2). After treatment with either amphetamine or phencyclidine, there was an expected main effect of time ($F_{2,34}$=10.4, p<0.001 and $F_{2,34}$=5.4, p=0.01, respectively), reflecting the increases in activity caused by these treatments. The lack of a main group effect or a time x group interaction suggested that the time course of the effects of either amphetamine or phencyclidine was not altered after mPFC-lesions. Lesioned animals tended to show increased phencyclidine responses (Figure 2, bottom panel); however, this was seen in only two out of nine rats. The analysis of the 5-HT concentrations in these two rats did not reveal any differences in the level of 5-HT depletion in comparison with the other rats. After a saline injection, the locomotor activity levels were very low, and there was no significant difference between the lesioned group and the sham-operated group (Figure 2).

The effects of the microinjection of 5,7-DHT on the startle response, habituation and prepulse inhibition

The startle amplitude in the pulse-alone trials and the habituation of the rats were not different between the mPFC-lesioned rats compared to the sham-operated controls (Figure 3). An ANOVA revealed that there was no significant main effect of group or of the habituation x group interaction. Figure 4 appeared to suggest that the mPFC-lesioned rats showed an increase in prepulse inhibition at PP2 and PP4 compared to the sham-operated controls; however, an ANOVA indicated that there was no significant main effect of group or of the prepulse x group interaction.

DISCUSSION

The behavioural assessment of rats with serotonergic lesions of the mPFC, using the locomotor hyperactivity and prepulse inhibition paradigms, revealed that there were no differences between the lesioned and control groups. The present findings suggest that normal regulation of locomotor activity and prepulse inhibition is independent of serotonin release from terminals in the mPFC.

Serotonin in the mPFC and psychotomimetic drug action

As previously reported [41], it is likely that serotonin release from terminals in the dorsal hippocampus has an inhibitory effect on glutamatergic projections to the core of the nucleus accumbens. Disruption of this inhibition may lead to increased glutamatergic transmission in the nucleus accumbens and enhancement of phencyclidine-induced hyperlocomotion. In addition, enhancement of glutamatergic transmission has been shown to have an opposite effect on amphetamine-induced hyperlocomotion [41].

It has been shown that phencyclidine enhances glutamate release in the prefrontal cortex to compensate for the blockade of NMDA receptors, which leads to the overstimulation of postsynaptic non-NMDA glutamate receptors [60, 61]. Additionally, the acute administration of phencyclidine promotes dopamine release in the prefrontal cortex [62]. It has been reported that group II metabotropic glutamate receptor agonists and non-NMDA receptor antagonists diminish phencyclidine-induced hyperlocomotion by preventing the responses of pyramidal cells of the rat mPFC [60, 61]. We suggest that serotonin depletion in the mPFC does not influence phencyclidine-induced dopamine or glutamate release in this brain region. Furthermore, our results suggest that glutamatergic transmission in the nucleus accumbens is not altered after the manipulation of serotonin release in the mPFC. We postulate that the effect of en-

hanced glutamatergic transmission on the amphetamine response depends on the balance of NMDA and non-NMDA receptor activation interacting with dopamine D_1 and D_2 receptors. Both NMDA and non-NMDA receptors in the nucleus accumbens are located at the presynaptic level on glutamatergic and dopaminergic terminals arising from the cortex, the hippocampus and the midbrain, respectively (for a review see [63]). Our results suggest that serotonin depletion in the mPFC does not influence either dopaminergic or glutamatergic transmission within the nucleus accumbens.

Serotonin in the mPFC and prepulse inhibition

Prepulse inhibition is thought to be mediated by a prefrontocortico-limbic-striato-pallidal circuit in which the mPFC plays an important role [64]. Manipulations that decrease dopamine levels in the mPFC disrupt prepulse inhibition [53, 54], presumably by disinhibition of the descending glutamatergic projections [64]. The mPFC sends direct glutamatergic projections to the nucleus accumbens and the ventral tegmental area (VTA) [65], from which dopaminergic projections ascend to the nucleus accumbens. Stimulation of the mPFC increases dopamine release in the nucleus accumbens, probably via the VTA [66, 67]. It is therefore possible that disinhibition of the mPFC glutamatergic output to the VTA increases dopamine release in the nucleus accumbens and thereby reduces prepulse inhibition [68]. Our results suggest that serotonin depletion in the mPFC does not alter mPFC output neurons to either the VTA or the nucleus accumbens, thus having no effect on sensorimotor gating.

In conclusion, serotonin depletion in the mPFC does not lead to the dysregulation of subcortical dopaminergic activity and does not cause aberrant responses to environmental stimuli. It is therefore clear that the behavioural effects of raphe lesions described in our initial studies [69, 70] are not mediated by serotonin depletion in the mPFC.

REFERENCES

1. Awad, A.G. and L.N. Voruganti, Impact of atypical antipsychotics on quality of life in patients with schizophrenia. CNS Drugs, 2004. 18(13): p. 877-893.
2. Harrison, P.J., The neuropathology of schizophrenia. Brain, 1999. 122: p. 593-624.
3. Carlsson, A. and M. Lindqvist, Effect of chlorpromazine or haloperidol on formation of 3-methoxytyramine and normetanephrine in mouse brain. Acta Pharmacol Toxicol, 1963. 20: p. 140-144.
4. Josselyn, S.A., R. Miller, and R.J. Beninger, Behavioral effects of clozapine and dopamine receptor subtypes. Neurosci Biobehav Rev, 1997. 21(5): p. 531-558.
5. Peroutka, S.J. and S.H. Synder, Relationship of neuroleptic drug effects at brain dopamine, serotonin, alpha-adrenergic, and histamine receptors to clinical potency. Am J Psychiatry, 1980. 137(12): p. 1518-1522.
6. Bymaster, F., et al., Olanzapine: a basic science update. Br J Psychiatry Suppl, 1999(37): p. 36-40.
7. Carlsson, A., N. Waters, and M.L. Carlsson, Neurotransmitter interactions in schizophrenia--therapeutic implications. Biol Psychiatry, 1999. 46(10): p. 1388-1395.
8. Weiner, D.M., et al., 5-hydroxytryptamine2A receptor inverse agonists as antipsychotics. J Pharmacol Exp Ther, 2001. 299(1): p. 268-276.
9. Costall, B. and R.J. Naylor, Serotonin and psychiatric disorders. A key to new therapeutic approaches. Arzneimittelforschung, 1992. 42(2A): p. 246-249.
10. Meston, C.M. and B.B. Gorzalka, Psychoactive drugs and human sexual behavior: the role of serotonergic activity. J Psychoactive Drugs, 1992. 24(1): p. 1-40.
11. Schlundt, D.G., et al., A sequential behavioral analysis of craving sweets in obese women. Addict Behav, 1993. 18(1): p. 67-80.
12. Azmitia, E.C. and P.M. Whitaker-Azmitia, Anatomy, cell biology, and plasticity of the serotonergic system. Neuropsychopharmacological implications for the actions of psychotropic drugs, in Psychopharmacology: the fourth generation of progress, F.E. Bloom and D.J. Kupfer, Editors. 1995, Raven Press: New York. p. 443-449.
13. Hornung, J.P., The human raphe nuclei and the serotonergic system. J Chem Neuroanat, 2003. 26(4): p. 331-343.
14. Adell, A. and R.D. Myers, Selective destruction of midbrain raphe nuclei by 5,7-DHT: is brain 5-HT involved in alcohol drinking in Sprague-Dawley rats? Brain Res, 1995. 693(1-2): p. 70-79.
15. McQuade, R. and T. Sharp, Functional mapping of dorsal and median raphe 5-hydroxytryptamine pathways in forebrain of the rat using microdialysis. J Neurochem, 1997. 69(2): p. 791-796.
16. Mokler, D.J., et al., Serotonin neuronal release from dorsal hippocampus following electrical stimulation of the dorsal and median raphe nuclei in conscious rats. Hippocampus, 1998. 8(3): p. 262-273.
17. Thomas, H., et al., Lesion of the median raphe nucleus: a combined behavioral and microdialysis study in rats. Pharmacol Biochem Behav, 2000. 65(1): p. 15-21.
18. Abi-Dargham, A., et al., The role of serotonin in the pathophysiology and treatment of schizophrenia. J Neuropsych Clin Neurosci, 1997. 9(1): p. 1-17.
19. Kapur, S. and G. Remington, Serotonin-dopamine interaction and its relevance to schizophrenia. Am J Psychiatry, 1996. 153(4): p. 466-476.
20. Geyer, M.A. and A. Markou, Animal models of psychiatric disorders, in Psychopharmacology: the fourth generation of progress, F. Bloom and D. Kupfer, Editors. 1995, Raven Press: New York. p. 787-798.
21. Koch, M., Can animal models help to understand human diseases? Commentary on Swerdlow et al., 'Animal models of deficient sensorimotor gating: what we know, what we think we know, and what we hope to know soon'. Behav Pharmacol, 2000. 11(3-4): p. 205-207.
22. Matthysse, S., Animal models in psychiatric research. Prog Brain Res, 1986. 65: p. 259-270.

23. Ellenbroek, B.A., Pre-attentive processing and schizophrenia: animal studies. Psychopharmacology (Berl), 2004. 174(1): p. 65-74.
24. Ellenbroek, B.A. and A.R. Cools, Animal models with construct validity for schizophrenia. Behav Pharmacol, 1990. 1(6): p. 469-490.
25. Ellenbroek, B.A. and A.R. Cools, Animal models for the negative symptoms of schizophrenia. Behav Pharmacol, 2000. 11(3-4): p. 223-233.
26. Seiden, L.S., K.E. Sabol, and G.A. Ricaurte, Amphetamine: effects on catecholamine systems and behavior. Annu Rev Pharmacol Toxicol, 1993. 33: p. 639-677.
27. Kelly, P.H., P.W. Seviour, and S.D. Iversen, Amphetamine and apomorphine responses in the rat following 6-OHDA lesions of the nucleus accumbens septi and corpus striatum. Brain Res, 1975. 94(3): p. 507-522.
28. Contreras, P.C., et al., Phencyclidine. Physiological actions, interactions with excitatory amino acids and endogenous ligands. Mol Neurobiol, 1987. 1(3): p. 191-211.
29. Javitt, D.C. and S.R. Zukin, Recent advances in the phencyclidine model of schizophrenia. Am J Psychiatry, 1991. 148(10): p. 1301-1308.
30. Pradhan, S.N., Phencyclidine (PCP): some human studies. Neurosci Biobehav Rev, 1984. 8(4): p. 493-501.
31. Geyer, M.A., et al., Startle response models of sensorimotor gating and habituation deficits in schizophrenia. Brain Res Bull, 1990. 25(3): p. 485-498.
32. Swerdlow, N.R., et al., Seroquel, clozapine and chlorpromazine restore sensorimotor gating in ketamine-treated rats. Psychopharmacology (Berl), 1998. 140(1): p. 75-80.
33. Mansbach, R.S., M.A. Geyer, and D.L. Braff, Dopaminergic stimulation disrupts sensorimotor gating in the rat. Psychopharmacology (Berl), 1988. 94(4): p. 507-514.
34. Swerdlow, N.R., D.L. Braff, and M.A. Geyer, GABAergic projection from nucleus accumbens to ventral pallidum mediates dopamine-induced sensorimotor gating deficits of acoustic startle in rats. Brain Res, 1990. 532(1-2): p. 146-150.
35. Wan, F.J., M.A. Geyer, and N.R. Swerdlow, Presynaptic dopamine-glutamate interactions in the nucleus accumbens regulate sensorimotor gating. Psychopharmacology (Berl), 1995. 120(4): p. 433-441.
36. Mansbach, R.S., D.L. Braff, and M.A. Geyer, Prepulse inhibition of the acoustic startle response is disrupted by N-ethyl-3,4-methylenedioxyamphetamine (MDEA) in the rat. Eur J Pharmacol, 1989. 167(1): p. 49-55.
37. Rigdon, G.C. and J.K. Weatherspoon, 5-Hydroxytryptamine 1a receptor agonists block prepulse inhibition of acoustic startle reflex. J Pharmacol Exp Ther, 1992. 263(2): p. 486-493.
38. Sipes, T.A. and M.A. Geyer, Multiple serotonin receptor subtypes modulate prepulse inhibition of the startle response in rats. Neuropharmacology, 1994. 33(3-4): p. 441-448.
39. Mansbach, R.S. and M.A. Geyer, Effects of phencyclidine and phencyclidine biologs on sensorimotor gating in the rat. Neuropsychopharmacology, 1989. 2(4): p. 299-308.
40. Braff, D. and M. Geyer, Sensorimotor gating and the neurobiology of schizophrenia: human and animal model studies, in Schizophrenia: Scientific Progress, S. Schulz and C. Tamminga, Editors. 1989, Oxford University Press: Oxford. p. 124-137.
41. Kusljic, S. and M. van den Buuse, Functional dissociation between serotonergic pathways in dorsal and ventral hippocampus in psychotomimetic drug-induced locomotor hyperactivity and prepulse inhibition in rats. Eur J Neurosci, 2004. 20(12): p. 3424-3432.
42. Kusljic, S. and M. van den Buuse, Differential involvement of 5-HT projections within the amygdala in prepulse inhibition but not in psychotomimetic drug-induced hyperlocomotion. Behav Brain Res, 2006. 168(1): p. 74-82.
43. Heidbreder, C.A. and H.J. Groenewegen, The medial prefrontal cortex in the rat: evidence for a dorso-ventral distinction based upon functional and anatomical characteristics. Neurosci Biobehav Rev, 2003. 27(6): p. 555-579.
44. Drevets, W.C., et al., Subgenual prefrontal cortex abnormalities in mood disorders. Nature, 1997. 386(6627): p. 824-827.
45. Mayberg, H.S., et al., Reciprocal limbic-cortical function and negative mood: converging PET findings in depression and normal sadness. Am J Psychiatry, 1999. 156(5): p. 675-682.
46. Kolb, B., Functions of the frontal cortex of the rat: a comparative review. Brain Res, 1984. 320(1): p. 65-98.
47. Vertes, R.P., Differential projections of the infralimbic and prelimbic cortex in the rat. Synapse, 2004. 51(1): p. 32-58.
48. Hajos, M., et al., In vivo inhibition of neuronal activity in the rat ventromedial prefrontal cortex by midbrain-raphe nuclei: role of 5-HT1A receptors. Neuropharmacology, 2003. 45(1): p. 72-81.
49. Grace, A.A., Phasic versus tonic dopamine release and the modulation of dopamine system responsivity: a hypothesis for the etiology of schizophrenia. Neuroscience, 1991. 41(1): p. 1-24.
50. Laruelle, M., et al., Selective abnormalities of prefrontal serotonergic receptors in schizophrenia. A postmortem study. Arch Gen Psychiatry, 1993. 50(10): p. 810-818.
51. Weinberger, D.R., K.F. Berman, and R.F. Zec, Physiologic dysfunction of dorsolateral prefrontal cortex in schizophrenia. I. Regional cerebral blood flow evidence. Arch Gen Psychiatry, 1986. 43(2): p. 114-124.
52. Weinberger, D.R. and B.K. Lipska, Cortical maldevelopment, anti-psychotic drugs, and schizophrenia: a search for common ground. Schizophrenia Res, 1995. 16(2): p. 87-110.
53. Ellenbroek, B.A., S. Budde, and A.R. Cools, Prepulse inhibition and latent inhibition: the role of dopamine in the medial prefrontal cortex. Neuroscience, 1996. 75(2): p. 535-542.
54. Koch, M. and M. Bubser, Deficient sensorimotor gating after 6-hydroxydopamine lesion of the rat medial prefrontal cortex is reversed by haloperidol. Eur J Neurosci, 1994. 6(12): p. 1837-1845.

55. Lacroix, L., et al., Effects of local infusions of dopaminergic drugs into the medial prefrontal cortex of rats on latent inhibition, prepulse inhibition and amphetamine induced activity. Behav Brain Res, 2000. 107(1-2): p. 111-121.
56. Jonsson, G., Chemical neurotoxins as denervation tools in neurobiology. Ann. Rev. Neurosci., 1980. 3: p. 169-187.
57. Paxinos, G. and C. Watson, The rat brain in stereotaxic co-ordinates, 5th edition. 5th ed. 2005, New York: Elsevier Academic press.
58. Van den Buuse, M., Deficient prepulse inhibition of acoustic startle in Hooded-Wistar rats compared with Sprague-Dawley rats. Clin Exp Pharmacol Physiol, 2003. 30: p. 254-261.
59. Gispen, W.H., P. Schotman, and E.R. De Kloet, Brain RNA and hypophysectomy: a topographical study. Neuroendocrinology, 1972. 9: p. 285-296.
60. Moghaddam, B., et al., Activation of glutamatergic neurotransmission by ketamine: a novel step in the pathway from NMDA receptor blockade to dopaminergic and cognitive disruptions associated with the prefrontal cortex. J Neurosci, 1997. 17(8): p. 2921-2927.
61. Moghaddam, B. and B.W. Adams, Reversal of phencyclidine effects by a group II metabotropic glutamate receptor agonist in rats. Science, 1998. 281(5381): p. 1349-1352.
62. Jentsch, J.D., et al., Alpha-noradrenergic receptor modulation of the phencyclidine- and delta9-tetrahydrocannabinol-induced increases in dopamine utilization in rat prefrontal cortex. Synapse, 1998. 28(1): p. 21-26.
63. Tarazi, F.I. and R.J. Baldessarini, Regional localization of dopamine and ionotropic glutamate receptor subtypes in striatolimbic brain regions. J Neurosci Res, 1999. 55(4): p. 401-410.
64. Swerdlow, N.R., M.A. Geyer, and D.L. Braff, Neural circuit regulation of prepulse inhibition of startle in the rat: current knowledge and future challenges. Psychopharmacology (Berl), 2001. 156(2-3): p. 194-215.
65. Sesack, S.R. and V.M. Pickel, Prefrontal cortical efferents in the rat synapse on unlabeled neuronal targets of catecholamine terminals in the nucleus accumbens septi and on dopamine neurons in the ventral tegmental area. J Comp Neurol, 1992. 320(2): p. 145-160.
66. Karreman, M. and B. Moghaddam, The prefrontal cortex regulates the basal release of dopamine in the limbic striatum: an effect mediated by ventral tegmental area. J Neurochem, 1996. 66(2): p. 589-598.
67. Taber, M.T., S. Das, and H.C. Fibiger, Cortical regulation of subcortical dopamine release: mediation via the ventral tegmental area. J Neurochem, 1995. 65(3): p. 1407-1410.
68. Koch, M., The neurobiology of startle. Prog Neurobiol, 1999. 59(2): p. 107-128.
69. Kusljic, S., et al., Brain serotonin depletion by lesions of the median raphe nucleus enhances the psychotomimetic action of phencyclidine, but not dizocilpine (MK-801), in rats. Brain Res, 2005. 1049(2): p. 217-226.
70. Kusljic, S., D.L. Copolov, and M. van den Buuse, Differential role of serotonergic projections arising from the dorsal and median raphe nuclei in locomotor hyperactivity and prepulse inhibition. Neuropsychopharmacology, 2003. 28(12): p. 2138-2147.

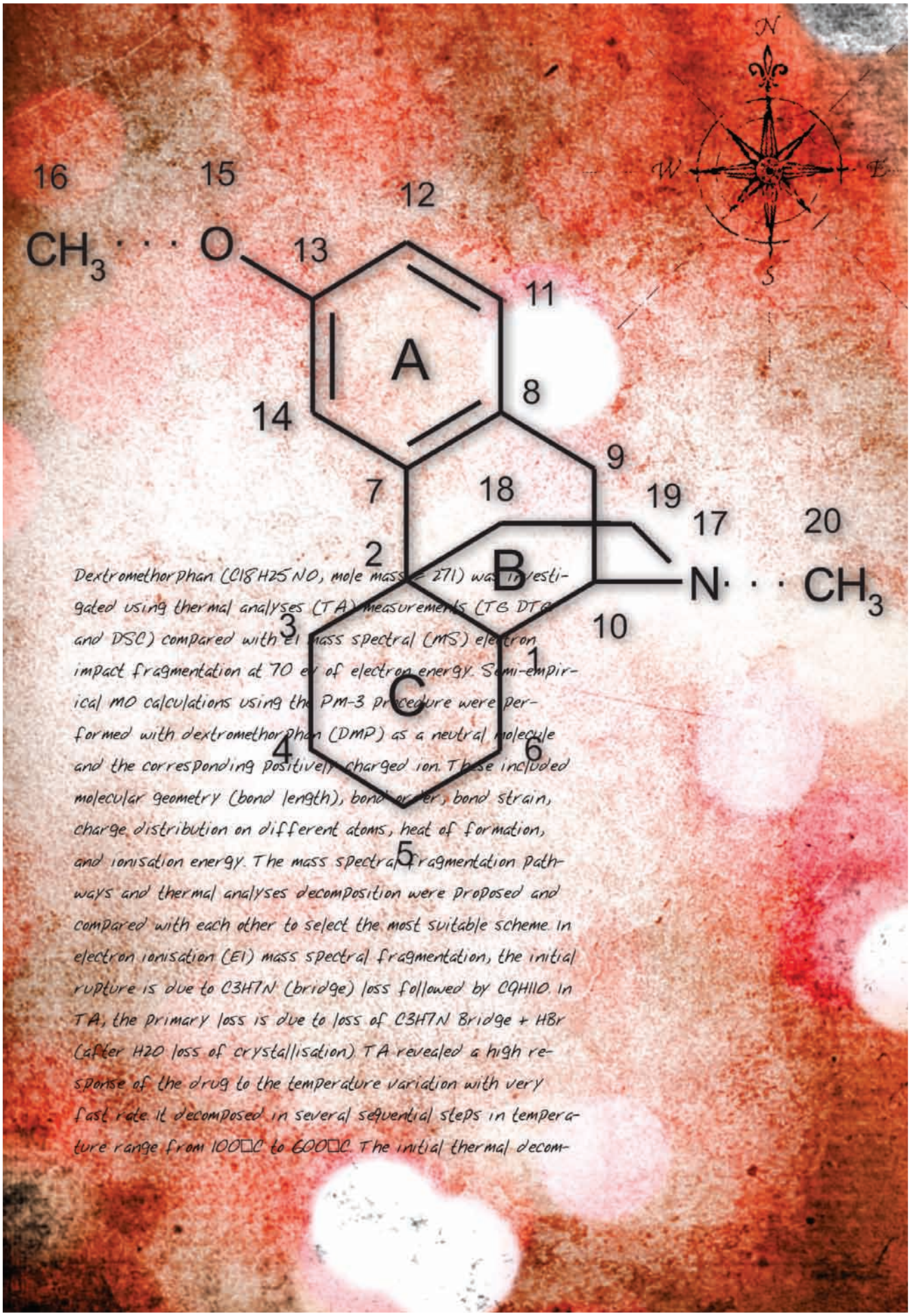

Dextromethorphan ($C_{18}H_{25}NO$, mole mass = 271) was investigated using thermal analyses (TA) measurements (TG DTG and DSC) compared with el mass spectral (MS) electron impact fragmentation at 70 ev of electron energy. Semi-empirical MO calculations using the PM-3 procedure were performed with dextromethorphan (DMP) as a neutral molecule and the corresponding positively charged ion. These included molecular geometry (bond length), bond order, bond strain, charge distribution on different atoms, heat of formation, and ionisation energy. The mass spectral fragmentation pathways and thermal analyses decomposition were proposed and compared with each other to select the most suitable scheme. In electron ionisation (EI) mass spectral fragmentation, the initial rupture is due to C_3H_7N (bridge) loss followed by $C_9H_{11}O$. In TA, the primary loss is due to loss of C_3H_7N Bridge + HBr (after H_2O loss of crystallisation). TA revealed a high response of the drug to the temperature variation with very fast rate. It decomposed in several sequential steps in temperature range from 100□C to 600□C. The initial thermal decom-

STRUCTURAL INVESTIGATION OF DEXTROMETHORPHAN USING MASS SPECTROMETRY AND THERMAL ANALYSES COMBINED WITH MO CALCULATIONS

M.A. Zayed[*1] , M.A. Fahmey [2], M.F. Hawash[2], S.A.M. Abdallah[3]
[1] Chemistry Department, Faculty of Science, Cairo University, 12316 Giza, Egypt.
[2] Nuclear Physics Dept., N.R.C., Atomic Energy Authority 13759, Cairo, Egypt.
[3] University of Workers, 10 Aswan, A.R. Egypt

Received / Primljen: 10. 03. 2011. Accepted / Prihvaćen: 07. 04. 2011.

ABSTRACT

($C_{18}H_{25}NO$, mole mass = 271) was investigated using thermal analyses (TA) measurements (TG/DTG and DSC) compared with EI mass spectral (MS) electron impact fragmentation at 70 eV of electron energy. Semi-empirical MO calculations using the PM-3 procedure were performed with dextromethorphan (DMP) as a neutral molecule and the corresponding positively charged ion. These included molecular geometry (bond length), bond order, bond strain, charge distribution on different atoms, heat of formation, and ionisation energy. The mass spectral fragmentation pathways and thermal analyses decomposition were proposed and compared with each other to select the most suitable scheme. In electron ionisation (EI) mass spectral fragmentation, the initial rupture is due to C_3H_7N (bridge) loss followed by $C_9H_{11}O$. In TA, the primary loss is due to loss of C_3H_7N Bridge + HBr (after H_2O loss of crystallisation). TA revealed a high response of the drug to the temperature variation with very fast rate. It decomposed in several sequential steps in temperature range from 100°C to 600°C. The initial thermal decomposition was similar to that obtained using MS. So, it is possible to select the proper pathway using both techniques. This comparison was successfully confirmed by MO calculation. The structural-reactivity effect on metabolism and the biological effect compared with codeine are discussed.

Keywords: *Dextromethorphan structure, Mass Spectrometry, Thermal analyses, MO calculation*

INTRODUCTION

Dextromethorphan (DMP, methoxy-methyl morphinan) is an antitussive agent used in many nonprescription cough and cold medications [1]. DM has an IUPAC name (+)-3-methoxy-17-methyl-(9α, 13α, 14α)- morphinan ($C_{18}H_{25}NO$, m/z=271) and is a synthetic product that is chemically related to codeine [2]. The drug is a safe, oral antitussive that is widely available [3 – 6]. The structural formula and numbering system of the drug is given in Fig. 1.

A number of methods have been reported to measure DM in biological fluids, including high-performance liquid chromatography (HPLC) [7, 8], gas chromatography (GC) [9, 10] and gas chromatography–mass spectrometry (GC–MS) [11-14, 1]. The latter technique is highly sensitive [5].

Rapid advances in biological sciences have led to an increased demand for chemical and structural information from biological systems. Mass spectrometry plays a pivotal role in the structural characterisation of biological molecules [15]. The technique is important because it provides a substantial amount of structural information using a small amount of sample. Moreover, the techniques offer comparative advantages in speed and productivity for pharmaceutical analysis [16]. In contrast, thermal analysis delivers extremely sensitive measurements of heat change, which can be applied on a broad scale with pharmaceutical development. These methods provide unique information relating to thermodynamic data of the system studied [17]. The increasing use of the combined techniques in TA could provide more specific information and thus facilities a more rapid interpretation of the curves obtained [17].

In the electron ionisation (EI) mass spectra, the fragmentation consists of competitive and consecutive unimolecular fragmentation [18]. The fragmentation of the ionised molecule depends mainly on their internal energy [19]. The thermo-gravimetric TG/DTG analysis provides quantitative information on weight losses due to decomposition and/or evaporation of low molecular weight fragments as a function of time and temperature. In conjunction with mass spectrometric analysis [20-22], the nature of the released fragments

UDK 615.233.074 / Ser J Exp Clin Res 2011; 12 (1): 21-28

Correspondence to: mazayed429@yahoo.com, Tel: 00202-22728437, 002-010577665.

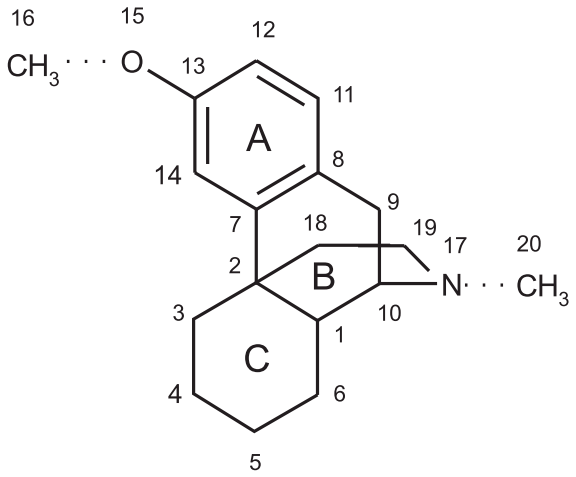

Dextromethorphan drug (DMP)

Figure 1. Structure and numbering system of DMP for, C, N and O skelton.

may be deduced, thus greatly facilitating the interpretation of thermal degradation processes. In contrast, the computational quantum chemistry could provide additional information about the atoms and bonds, which could be used successfully in an interpretation of experimental results [23]. The application of the computational quantum chemistry in addition to experimental results (MS and TA) gives valuable information about the atoms and bonds, which helps in the description and prediction of the primary fragmentation site of cleavage and subsequent ones [24-28].

Although the literature is wealthy in information related to the biological activities of DMP and its metabolites *in vivo* and *in vitro* [3-6], there seems to be a lack of any correlation between chemical behaviour and its electronic structure.

The main aim of this work was to perform an experimental and theoretical investigation of DM using thermal analyses (TA) and EI mass spectral (MS) fragmentation at 70 eV. In addition, MO calculations were performed using the PM3 procedure on the neutral molecule and charged molecule to investigate geometrical parameters (bond length, bond order, bond strain, heats of formation ionisation energy) and charge distribution.

The calculations correlated the experimental results [TA and MS] to obtained information regarding the stability of the drug and the prediction of the site of primary fragmentation and subsequent ones. This study could be helpful in establishing a quantitative and qualitative structure–activity relationship for the drug, which is the main objective of this work. It is worth mentioning that there is scant literature concerning such a comparative study.

Moreover, the authors tried to correlate and discuss the structure reactivity and relationship between DM and Codeine [26], which are chemically related to each other [2] and which affect the O and OH on MS and TA and MO parameters. In addition, they attempted to find the metabolite structures in the mass spectrum and correlated the biological behaviour of the two drugs.

EXPERIMENTAL

Mass spectrometry (MS)

The electron ionisation (EI) mass spectrum of DMP was obtained using a Shimadzu GC-MS-Qp 1000 PX quadruple mass spectrometer with an electron multiplier detector equipped with the GC-MS data system. The direct probe for solid material was used in this study. The sample was put into a glass sample micro vial by a needle (≃ 1 µg max). The vial was installed on the tip of the DP containing the heating cable and was inserted into the evacuated ion source. The sample was ionised by an electron beam emitted from the filament with the generated ions being effectively introduced into the analyser by the focusing and extractor lens systems. The MS was continuously scanned, and the spectra obtained were stored. The electron ionisation mass spectra were obtained at an ionising energy value of 70 eV, ionisation current of 60 µA and a vacuum greater than 10^{-6} torr.

Thermal analysis (TA)

The thermal analyses of DMP were made using a conventional thermal analyser (Shimadzu system of DTA-50 and 30 series TG-50). The mass loss for 5 mg of sample and the heat response to changes in the sample were measured from room temperature up to 600°C. The heating rate in an inert argon atmosphere was 10°C min^{-1}. These instruments were calibrated using indium metal as a thermal stable material. The reproducibility of the instrument reading was determined by repeating each experiment more than twice.

Quantum chemical calculations

The MO calculations were performed using a semi-empirical molecular orbital calculation. The method used in these computations was the parametric PM-3 method described by Stewart [29]. The geometry of all stable species studied was completely optimised with respect to all geometrical variables using the Eigen vector following (EF) routine [30]. The program was run under the molecular orbital calculation package MOPAC2000 by Stewart [31] for microcomputers.

RESULTS AND DISCUSSION

The chemistry and reactivity of pharmaceutical drugs are of great interest because of their importance in treating various diseases. Knowledge of the thermal decomposition mechanism of the drug is very important to understand the chemical processes in biological systems. It is difficult to establish the exact major fragmentation pathway in EI using conventional MS. However, the combination of experimental techniques (TA and MS) and MO calculation is very important to understand the following topics:

1 -The primary site fragmentation process and its major fragmentation pathways in both techniques.
2 -The stability of the drug as a neutral molecule in the solid-state phase and molecular ion in the gas phase.
3 -Selection of the most probable decomposition pathway in both TA and MS.

Thermal analysis (TA)

The TG/DTA curves of DMP (Fig. 2) were displayed between 25°C and 600°C. The drug has the general formula $C_{18}H_{25}NO.HBr.H_2O$ in solid-state phase with a molecular weight (MW) of 370.3 and melting point (m.p.) ≅ 125 °C.

It is clear from the thermal survey of the drug that there are four mass losses in the TGA (Table 1). The first one appeared at 100-150°C with a mass loss % of 4.1, which may be attributed to the loss of water present in the drug (cal. mass loss % = 4.8). The second mass loss was approximately 32.5% and occurred at 150-350°C. The third one was 54.57% and occurred at 350-450°C. The final one was 5.68% and occurred at 450-600°C, which may be attributed to the loss of the remainder. These mass losses were observed at the three main peaks at values: 120.8°C, 287.2°C and 378.6°C in DTG, respectively. These mass losses also appeared as two endothermic peaks in the DTA. The first one appeared at 110.77°C, requiring an energy E_1= +242.6 J/g, and the second one appeared at 362°C, requiring an energy E_2 = + 356.75 J/g. The fragmentation of this compound and its chemical changes occurring after this thermal degradation appeared at 555.56°C as a very strong exothermic peak requiring an energy E_3 = 513.5 J/g.

Mass spectral behaviour of dextromethorphan (MS)

The electron impact (EI) mass spectrum for DMP drug at 70 eV was recorded and investigated. A typical mass spectrum (barograph) of the drug is shown in Fig. 3.

Scheme 1 shows the proposed principal fragmentation pathways of DMP following electron impact at 70 eV. In addition, prominent ions and their relative intensities with some common ions formed from codeine [26] are listed

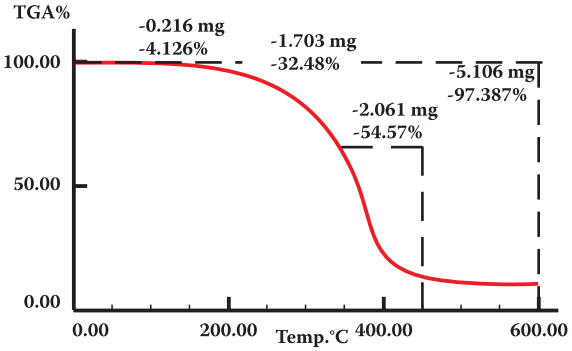

Fig.2a : TGA curve of Dextromethorphan Hydrobromide

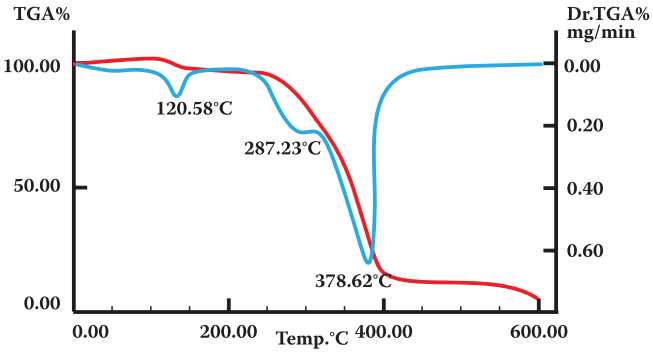

Fig.2b : Dr.TGA of Dextromethorphan Hydrobromide

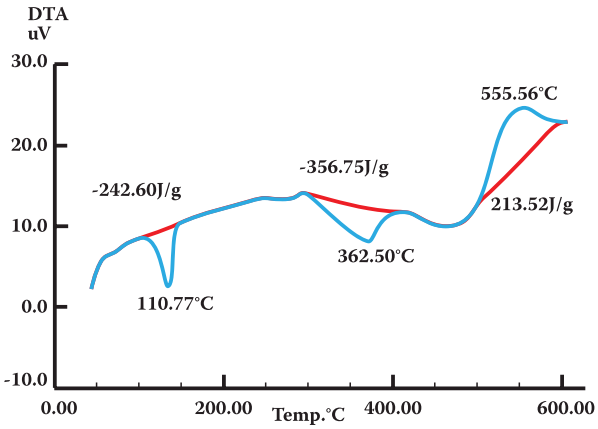

Fig 2 C: DTA of Dextromethorphan Hydrobromide

Table 1: Structure identification of Dextromethorphan Hydrobromide

TGA		DTA		
Wt. loss%	Temp.range °C	Peak temp. °C	Descripion	E J/g
4.10	100-150	118.77	Endothermic	+242.6
32.50	150-350	367.6	endothermic	+365.75
54.57	350-450	555.56	St.exothermic peak	-613.5
5.68 ΣWt.loss %=96.85	450-600			

*Dr. TGA gives three main peaks temperatures at 120.58, 287.23 and 378.62 oC.

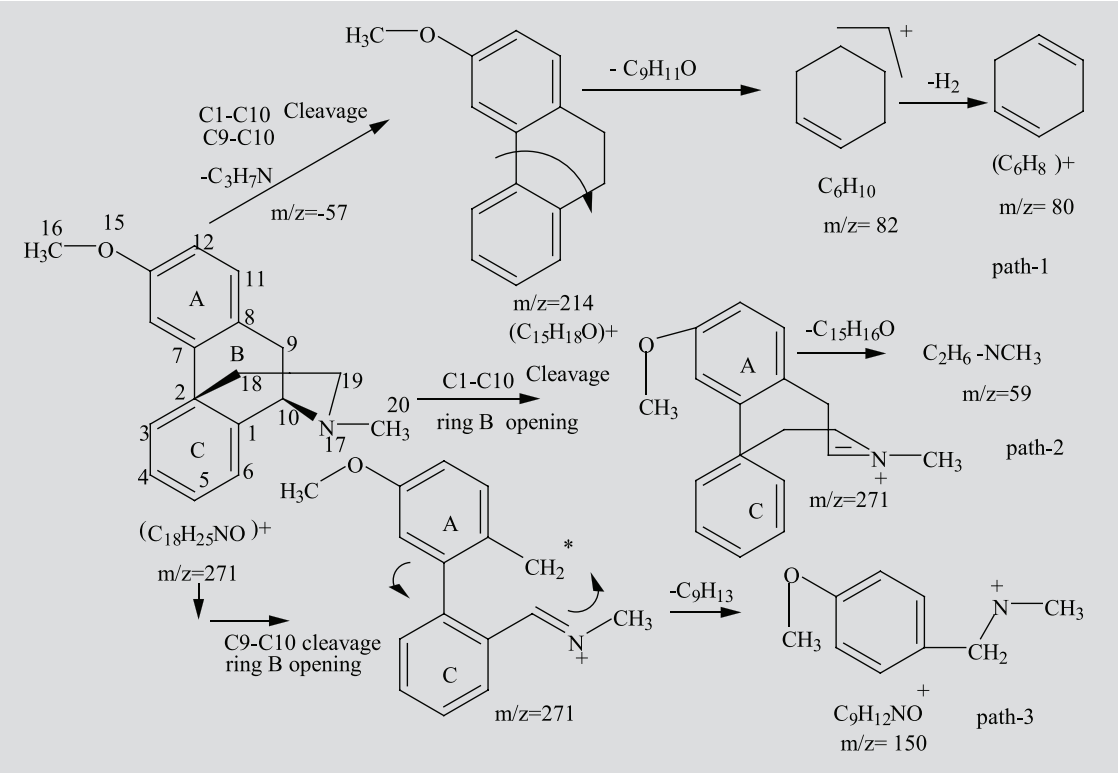

Scheme (1): Mass spectral fargmentation pathways of Dextromethorphan

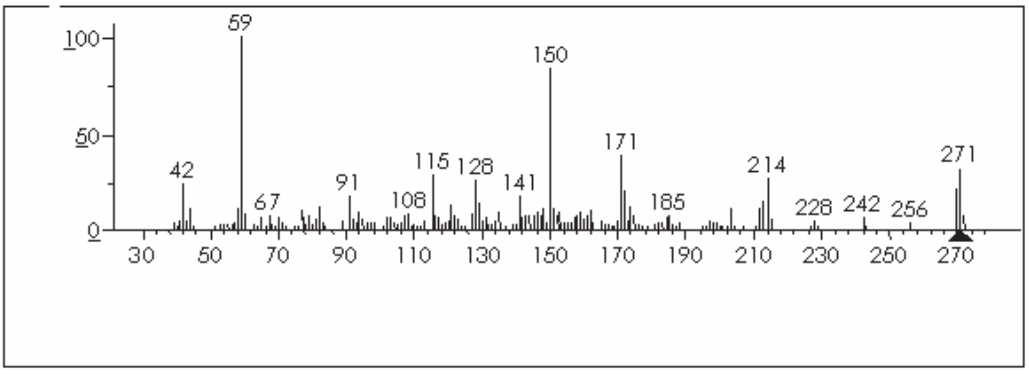

Fig. (3): Mass spectrum of DMP at 70 eV.

Dextromethorphan				Codeine		
m/z	R.I.	Structure	Process	m/z	Process	R.I.
271	31.6	$C_{18}H_{25}NO^+$	M^+	299	M^+	100%
270	20.3	$C_{18}H_{24}NO^+$	$[M-1]^+$	298	$[M-1]^+$	14.3
214	26.6	$C_{15}H_{18}O^+$	$[M-C_3H_7N]^+$	242	$[M-C_3H_7N^+]$	9.3
150	83.0	$C_9H_{12}NO^+$	$[M-C_9H_{13}]^+$			
82	12.5	$C_6H_{10}^+$	$[M-C_3H_7N-C_9H_8O]^+$			
59	100%	$C_3H_9N^+$	$[M-C_{15}H_{16}O]^+$			

Table 2: The prominent ions in the mass spectrum of DMP drug in comparison with codeine drug [26].

in Table 2. The mass spectrum of DMP showed that the molecular ion ($C_{18}H_{25}NO+$, m/z = 271) signal represented approximately 30% of the base peak (= 100%) at m/z = 59 [C3H9N$^+$], indicating a moderate stability of the molecular ion in gas phase compared with codeine [26].

The main fragmentation pathway for DMP after ionisation at 8.83 eV consists of three principal pathways (paths 1-3) as rationalised in scheme 1. The formation of the fragment ion at signal m/z = 214 (path 1, scheme 1) with R.I. = 26.6% is mainly due to the formation of $[M\text{-}C_3H_7N]^+$ as a loss of the C_3H_7N bridge by disruption of the C_2–C_{18} and C_{10}–C_{17} bonds. It is worth mentioning that this fragment ion, $C_{15}H_{18}O+$ ($M\text{-}C_3H_7$), was formed directly from the molecular ion. This formation was confirmed by the full scan positive ion mass spectrum using tandem mass spectrometry (MS/MS) [6] as a prominent peak. Subsequent cleavage of the C_7–C_2 and C_1–C_{10} bonds (ring B) occurred forming the $C_6H_{10}^+$ fragment ion (m/z = 82, R.I. = 12.5%) (path 1 scheme 1).

Two important possible modes of fragmentation (paths 2 and 3 scheme 1) are due to the cleavage of the two bonds ß to the nitrogen atom (i.e., cleavage of C_1–C_{10} and C_9–C_{10} competitively forming two important fragment ions in the mass spectrum.) First, cleavage of the C_1–C_{10} bond and formation of the most prominent fragment (the base peak) at m/z = 59 (path 2) of formula C_3H_9N. Also, cleavage of the C_9–C_{10} bond formed the second prominent peak at m/z = 150 (R.I. = 83.0%) with the structure $C_9H_{12}NO$ (path 3).

Structural determinations for the compounds of unknown structure are generally based upon information obtained through the use of a variety of modern instruments. The instrumental methods usually include mass spectrometric studies, and the techniques are well known to organic chemists and scientists [32].

It is known that DMP is chemically related to codeine [2] but that it differs in biological effect. DMP is an antitussive agent used in many nonprescription cough and cold medications [1]. Codeine has an analgesic effect [26]. Biotransformation (metabolites) *in vivo* and *in vitro* of the two drugs has been investigated by many investigators [3–6]. Metabolism studies often lead to compounds with unknown structures that are related to the material under study. The chemical structure and metabolic pathway of DMP were rationalised [5] in Fig. 3.

The metabolism of DMP is primarily by o-demethylation to dextrophan. DMP is also metabolised to 3-methoxymorphinan and 3-hydroxymorphinan.

It was noted that from mass spectrum of DMP, the signal due to C_2H_4 loss was observed with minor abundance m/z = 243, R.I. = 1.21, which may be due to the formation of hydroxymorphinan.

Comparing the fragmentation pathway of DMP to codeine [26], one can notice that the two drugs are similar in the initial processes (i.e., loss of the bridge C_3H_7N and the ring opening of the two bonds ßto the nitrogen atom). The subsequent fragmentation differed because of the presence of different substituent groups (O and OH).

Computation

Molecular orbital calculations gave valuable information regarding the structure and reactivity of the molecules and molecular ions. The computational data supports the experimental data. The parameters calculated using the MO calculation include geometry, bond order, bond strain, charge distribution, heat of formation and ionisation energy.

The investigation of the molecular structure of DMP with the common formula $C_{18}H_{25}NO$ was of interest in this work, and this investigation aimed to predict the weakest bond cleavage and the stability of the neutral molecule by TA and the charged molecular by MS.

Table 3 shows the comparison of computed bond length, bond order and bond strain using the PM3 method for neutral and molecular cationic forms. Table 4 shows a comparison of computed partial charges of neutral and charged species. The computations reveal some important results.

1 The charge density localised on the nitrogen atom increased from -0.076 to 0.489 from a neutral to charged atom, which reveals that the electron disruption upon ionisation at 8.83 eV occurs in the nitrogen atom. No appreciable change in the charge on the other atom was due to ionisation of the molecule.
2 C_2–C_{18} is the lowest bond order for neutral molecule (0.964) and charged cationic form (0.967).

Correlation of TA, MS and MO-calculations.

DMP is an essential cough and cold medication [1]. The drug is chemically related to codeine [2]. As indicated previously [32], a determination of initial bond cleavage is an important first step.

The scope of this investigation was restricted to a search or prediction and discerned the features of initial bond disruption during the course of fragmentation of DMP. Empirical observations indicate that the course of subsequent fragmentation is determined to a large extent by the initial bond disruption of the molecular ion in MS [34]. It is quite acceptable to say that the computational quantum chemistry can provide additional data, which can be used successfully to interpret both TA and MS experimental results. These theoretical data are particularly valuable for mass spectral scientists. These scientists study gas-phase species, which can be handled much more easily by quantum chemistry [33].

The mass spectrum of DMP in gas-phase ion revealed three competitive processes (1 – 3, scheme 1).

PM3 calculation (Table 3) revealed that C_{10}–N_{17} was the weakest bond in the charged system (weakest bond order at 0.961, large bond length = 1.484 A° and bond strain). Moreover, the weakness of this bond (C_{10}–N_{17}) was due to the presence of a lone pair on the nitrogen. Table 3 shows that the electron disruption upon ionisation occurred from the nitrogen, which increased the weak-

Bond	Bond length (Å)		Bond order		Bond strain (k Cal/mol)	
	Neutral	Ionic	Neutral	Ionic	Neutral	Ionic
C1-C2	1.541	1.542	0.965	0.970	0.206	0.189
Cl-C6	1.525	1.531	0.984	0.983	0.049	0.208
Cl-C10	1.533	1.542	0.973	0.962	0.049	0.101
C2-C3	1.548	1.547	0.969	0.971	0.457	0.639
C2-C7	1.518	1.520	0.969	0.974	0.252	0.290
C3-C4	1.519	1.519	0.993	0.996	0.034	0.071
C4-C5	1.518	1.515	0.992	0.997	0.107	0.004
C5-C6	1.526	1.522	0.987	0.992	0.174	0.095
C7-C8	1.403	1.405	1.376	1.365	0.082	0.140
C7-C14	1.395	1.393	1.424	1.442	0.084	0.097
C8-C9	1.493	1.491	0.990	0.997	0.035	0.058
C8-C11	1.396	1.397	1.409	1.401	0.044	0.047
C9-C10	1.533	1.535	0.971	0.959	0.073	0.115
C11-C12	1.388	1.387	1.429	1.444	0.007	0.003
C12-C13	1.389	1.401	1.373	1.360	0.015	0.010
C13-C14	1.400	1.405	1.371	1.351	0.012	0.015
C13-C15	1.382	1.372	1.029	1.067	0.038	0.038
C15-C16	1.406	1.409	0.987	0.980	0.008	0.009
C10-N17	1.503	1.484	0.972	0.961	0.226	0.192
C2-C18	1.545	1.547	0.964	0.967	0.118	0.178
C18-C19	1.524	1.525	0.990	0.980	0.075	0.031
N17-C20	1.480	1.450	0.997	1.013	0.057	0.063
C19-N17	1.492	1.460	0.980	0.994	0.092	0.059

Table 3: Comparison of computed bond length, bond order and bond strain (k Cal mol^{-1}) using PM3 method for neutral and molecular cation.

ness of the bond. After an easy disruption of this bond, the subsequent bond is C_2–C_{18} (bond order = 0.967, bond length = 1.54 7A° and bond strain = 0.178 K cal mol^{-1}). Disruption of these two bonds (C10–N_{17} and C_2–C_{18}) formed a fragment ion at m/z = 214 by loss C_3H_7N (bridge) from the molecular ion. The subsequent loss of $C_9H_{11}O$ (rupture of the B ring) formed the fragment ion C_6H_{10} at m/z = 82, which can lead to a loss of H_2 to form the fragment ion C_6H_8 at m/z = 80 (process 1, scheme 1). One can conclude that process 1 is the principal one for DMP, which can help to interpret TA decomposition.

The primary TA decomposition of DMP (wt loss = 4.1%) between 100 °C and 150°C was mainly due to loss of water. It was followed by a mass loss of 32.5% between 150 °C and 350°C. On the basis of the MO calculation (Table 2), C_2–C_{18} was the first bond cleavage of neutral system having the lowest bond order at 0.964 with a long bond length (1.545 °A) and large bond strain (0.118 k cal mol^{-1}) followed by C_{10}–N_{17} (bond order = 0.972, bond length = 1.503 A° and bond strain = 0.226 k cal mol^{-1}). As a result of the disruption of these two bonds, C_2–C18 and C_{10}–N_{17} lost the bridge C_3H_7N. The wt loss of 32.5% resulted from the bridge and HBr molecule (C_3H_7N + HBr). The subsequent third mass loss of 54.57% occurred at 350-450°C and may be attributed to the loss of $OCH_3C_6H_4CH_2CH_2$ (i.e., $C_9H_{11}O$) via the cleavage of the B-ring (C_2–C_7 and C_1–C_{10}).

The final mass loss of 5.68%, which occurred at temperature range 450-600°C, may be attributed to the loss of the remainder of the drug molecule. It is possible to rationalise the thermal degradation scheme 2 as follows.

The dextromethorphan (DMP-HBr) neutral compound is stable up to 150°C before being fragmented by the loss of the bridge C_3H_7N + HBr, whereas codeine fragments at 160°C [26]. In contrast, the molecular ion of DMP is RI = 30%, while the molecular ion of codeine is considered the base peak (RI = 100%). This high stability of codeine may be due to the presence of OH and O atoms in its skeleton.

This work provides further insights into utility of experimental TA and MS techniques and a theoretical investigation with MO calculation using the semi-empirical PM3 procedure on DMP. From the practical and theoretical techniques, we concluded that the primary fragmentation of DMP is initiated by the loss of C_3H_7N + HBr in

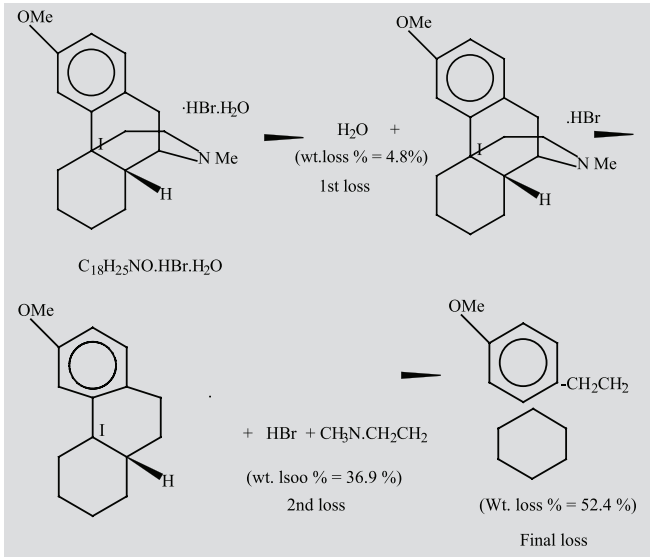

Scheme (2) : Thermal Decomposition of Dextrometharphan Hydrobromide Drug

Atom	Partial Charge	
	Neutral	cation
C1	- 0.073	- 0.072
C2	0.013	0.014
C3	- 0.107	- 0.106
C4	- 0.093	- 0.097
C5	- 0.091	- 0.096
C6	- 0.098	- 0.094
C7	- 0.019	- 0.047
C8	- 0.102	- 0.174
C9	- 0.080	- 0.050
C10	- 0.048	- 0.144
C11	- 0.073	- 0.042
C12	- 0.181	- 0.164
C13	0.087	0.124
C14	- 0.150	- 0.142
O15	- 0.189	- 0.177
C16	0.051	0.047
N17	- 0.076	0.489
C18	- 0.095	- 0.116
C19	- 0.077	- 0.169
C20	- 0.094	- 0.198

Table 4: Comparison of computed partial charge using PM3 procedure for neutral and molecular ion for DMP drug.

TA and C_3H_7N in MS. MO-calculation confirmed these processes. Subsequent cleavage in both techniques is due to the cleavage of the B ring and loss of the neutral fragment $C_9H_{11}O$. DMP can be completely dissociated between 150 and 600°C in TA, while in MS, the molecule can be fragmented after a few electron volts above the ionisation energy of 8.83 eV. Theoretical calculation can help to select the most probable fragmentation pathway in both techniques.

Signal at m/z = 243 and R.I. = 1.2% may have the structure $C_{16}H_{21}NO$ (hydroxymorphinan structure), which is the metabolite of DMP by the loss of $CH_2 + CH_2$.

Compared with codeine, we noticed the following occurrences due to the presence of O and OH atoms.

1 -DMP is less stable than codeine in TA (decomposes ≅ 10°C before codeine).
2 -The stability of the molecular ion of DMP in gas phase (MS) is about 30% compared with codeine (100%).
3 -The biological behaviour of DMP is significantly different from codeine due to the presence of two excess O-atoms in the skeleton of the latter, which may help its transport to the brain and its differential effect.

REFERENCES

1. Kim JY, Suh SI, K. Paeng In-JMK. Determination of Dextromethorphan and its Metabolite Dextrorphan in Human Hair by Gas Chromatography–Mass Spectrometry. Chromatographia 2004; 60: 703-707.
2. Intelligence Bulletin, DXM (Dextromethorphan), Product no. 2004; L0424-029.
3. Lutz U, Volkel W, Lutz RW, Lutz WK. Microbial Transformation of Dextromethorphan by Cunninghamella blakesleeana AS 3.153 J. Chromatography B 2004; 813: 217-225.
4. Arellano C, Philibert C, Dane à Yakan EN, Vachoux C, Lacombe O, Woodley J, Houin G. Validation of a liquid chromatography-mass spectrometry method to assess the metabolism of dextromethorphan in rat everted gut sacs. J. Chromatography B 2005; 819: 105-113.
5. Bagheri H, Es-haghi A, Rouini MR. Sol-gel-based solid-phase microextraction and gas chromatography-mass spectrometry determination of dextromethorphan and dextrorphan in human plasma. J. Chromatography B 2005; 818: 147-157.
6. Constanzer ML, Cavez-Eng CM, Fu I, Woolf EJ, Matuszewski BK. Determination of dextromethorphan and its metabolite dextrorphan in human urine using high performance liquid chromatography with atmospheric pressure chemical ionization tandem mass spectrometry: a study of selectivity of a tandem mass spectrometric assay. J. Chromatography B 2005; 816: 297-308.
7. Bendriss EK, Markoglou N, Wainer IW. High-performance liquid chromatography assay for simultaneous determination of dextromethorphan. J. Cromatography B 2001; 754: 2009-215.
8. Hendrickson HP, Gurley BJ, Wessinger WD. Determination of dextromethorphan and its metabolites in rat serum by liquid-liquid extraction and liquid chromatography with fluorescence detection. .J. Chromatography B 2003; 260: 261-268.

9. Salsali M, Coutts RT, Baker GB. Analysis of dextrorphan, a metabolite of dextromethorphan, using gas chromatography with electron-capture detection - role of CYP2C9, CYP2C19, CYP2D6, and CYP3A J.Pharmacol. Toxicol 1999; 41: 143-146.
10. Wu YJ, Cheng YY, Zeng S, Ma MM. Determination of dextromethorphan and its metabolite dextrorphan in human urine by capillary gas chromatography without derivatization. J. Chrpmatography B 2003; 784: 219-224.
11. Eichhold TH, Quijano M, Seibel WL, Wehmeyer KR. Highly sensitive high-performance liquid chromatographic-tandem mass spectrometric method for the analysis of dextromethorphan in human plasma. J. Chromatography B 1997; 698: 147-154.
12. Mccauley-Myers DL, Eichhold TH, Hoke II SH. Rapid bioanalytical determination of dextromethorphan in canine plasma by dilute-and-shoot preparation combined with one minute per sample LC-MS/MS analysis to optimize formulations for drug delivery. J. Pharm. Biomed. Anal. 2000; 2: 825-835.
13. Bolden RD, Hoke II SH, Eichhold TH, Wehmeyer KR. Semi-automated liquid--liquid back-extraction in a 96-well format to decrease sample preparation time for the determination of dextromethorphan and dextrorphan in human plasma. J. Chromatography B 2002; 772(1): 1-10.
14. Vengurlekar SS, Heitkamp J, McCush F, Velagaleti PR, Brisson JH, Bramer SL. A sensitive LC-MS/MS assay for the determination of dextromethorphan and metabolites in human urine--application for drug interaction studies assessing potential CYP3A and CYP2D6 inhibition. J. Pharm. Biomed. Anal. 2002; 30(1): 113-124.
15. Ed: Larson BS, Meewen CN. Mass Spectrometry of Biological Materials. Marcel Dakker, Inc, New York, Bqsel, Hong Kong 1998.
16. Kerns EH, Rourich RA, Volk KJ, Lee MS. Buspirone metabolite structure profile using a standard liquid chromatographic-mass spectrometric protocol. J. Chromatogr. B 1997; 698: 133-145.
17. Giron D, Goldbrown G. PSTT1, 1998.
18. Levsen K. Fundamental Aspects of Organic Mass Spectrometry. Verlag Chemie, Weinheim, New York 1978.
19. Bourcier S, Hoppilliard Y. Fragmentation mechanisms of protonated benzylamines. Electrospray ionisation-tandem mass spectrometry study and ab initio molecular orbital calculations. Eur. J. Mass Spectrom 2003; 9: 351-360.
20. Fahmey MA, Zayed MA, Keshek YH. 2001 Comparative study on the fragmentation of some simple phenolic compounds using mass spectrometry and thermal analyses. Therm. Chem. Acta. 2003; 366: 183-188.
21. Fahmey MA, Zayed MA. Phenolic-iodine redox products. Mass spectrometry, thermal analysis and other Physicochemical Methods of Analyses. J. Therm. Anal. Calor. 2002; 67: 163-165.
22. Fahmey MA, Zayed MA, El-Shobaky HG. Study of some phenolic-iodine redox polymeric products by thermal analyses and mass spectrometry. J. Therm. Anal Calor. 2005; 82: 137-142.
23. Mayer I, Gömöry Á. Semiempirical quantum chemical method for predicting mass spectrometric fragmentations. J. Molec. Struct. Theochem. 1994; 311: 331-341.
24. Zayed MA, Fahmey MA, Hawash MF. Investigation of malomananilide and its dinitro-isomers using thermal analyses, mass spectrometry and semi-empirical MO calculations. Egypt. J. Chem. 2005; 48(1): 43-57.
25. Zayed MA, Fahmey MA, Hawash MF. Investigation of diazepam drug using thermal analyses, mass spectra and semi-empirical MO calculations. Spectrochimica Acta, part A 2005; 61:799-805.
26. Zayed MA, Hawash MF, Fahmey MA. Structure investigation of codeine drug using mass spectra, thermal analyses and semi-empirical MO calculations. Spectrochemica Acta A 2006; 64: 363-371.
27. Zayed MA, Fahmey MA, Hawash MF, El-Habeeb AA. Mass spectrometric investigation of buspirone drug in comparison with thermal analyses and molecular orbital calculations. Spectrochemica Acta A 2007; 67: 522-530.
28. Zayed MA, Hawash MF, Fahmey MA, El Haeeb AA. Structure investigation of Sertraline drug and its iodine prodcut using mass spectrometry, thermal analyses and MO-Calculations. Spectrochemica Acta, Part A 2007; 68: 970-978.
29. Stewart JJP. Optimization of parameters for semiempirical methods. J Comp Chem. 2004; 10 (2): 209-220.
30. Baker J. An algorithm for the location of transition states. J. Com. Chem. 2004; 7 (4): 385-395.
31. Stewart JJP. "MOPAC 2000" Fujitsu Limited, Tokyo, Japan 1999.
32. Horning EC. Advances in Mass Spectrometry, Ed: J.F.J. Todd. 3, 1985.
33. Mayer I, Gömöry Á. Semiempirical quantum chemical method for predicting mass spectrometric fragmentations. Journal of Molecular Structure 1994; 311: 331-341.
34. Loew G, Chadwick M, Smith D. Applications of molecular orbital theory to the interpretation of mass spectra. Prediction of primary fragmentation sites in organic molecules. Org Mass Spectrom 1973; 7: 1241-1251.

EXPERIMENTAL MODELS OF DIABETES MELLITUS

Jelena Pantic[1], Vladislav Volarevic[1], Aleksandar Djukic[1]
[1]Faculty of Medicine, University of Kragujevac

EKSPERIMENTALNI MODELI DIJABETES MELITUSA

Jelena Pantić[1], Vladislav Volarević[1], Aleksandar Đukić[1]
[1]Medicinski fakultet, Univerzitet u Kragujevcu

Received / Primljen: 27. 07. 2010. Accepted / Prihvaćen: 03. 03. 2011.

APSTRAKT

Early studies on pancreatectomised dogs confirmed the central role of the pancreas in the homeostasis of glycemia and resulted in the discovery of insulin. Today, hundreds of different animal models are used in experimental studies of diabetes. The aim of this review is to present experimental models of type 1 and type 2 diabetes. In preparing for this review, we searched the electronic databases ***Medline, Highwire, and Hinari.***

The majority of the experiments are conducted on rodent models (mice and rats). Selective inbreeding resulted in the development of numerous models with pathogenic characteristics and the manifestation of type 1 and 2 diabetes and the related phenotypes of obesity and insulin resistance. In addition to analyzing the pathogenic mechanisms of the disease and its complications, these models are used to evaluate new treatment solutions as well as the transplantation of beta cells and disease prevention. New animal models have been created using techniques based in molecular biology and genetic engineering: transgenic, knockout and tissue-specific knockout models. These are very powerful methods, which may lead to exciting results in the future.

Key words: *animal models, experimental diabetes, mouse, rat*

SAŽETAK

Prve studije rađene na psima kojima je prethodno uklonjen pankreas potvrdile su centralnu ulogu pankreasa u homeostazi glikemije i doprineli otkriću insulina. Danas, veliki broj različitih eksperimentalnih modela se koristi u istraživanjima u oblasti dijabetesa. Cilj ovog revijskog rada je da predstavi neke od ovih modela, koristeći kao literaturu originalne i revijske radove elektronskih baza ***Medline, Highwire i Hinari.***

Većina laboratorija koristi selektivnim inbridingom dobijene miševe i pacove, kao i transgene i nokaut životinje dobijene genetskim inženjeringom, koje zbog svojih karakteristika (npr. gojaznost, rezistencija na insulin) predstavljaju idealne eksperimentalne modele za dijabetes tip 1 ili 2. Ovi eksperimentalni modeli koriste se kako za ispitivanje patogeneze dijabetesa tako i za ispitivanja novih terapijskih sredstava u lečenju šećerne bolesti.

Ključne reči: *animalni modeli, eksperimentalni dijabetes, miš, pacov*

UDK 616.379-008.64 / Ser J Exp Clin Res 2011; 12 (1): 29-35

Correspondence to: Jelena Pantic, Address: Janka Veselinovica 3/3, 11000 Beograd
Tel: 064/1550001, 011/3861942, E-mail: panticjelena@open.telekom.rs

INTRODUCTION

Since 1880, when von Mering and Minkowski removed the pancreas from a dog displaying symptoms of diabetes mellitus (1), many experiments have been conducted on mice, rats, rabbits, and dogs, which were all used as experimental models for this disease.

The rodents (mice and rats) are most frequently used in laboratory research of type 1 and type 2 diabetes because they are biologically and genetically similar to people, their reproductive potential is high, their life span is short, and they are cheap and easy to handle (1). The main drawback of these models is that sometimes they are unable to successfully simulate pathological processes occurring in humans; in those situations, the use of cats, dogs, pigs or primates is justifiable.

Models of experimental diabetes are:
1. induced (experimental)
2. spontaneous (genetically induced) or
3. transgenic and knock-out models (resulting from genetic engineering).

Hyperglycemia is induced by:
1. surgical method (partial or total pancreatectomy)
2. non-surgical method (using a diabetogenic toxin in experimental animals) (Table 1) (2).

MATERIALS AND METHODS

We searched the electronic databases *Medline, Highwire,* and *Hinari*. Selected papers, both original and review, have been summarized and cited with regard to their scientific relevance for this research field.

EXPERIMENTAL MODELS OF TYPE 1 DIABETES MELLITUS

A) Induced models

Multiple low-dose streptozotocin-induced diabetes

Streptozotocin (STZ) is a derivative of nitrosourea that has been isolated from *Streptomyces achromogenes*. It is a strong alkylating agent that affects glucose transport (the role of glucokinase) and induces numerous lesions in the beta-cell DNA chain (3-5). It can selectively bind to glucose-transport protein 2 (GLUT2), which is predominantly expressed on the membranes of pancreatic beta-cells (3).

Toxin	Diabetogenic effect
Streptozotocin	Hyperglycemia, glucose intolerance
Alloxan	Hyperglycemia, glucose intolerance
Chlorozotocin	Hyperglycemia, glucose intolerance
Dithizone	Hyperglycemia, glucose intolerance
Vacor	Hyperglycemia
Oxine	Hyperglycemia
Methylnitrosurea	Glucose intolerance
Cyproheptadine	Glucose intolerance

Table 1. Toxins with diabetogenic effect

Toxicity of the streptozotocin on beta-cells is complex and includes genetic and non-genetic mechanisms (6). Nitric oxide (NO) and other free radicals influenced by streptozotocin result in spontaneous lesions of the DNA chain (7). Damaged DNA chains activate poly-(ADP-ribose) polymerase (PARP) as a reparatory mechanism, which in case of over-activation may have proapoptotic effects (8). PARP knockout mice were shown to be resistant for streptozotocin-induced diabetes (8).

In addition, the toxicity of streptozotocin is associated with a drastic decrease of insulin reserves within beta cells, resulting from the fast catabolism of nicotinamide-adenine-dinucleotide+ (NAD+), a substrate for PARP activation (9). Decrease of NAD+ and ATP+ provokes significant depletion of insulin secretion as well as other basic processes inside the cell. While excessive activation of PARP represents a proapoptotic stimulus, the reduction of necessary cell energy results in cellular necrotic death.

A single high dose of streptozotocin provokes diabetes in rodents, possibly as a result of the direct toxic effect. Multiple low-dose streptozotocin-induced diabetes (when streptozotocin is administered in lower doses (40 mg/kg) during five consecutive days) is an experimental model of type 1 diabetes and immune-mediated insulitis and is widely used for studying the immunological background of this disease (10).

Partial pancreatectomy

The partially pancreatectomised rat was one of the first experimental models of diabetes (11). The surgical removal of 90% of the pancreatic tissue resulted in a slow development of hyperglycemia over the course of 12 weeks to 20 months (12). The period of post-surgical euglycemia is followed by the development of chronic hyperglycemia as a consequence of a further failure of the remaining beta cells.

The first stage of disease refers to glucose intolerance followed by a compensatory hyper-function of beta-cells, the exhaustion of the remaining beta cells and their further breakdown 14 weeks after surgery (12). Altered beta cell gene expression is associated with a decreased production of islet amylin polypeptide (IAPP), transcription factors, ionic canals and pumps, including GLUT2, glucokinase, mitochondrial glycerophosphate dehydrogenase (mGPD) and pyruvate carboxylase (13). A reduction of insulin secretion follows even in conditions of high concentrations of glucose and even after application of insulin secretagogues (14).

Histopathological findings demonstrate hypertrophy and fibrosis of pancreatic islets related to the level of hyperglycemia (13). Insulitis, demonstrated as the infiltration of inflammatory cells, may be depressed, thus slowing down the process of cell degeneration (15).

B) Spontaneous models

The most frequently used spontaneous models of type 1 diabetes are the non-obese diabetic (NOD) mouse and the bio-breeding (BB) rat. These two strains are the result of laboratory inbreeding (keen cross-breeding) of a large number of generations; they develop the disease spontaneously, similar to type 1 human diabetes.

NOD mouse

The NOD mouse is an inbred, homozygous strain discovered in 1974 in Shionogi Research Laboratories in Osaka, Japan. It was a result of keen cross-breeding from normoglycemic strains used for cataract research (Jcl-ICR mouse) and bred in sterile conditions, free from species-specific pathogens (16). The NOD mouse developed insulitis detectable by electronic microscopy after 2 weeks, and within 4-5 weeks it becomes visible under standard microscopy (17). The infiltration is mainly characterized by the presence of a large number of CD 4+ T lymphocytes, while CD 8+ T and B lymphocytes, as well as NK cells are not so numerous (18). Insulitis is progressive and accompanied by the destruction of beta cells and a decrease of insulin levels in serum. In contrast to the disease in the human population, these strains have mild ketoacidosis and can survive for weeks without insulin substitution (1). Incidence of this disease differs between genders (90% among females and 60% among males) (1).

Similar to the human population, the main autoantigenes in pathogenesis of this disease, recognized by secreted antibodies, are insulin, glutamic acid decarboxylase (GAD), and tyrosine phosphatase (ICA512, known as IA-2) (19).

The genetic background of diabetes in this model highlights the role of a major histocompatibile complex (MHC) class II gene that codes for molecule I-A^{g7} (20-21). The expression of MHC molecule class I refers to proteins K^d and D^b (22). An alteration of INS gene expression, controlling the expression of insulin in the thymus and the deletion of T reactive lymphocytes in the case of central tolerance, is related to an initiation of the autoimmune process (22). A similar situation is observed with the cytotoxic T lymphocyte antigen 4 (CTLA-4) gene, which codes for a negative signal molecule for CD8+ T cells and controls the activation and expansion of T lymphocytes (22). The protein tyrosine phosphatase non-receptor type 22 (PTPN22) gene, associated with autoimmune diabetes, codes for tyrosine phosphatase (LYP or PEP), a negative regulator of T cells (22). Variations of genes coding for IL2 and CD25 $FoxP3^+$ that a key role in maintaining immune homeostasis are common for both human and NOD mice (22).

BB rat

The BB rat was discovered in 1974 within the commercial campaign of the Company Bio Breeding Laboratories, Ottawa. It develops diabetes spontaneously (decrease of body weight, polyuria, polydipsia, hyperglycemia and insulopenia) during puberty—approximately the 12^{th} week of life (1). Similar to the human population, the BB rat develops serious/fatal ketoacidosis unless insulin substitution is administered. (1) The disorder is autoimmune, and insulitis is characterized by the infiltration of T lymphocytes, B lymphocytes, macrophages and NK cells (23). Typical for this species is extreme lymphopenia associated with a decreased number of T lymphocytes with an elevated expression of ADP-ribosyltransferase 2 (ART2); this has not been registered in the human population (24). A transfusion of histocompatible T ART2+ lymphocytes prevents spontaneous hyperglycemia in this model (24).

Recent studies show that BB rat diabetic syndrome is a complex, polygenic disease that may share additional susceptibility genes aside from MHC class II with human type 1 diabetes (25). The expression of two main susceptibility genes is responsible for the development of diabetes in the BB rat: MHC (RT1) class II u haplotype (Iddm1) and the Gimap5 (GTPase immunity associated protein family member 5) gene, a key genetic factor for lymphopenia in spontaneous BB rat diabetes (Iddm2) (25).

EXPERIMENTAL MODELS OF TYPE 2 DIABETES

A) Induced models

C57BL/6J mouse fed a high-fat diet

This model was originally introduced by Surwit et al. in 1988 as a robust model of impaired glucose tolerance (IGT) and early type 2 diabetes (26). C57BL/6J mice fed a high-fat diet (58% energy by fat, a "Western diet") developed hyperglycemia, hyperinsulinemia, hyperlipidemia and increased adiposity (27). High-fat diet results in insulin resistance with compensatory hyperinsulinemia. After one week on the diet, baseline plasma glucose and insulin are significantly elevated and intravenous glucose tolerance test (IVGTT) shows reduced glucose elimination and impaired insulin secretion (28). The model thus shows two important pathophysiological characteristics for impaired glucose tolerance (IGT) and type 2 diabetes: insulin resistance and islet dysfunction.

In this model, the weight gain is due primarily to an increase in mesenteric adiposity. In high-fat diet-fed mice, energy intake is higher and metabolic efficiency index is lower compared to normal diet-fed mice (28). Despite obesity, plasma leptin levels are significantly lower than in the control group in the absence of hyperphagia (29). Increased serum lipid levels develop concomitantly with the development of hyperglycemia, thus deteriorating insulin resistance and producing lipid deposits in non-adipose cells, including beta cells and skeletal muscle cells (30). Microscopically, a high-fat diet induces hypertrophy of pancreatic islets (31).

This model is suitable for examining novel therapeutic interventions. The dipeptidyl peptidase-IV (DPP-IV) inhibitor is efficient in improving glucose tolerance and insulin secretion in the high-fat diet-fed mouse model (28).

Partial pancreatectomy as a surgical method of inducing diabetes was described above.

B) Spontaneous models

Goto Kakizaki Rat

The Goto Kakizaki (GK) rat is skinny, diabetic rat developed in Japan in 1975 from Wistar species (6). Both insulin resistance and impaired insulin secretion are present in this model (32). GK rats have a decreased numbers of beta cells at birth, which is probably the consequence of their apoptosis during embryonic development (16-18 day). However, GK rats are still normoglycemic and without marked changes in islet morphology at birth (33). The characteristics of diabetes type 2 in this model are mild hyperglycemia (9 mmol/l) in the fourth week and the increase of basal insulin secretion and insulin resistance followed by a decrease in glucose tolerance (34). GK rats are resistant to food intake restrictions (35).

Starting from the 8th week, insulin islets show signs of fibrosis with a marked elevation of hyperglycemia (36). In addition, the expression of CD38 and GLUT2 proteins is reduced in GK islets (37-38). Microscopically, numerous macrophages (major histocompatibility complex class II^{+} and CD68^{+}) and granulocytes were found in and around pancreatic islets (39). Elevated islet IL-1β activity in GK rat promotes cytokine and chemokine expression, leading to the recruitment of innate immune cells (40). Treatment of GK rats with IL-1 receptor antagonists decreases hyperglycemia, reduces the proinsulin/insulin ratio and improves insulin sensitivity (40).

The most important factor for the disorder of insulin secretion is the dysfunction of glucose metabolism connected with a deficiency of enzymes that control oxidative glycolysis (6). The GK rat develops some features that can be compared with the complications of diabetes seen in humans (1).

Zucker Fatty and Zucker Fatty Diabetic Rat

The Zucker Fatty (ZF) rat has a defect of a gene that codes for leptin receptors (fa/fa), resulting in the development of obesity and hypertension with associated renal and cardiovascular disease (6). The Zucker Fatty Diabetic Rat (ZDF) has the identical genetic mutation and, additionally, a mutation which leads to the spontaneous development of hyperglycemia in males during the 7th-10th week (41). The females become hyperglycemic only after high-fat diet, and it is supposed that this additional mutation is expressed in beta cells (42).

Leptin suppresses insulin secretion and controls food intake. The fa/fa mutation of the leptin receptor results in insulin resistance with severe glucose intolerance (6). ZF and ZDF rats are hyperphagic due to the reduction in leptin signalling that results in obesity (6). These animals, in adulthood, become extremely dislipemic with increased concentration of free fatty acids, cholesterol, and triglycerides in plasma with a consequent development of diabetes mellitus complications (cardiovascular, renal, and peripheral neuropathy) (6, 43-44).

Pancreatic islets in adults show increased beta cell activity, with marked characteristics of a prediabetic state (6). After the onset of diabetes, pancreatic islets become irregular as a result of hyperplasia, hypertrophy and infiltration of inflammatory cells (45). An almost complete absence of beta cells was detected by the 14th week of age (45).

Reduced expression of mGDP and pyruvate carboxylase activity was noticed in this model (46).

Otsuka Long Evans Tokushima Fatty Rat

The Otsuka Long Evans Tokushima Fatty Rat (OLETF) is derived by inbreeding from the glucose-intolerant Long-Evans colony of rats (47). These animals develop hyperglycemia slowly, by 40 weeks of age, with greater incidence in males than in females (1). Adult animals are mildly obese and hyperglycemic, with increased appetite and renal glomerulosclerosis. These changes are the result of a deletion of the gene for cholecystokinin 1 receptors. Diet and exercise prevent type 2 diabetes in this model (48).

Histopathologic changes inside the islets during the 8th-10th week show an infiltration of inflammatory cells followed by tissue damage. Beta cell hyperplasia and proliferation occur between the 20th and 40th weeks, while atrophy and fibrosis of the islets start after the 40th week (47). From the 72nd week, inflammatory cytokines (tumour necrosis factor- (TNF-), interleukin-1β (IL-1β) and interleukin-6 (IL-6)) are detectable by immunohistochemical method (49).

Psammomys obesus

The Psammomys obesus is rat from North America and the Middle East. It usually feeds on a low-calorie diet and demonstrates the strong effect of a high-calorie diet by developing hyperglycemia within 4-7 days (6).

Pathogenesis of the disorders goes through four typical stages: normoglycemia and normoinsulinemia, normoglycemia with hyperinsulinemia (indicating insulin resistance), hyperglycemia with hyperinsulinemia, and hyperglycemia with hypoinsulinemia (50). The last stage is characterized by marked apoptosis and a reduction of beta cell mass (51). Returning to a low-calorie diet results in the recovery of beta cells, indicating that the irreversible loss of beta cell mass is a late event (52).

TRANSGENIC AND KNOCKOUT MODELS OF DIABETES MELLITUS

In experimental diabetes, numerous transgenic and knockout models are being used. These models have been created by genetic manipulations using either transgene insertion and/or targeted gene-deletion approaches.

Still, these techniques have some limitations. Some homozygotes may die in the womb, which makes studies in adults impossible. Several genes could function differently during embryogenesis and in adulthood. Finally, some models' gene expression is altered in soft tissues, and therefore it is impossible to analyze their function in the desired tissue. Tissue-specific knockout models for diabetes, in which the gene being studied is only knocked out in specific tissues, were created to address this issue.

Mouse/rat model	Phenotype	Reference
IR +/-	Mild insulin resistance	53, 54
IR -/-	Severe hyperglycemia, neonatal death from ketoacidosis	54
IRS-1 -/-	Mild insulin resistance, normoglycemia, elevated serume triglycerides, hypertension, growth retardation	55
IRS-2 -/-	Insulin resistance, hyperglycemia, reduced beta-cell mass	56
IRS-1 -/- IRS-3 -/-	Hyperglycemia, lipatrophy, decreased plasma levels of leptin, hyperinsulinemia	57
IRS-1+/- IR +/-	Insulin resistance, beta-cell hyperplasia	58
GK -/-	Hyperglycemia, perinatal death	59
GK +/-	Glucose intolerance	59
GLUT4 -/-	Mild changes in glucose hemostasis, growth retardation, reduction of fat, cardiac hypertrophy	60
PPARγ +/-	Mild insulin resistance	61
PPARγ2 -/-	Insulin resistance, reduction of white adipose tissue	62
PPARα -/-	No phenotypical defect without pharmacological intervention	63
hIAPP +/+ rat	Decreased proliferation and increased apoptosis of beta cell, hyaline replacement of islet cells	64

homozygous (-/-), heterozygous (-/+)

Table 2. Transgenic and knockout models of Diabetes mellitus

The first knockout models of insulin resistance aimed at the disruption of major molecules in insulin receptor (IR) signaling. Heterozygous IR knockout mice show 50% of IR expression, which is sufficient for the maintenance of physiological blood glucose contentrations (53). In contrast, homozygous IR-deficient mice rapidly develop diabetic ketoacidosis and die within 3-7 days after birth, showing the central role of IR in glucose metabolism (54). Aside from IR knockouts, various molecules of the signal transduction pathway initiated by IR have been disrupted, such as insulin receptor substrates (IRS-1, IRS-2, IRS-3) (55-58). Insulin resistance and insulin secretory defects have also been presented by a generation of mice deficient in beta cell glucokinase (GK). The heterozygous beta cell GK knockout mouse is characterised by decreased insulin secretion in response to glucose (59). The homozygous knockout mouse model with a disrupted gene for the glucose transporter 4 (GLUT4), which mediates glucose transport in muscle and adipose tissue in response to insulin, is characterised by mild changes in glucose hemostasis, growth retardation, reduction of fat and cardiac hypertrophy (60). The important physiological role of peroxisome proliferator-activator receptors (PPARα and PPARγ) was deduced from findings identifying the PPARs as primary targets of tiasolidinedione insulin sensitizers and fibrates that have been used in the successful treatment of diabetes and dyslipidemia. Diverse knockout models have been created to study the function of single PPARs isoforms (61-63). Similar to other mouse models, a transgenic human islet amyloid polypeptide-expressing rat has been recently developed (64). This model shows pancreatic amyloidosis, insulin resistance, and reduced β-cell mass with resulting hyperglycemia (64). Some of the transgenic/knockout and tissue-specific knockout models are presented in Table 2.

REFERENCES

1. Rees DA, Alcolado JC. Animal models of diabetes mellitus. Diabetic medicine 2005; 22: 359-370.
2. Wilson GL, LeDoux SP. The Role of Chemicals in the Etiology of Diabetes Mellitus. Toxicologic Pathology 1989; 17(2): 357.
3. Wang Z, Gleichmann H. GLUT2 in pancreatic islets: crucial target molecule in diabetes induced with multiple low-doses of streptozotocin in mice. Diabetes 1998; 47: 50-56.
4. Zahner D, MalaisseWJ. Kinetic behaviour of liver glucokinase in diabetes, I, Alteration in streptozotocin-diabetic rats. Diabetes Res 1990; 14: 101-108.
5. Bolzan AD, Bianchi MS. Genotoxicity of streptozotocin. Mutat Res 2002; 512: 121-134.
6. Nugent DA, Smith DM, Jones HB. A Rewiew of Islet of Langerhans Degeneration in Rodent Models of Type 2 Diabetes. Toxicologic Pathology 2008; 36(4): 529-551.
7. Wada R, Yagihasi S. Nitric oxide generation and poly (ADP ribose) polymerase activation precede beta-cell death in rats with a single high-dose injection of streptozotocin. Virchows Arch 2004; 444: 375-82.
8. Peiper AA, Brat DJ, Krug DK, Watkins CC, Gupta A, BlackshawB S, Verma A, Wang ZQ, Snyder SH. Poly(ADP-ribose) polymerase-deficient mice are protected from streptozotocin-induced diabetes. Proc Natl Acad Sci USA 1999; 96: 3059-62.
9. Cardinal JW, Allan DJ, Cameron DR. Poly(ADP-ribose) polymerase activation determines strain sensitivity to streptozotocin-induced β cell death in inbred mice. J Mol Endocrinol 1999; 22: 65-70.
10. Mensah-Brown EP, Stosic Grujicic S, Maksimovic D, Jasima A, Lukic ML. Downregulation of apoptosis in the target tissue prevents low-dose streptozotocin-induced autoimmune diabetes. Mol Immunol 2002; 38: 941-946.

11. Lewis JT, Foglia VG, Rodriguez RR. The effects of steroids on the incidence of diabetes in rats after subtotal pancreatectomy. Endocrinology 1950; 46: 111-21.
12. Yomemura Y, Takashima T, Matsuki N, Hagino S, Sawa T, Takashima S, Miwa K, Miyazaki I. The pathogenesis of diabetes produced by subtotal pancreatectomyp, with special reference to the cell kinetics of the islet cells. Nippon Geka Gakkai Zasshi 1984; 85: 356-62.
13. Laybutt DR, Glandt M, Xu G, Ahn YB, Trivedi N, Bonner-Weir S, Weir GC. Critical reduction in beta-cell mass results in two distinct outcomes over time. Adaption with impaired glucose tolerance or decompensated diabetes. J Biol Chem 2003; 278: 2997-3005.
14. Rossetti L, Shulman GI, Zawalich W, DeFronzo RA. Effect of chronic hyperglycaemia on in vivo insulin secretion in partially pancreatectomized rat.J Clin Invest 1887; 80: 1037-1044.
15. Lampeter EF, Tubes M, Klemens C, Brocker U, Friemann J, Kolb-Bachofen V, Gries FA, Kolb H. Insulitis and islet-cell antibody formation in rats with experimentally reduced beta-cell mass. Diabetologia 1995; 38: 1397-04.
16. Hanafusa T, Miyagawa J, Nakajima H, Tomita K, Kuwajima M, Matsuzawa Y, Tarui S. The NOD mouse. Diabetes Research and Clinical Practice 1994; 24: 307-311.
17. Fijino-Kurihara H, Fujita H, Hakura $, Nonaka K, Tarui S. Morphological aspects of non-obese diabetic (NOD) mice. Virchows Arch 1885; 149: 107-120.
18. Miyazaki A, Hanafusa T, Yamada K. Predominance of T lymphocytes in pancreatic islets and spleen of prediabetic non-obese diabetic (NOD) mice: a longitudinal study. Clin Exp Immunol 1985; 60: 622-630.
19. Wong FS, Janeway CA Jr. Insulin-dependent diabetes mellitus and its animal models. Curr Opin in Immunol 1999; 11: 643-647.
20. Murphy K, Travers P, Walport M. Janeways Immunobiology. Garland Science 2008; Chapter 14: 600-609.
21. Serreze DV, Leiter EH. Genetic and pathogenic basis of autoimmune diabetes in NOD mice. Curr Opin in Immunol 1994; 6: 900-906.
22. Wicker LS, Clark J, Fraser HI et all. Type 1 diabetes genes and pathways shared by humans and NOD mice. Journal of Autoimmunity 2005; 25: 29-33.
23. Lally FJ, Ratcliff H, Bone AJ. Apoptosis and disease progression in the spontaneosly diabetic BB/S rat. Diabetologia 2001; 44: 320-324.
24. Bortel R, Waite DJ, Whalen BJ, Todd D, Leif JH, Lesma E et all. Levels of Art2+ cells but not soluble Art 2 protein corelate with expression of autoimune diabetes in the BB rat. Autoimmunity 2001; 33: 199-211.
25. Wallis RH, Wang K. Type 1 Diabetes in the BB rat: A Polygenic Disease. Diabetes 2009; 58(4): 1077-11.
26. Surwit RS, Kuhn CM, Cochrane C, McCubbin JA, Feinglos MN. Diet-induced type 2 diabetes in C57BL/6J mice. Diabetes 1988; 37: 1163-1167.
27. Rebuffe-Scrive M, Surwit RS, Feinglos MN et al. Regional fat distribution and metabolism in a new mouse model (C57BL/6J) of non-insulin-dependent diabetes mellitus. Metabolism 1993; 42: 1405-1409.
28. Winzell MS, Ahren B. The high-fat diet-fed mouse A model for studying mechanisms and treatment of impared glucose tolerance and type 2 diabetes. Diabetes 2004; 53(3): S215-S219.
29. Parekh PI, Petro AE, Tiller JM et al. Reversal of diet-induced obesity and diabetes in C57BL/6J mice. Metabolism 1998; 47: 1089-1096.
30. Shimabukuro M, Zhou YT, Moshe L, Unger RH. Fatty acid-induced β cell apoptosis: a link between obesity and diabetes. Proc Natl Acad Sci USA 1998; 95: 2498-502.
31. Hull RL, Kodama K, Utzschneider KM, Carr DB, Prigeon RL, Kahn SE. Dietary fat-induced obesity in mice results in beta cell hyperplasia but not increased insulin release: evidence for specificity of impaired beta cell adaptation. Diabetologia 2005; 48: 1350-1358.
32. Bisbis S, Bailbe D, Tormo MA, Picarel-Blanchot F, Derouet M, Simon J, Portha B. Insulin resistance in the GK rat: decreased receptor number but normal kinase activity in liver. Am J Physiol 1993; 265: E807-813.
33. Portha B, Giroix MH, Serradas P, Gangrenau MN, Movassat J, Rajas, F, Bailbe D, Plachot C, Mithieux G, & Marie, JC. (2001). Beta-cell function and viability in the spontaneously diabetic GK rat: information from the GK/Par colony. Diabetes 2001; 50: S89-93.
34. Ostenson CG, Khan A, Abdel-Halim SM, Guenifi A, Suzuki K, Goto Y, Efendic S. Abnormal insulin secretion and glucose metabolism in pancreatic islets from the spontaneously diabetic GK rat. Diabetologia 1993; 36: 3-8.
35. Alvarez, C, Bailbe D, Picarel-Blanchot F, Bertin E, Pascual-Leone AM, Portha B. Effect of early dietary restriction on insulin action and secretion in the GK rat, a spontaneous model of NIDDM. Am J Physiol Endocrinol Metab 2000; 278 : E1097-103.
36. Guenifi A, Abdel-Halmi SM, Hoog A, Falkmer S, Ostenson CG. Preserved beta-cell density in the endocrine pancreas of young, spontaneously diabetic Goto-Kakizaki (GK) rats. Pancreas 1995; 10: 148-153.
37. Matsuoka T, Kajimoto Y, Watada H, Umayahara Y, Kubota M, Kawamori R, Yamasaki Y, Kamada T. Expression of CD38 gene, but not of mitochondrial glycerol-3-phosphate dehydrogenase, is impaired in pancreatic islets of GK rats. Biochem Biophys Res Commun 1995; 214: 239-246.
38. Ohneda M, Johnson JH, Inman LR, Chen L, Suzuki K, Goto Y, Alam T, Ravazzola M, Ocri L, Unger RH. GLUT2 expression and function in the beta-cells of GK rats with NIDDM. Dissociation between reductions in glucose transport and glucose-stimulated insulin secretion. Diabetes 1993; 42: 1065-1072.
39. Homo-Delarche F, Calderari S, Irminder JC, Gangnerau MN, Coulaud J, Rickenbach K, Dolz M, Halban P, Portha B. Islet inflammation and fibrosis in a spontaneous model of type 2 the GK rat. Diabetes 2006; 55: 1625-1633.

40. Ehses JA, Lacraz G, Giroix MH, Schmidlin F, Coulaud J, Kassis N, Irminger JC, Kergoat M, Portha B, Homo-Delarche F, Donath MY. IL-1 antagonism reduces hyperglycemia and tissue inflammation in the type 2 diabetic GK rat. PNAS 2009; 106: 13998-14003.
41. Peterson RG, Shaw WN, Neel MA, Little LA, Eichberg J. (1990). Zucker diabetic fatty rat as a model for non-insulin dependent diabetes mellitus. ILAR J 1990; 32: 16-19.
42. Coresttis JP, Sparks, JD, Peterson, RG, Smith, RL, & Sparks, CE. Effect of dietary fat on the development of non-insulin dependent diabetes mellitus in obese Zucker diabetic fatty male and female rats. Atherosclerosis 1999; 148: 231-41.
43. Lee Y, Hirose H, Zhou YT, Esser V, McGarry JD, Unger RH. Increased lipogenic capacity of the islets of obese rats: a role in the pathogenesis of NIDDM. Diabetes 1997; 46: 408-13.
44. Erdely A, Freshour G, Maddox, D, Olson, J, Samsell L, Baylis C. Renal disease in rats with type 2 diabetes is associated with decreased renal nitric oxide production. Diabetologia 2004; 47: 1672-6.
45. Finegood DT, McArthur, MD, Kojwang D, Thomas, MJ, Topp BG, Leonard, T, Buckingham RE. β-Cell mass dynamics in Zucker diabetic fatty rats. Rosiglitazone prevents the rise in net cell death. Diabetes 2001; 50: 1021-9.
46. MacDonald MJ, Tang J, Polonsky KS. Low mitochondrial glycerol phosphate carboxylase in pancreatic islets of Zucker diabetic fatty rats. Diabetes 1996; 45: 1326-1330.
47. Kawano K, Hirashima T, Mori S, Saitoh Y, Kurosumi M, Natori T. Spontaneous long-term hyperglycaemic rat with diabetic complications Otsuka Long-Evans Tokushima Fatty (OLETF) strain. Diabetes 1992; 41: 1422-8.
48. Moran TH, Bi S. Hyperphagia and obesity of OLETF rats lacking CCK1 receptors: developmental aspects. Dev Psychobiol 2006; 48: 360-7.
49. Jia D, Taguchi, M, Otsuki M. (2005). Synthetic protease inhibitor camostat prevents and reverses dyslipidemia insulin secretory defects, and histological abnormalities of the pancreas in genetically obese and diabetic rats. Metabolism 2005; 54: 619-27.
50. Lewandowski PA, Cameron-Smith D, Jackson CJ, Kultys ER, Collier GR. The role of lipogenesis in the development of obesity and diabetes in Israeli sand rats (Psammomys obesus). J Nutr 1998; 128: 1984-8.
51. Bar-On H, Ben-Sasson R, Ziv E, Arar N, Shafrir E. Irreversibility of nutritionally induced NIDDM in Psammomys obesus is related to beta-cell apoptosis. Pancreas 1999; 18: 259-265..
52. Kaiser N, Yuli M, Uckaya G, Oprescu A, Berthault MF, Kargar C, Donath M, Erol C, Ktorza A. Dynamic changes in β-cell mass and pancreatic insulin during the evolution of nutrition-dependent diabetes in Psammomys obesus. Impact of glycemic control. Diabetes 2005b; 54: 138-145.
53. Plum L, Wunderlich FT, Baudler S, Krone W, Bruning JC. Transgenic and Knockout Mice in Diabetes Research: Novel Insights into Pathophysiology, Limitations, and Perspectives. Physiology 2005; 20(3): 152-161.
54. Accili D, Drago J, Lee EJ, Johnson MD, Cool MH, Salvatore P, Asico LD, Jose PA, Taylor SI, Westphal H. Early neonatal death in mice homozygous for a null allele of the insulin receptor gene. Nat Genet 1996; 12: 106–109.
55. Abe H, Yamada N, Kamata K, Kuwaki T, Shimada M, Osuga J, Shionoiri F, Yahagi N, Kadowaki T, Tamemoto H, Ishibashi S, Yazaki Y, Makuuchi M. Hypertension, hypertriglyceridemia, and impaired endothelium-dependent vascular relaxation in mice lacking insulin receptor substrate-1. J Clin Invest 1998; 101: 1784–1788.
56. Previs SF, Withers DJ, Ren JM, White MF, Shulman GI. Contrasting effects of IRS-1 versus IRS-2 gene disruption on carbohydrate and lipid metabolism in vivo. J Biol Chem 2000; 275: 38990–38994.
57. Laustsen PG, Michael MD, Crute BE, Cohen SE, Ueki K, Kulkarni RN, Keller SR, Lienhard GE, and Kahn CR. Lipoatrophic diabetes in Irs1(–/–)/Irs3(–/–) double knockout mice. Genes Dev 2002; 16: 3213–3222.
58. Bruning JC, Winnay J, Bonner-Weir S, Taylor SI, Accili D, and Kahn CR. Development of a novel polygenic model of NIDDM in mice heterozygous for IR and IRS-1 null alleles. Cell 1997; 88: 561–572.
59. Grupe A, Hutlgren B, Ma YH, Bauer M, Stewart TA. Transgenic knockouts reveal a critical requirement for pancreatic P cell glucokinase in maintaining glucose homeostasis. Cell 1995; 83- 69-78.
60. Katz EB, Stenbit AE, Hatton K, DePinho R, and Charron MJ. Cardiac and adipose tissue abnormalities but not diabetes in mice deficient in GLUT4. Nature 1995; 377: 151–155.
61. Kubota N, Terauchi Y, Miki H, Tamemoto H, Yamauchi T, Komeda K, Satoh S, Nakano R, Ishii C, Sugiyama T, Eto K, Tsubamoto Y, Okuno A, Murakami K, Sekihara H, Hasegawa G, Naito M, Toyoshima Y, Tanaka S, Shiota K, Kitamura T, Fujita T, Ezaki O, Aizawa S, Kadowaki T. PPAR mediates high-fat diet-induced adipocyte hypertrophy and insulin resistance. Mol Cell 1999; 4: 597–609.
62. Zhang J, Fu M, Cui T, Xiong C, Xu K, Zhong W, Xiao Y, Floyd D, Liang J, Li E, Song Q, Chen YE. Selective disruption of PPAR 2 impairs the development of adipose tissue and insulin sensitivity. Proc Natl Acad Sci USA 2004; 101: 10703–10708.
63. Djouadi F, Weinheimer CJ, Saffitz JE, Pitchford C, Bastin J, Gonzalez FJ, and Kelly DP. A gender-related defect in lipid metabolism and glucose homeostasis in peroxisome proliferator-activated receptor -deficient mice. J Clin Invest 1998; 102: 1083–1091.
64. Butler, AE, Jang, J, Gurlo T, Carty MD, Soeller WC, & Butler, PC. Diabetes due to a progressive defect in β-cell mass in rats transgenic for human islet amyloid polypeptide (HIP rat). Diabetes 2004; 53: 1509-1516.


Renal disease/Hemodialysis
/PTH/
Bone disease
LBMD/ABD/High turnov
media thickness
Cardiovascular diseases present a leading caus
patients treated with haemodialysis The
mortality in this population is
basis, with left ventricul
eases and heart f
Left ventricular
haemodialys
for th
volume of extr
flow through the vasc
tricular hypertrop
echo
hypertrophy, the
ent, and the realisation and
of risk factors decelerates the
phy and leads to the regression of
hypertrophy, the reduction of cardiovascul
and mortality rates and the improvement of the
life of patients treated with haemodialysis

DIAGNOSTICS AND THERAPY OF LEFT VENTRICULAR HYPERTROPHY IN HAEMODIALYSIS PATIENTS

Dejan Petrovic[1], Nikola Jagic[2], Vladimir Miloradovic[3], Aleksandra Nikolic[3], Biljana Stojimirovic[4]
[1]Clinic for Urology and Nephrology, Center for Nephrology and Dialysis, Clinical Center "Kragujevac", Kragujevac
[2]Center for Radiology Diagnostics, Department for Interventional Radiology, Clinical Center "Kragujevac",Kragujevac
[3]Clinic for Internal Medicine, Clinical Center "Kragujevac", Kragujevac
[4]Institut for Urology and Nephrology, Clinic for Nephrology, Clinical Center of Serbia, Belgrade, Serbia

DIJAGNOSTIKA I LEČENJE HIPERTROFIJE LEVE KOMORE KOD BOLESNIKA NA HEMODIJALIZI

Dejan Petrović[1], Nikola Jagić[2], Vladimir Miloradović[3], Aleksandra Nikolić[3],Biljana Stojimirović[4]
[1]Klinika za urologiju i nefrologiju, Centar za nefrologiju i dijalizu, KC Kragujevac, Kragujevac
[2]Centar za radiologiju, Odsek interventne radiologije, KC "Kragujevac", Kragujevac
[3]Klinika za internu medicinu, KC "Kragujevac", Kragujevac
[4]Institut za urologiju i nefrologiju, Klinika za nefrologiju, KC Srbije, Beograd, Srbija

Received / Primljen: 10. 01. 2011. Accepted / Prihvaćen: 03. 04. 2011.

ABSTRACT

Cardiovascular diseases present a leading cause of death in patients treated with haemodialysis. The rate of cardiovascular mortality in this population is approximately 9% on an annual basis, with left ventricular hypertrophy, ischemic heart diseases and heart failure having the highest rates of mortality. Left ventricular hypertrophy is present in 75-80 % of haemodialysis-treated patients. The most important risk factors for the progression of left ventricular hypertrophy are: hypertension, arteriosclerosis, secondary aortic stenosis, anaemia, increased volume of extracellular fluid and increased blood flow through the vascular access for haemodialysis. Left ventricular hypertrophy is present when the left ventricular mass index on echocardiography exceeds 131 g/m^2 in males and 100 g/m^2 in females. Left ventricular hypertrophy is a risk factor of unfavourable outcome in patients treated with haemodialysis. The identification of patients with increased risk of progression of left ventricular hypertrophy, the timely implementation of adequate treatment, and the realisation and maintenance of targeted values of risk factors decelerates the progression of the hypertrophy and leads to the regression of existing left ventricular hypertrophy, the reduction of cardiovascular morbidity and mortality rates and the improvement of the quality of life of patients treated with haemodialysis.

Key words: *risk factors, left ventricular hypertrophy, echocardiography, haemodialysis*

SAŽETAK

Kardiovaskularne bolesti su vodeći uzrok smrti bolesnika koji se leče hemodijalizom. Stopa kardiovaskularnog mortaliteta kod ovih bolesnika iznosi približno 9% godišnje, a među kardiovaskularnim bolestima najveća je prevalencija hipertrofije leve komore, ishemijske bolesti srca i srčane slabosti. Hipertrofiju leve komore ima 75-80% bolesnika koji se leče hemodijalizom. Najznačajniji faktori rizika za razvoj hipertrofije leve komore su: hipertenzija, arterioskleroza, sekundarna aortna stenoza, anemija, povećan volumen ekstracelularne tečnosti i povećan protok krvi kroz vaskularni pristup za hemodijalizu. Hipertrofija leve komore je prisutna ako je na ehokardiografskom pregledu indeks mase leve komore veći od 131 g/m2 kod muškaraca i veći od 100 g/m2 kod žena. Hipertrofija leve komore je faktor rizika za nepovoljan ishod bolesnika koji se leče hemodijalizom. Izdvajanje bolesnika koji imaju povećan rizik za razvoj hipertrofije leve komore, pravovremena primena odgovarajućeg lečenja, ostvarivanje i održavanje ciljnih vrednosti faktora rizika usporavaju razvoj i dovode do regresije postojeće hipertrofije leve komore, do smanjenja stope kardiovaskularnog morbiditeta i mortaliteta, i poboljšanja kvaliteta života bolesnika koji se leče hemodijalizom.

Ključne reči: *faktori rizika, hipertrofija leve komore, ehokardiografija, hemodijaliza*

UDK 616.61-78-06 ; 616.1 / Ser J Exp Clin Res 2011; 12 (1): 37-40

Correspondence: Doc. Dr Dejan Petrovic, Clinic for Urology and Nephrology, Center for Nephrology and Dialysis, Clinical Center "Kragujevac", Kragujevac, Zmaj Jovina 30, 34000 Kragujevac, Tel.: +381 34 370302, Fax: +381 34 300380, e-mail: aca96@eunet.rs

INTRODUCTION

Cardiovascular diseases present a leading cause of death in patients treated with haemodialysis [1, 2]. The rate of cardiovascular mortality in this population is approximately 9% on an annual basis, with left ventricular hypertrophy, ischemic heart diseases and heart failure having the highest rates of mortality [1, 2].

METHODS

For this study, the Medline database was used. The following key words were used for searching: risk factors, left ventricular hypertrophy, echocardiography, and haemodialysis. About 40.000 references were found dealing with these types of problems. Systematic review articles and well-controlled clinical studies were singled out. Editor's letters and uncontrolled clinical studies were not used. Systematic review articles were used and analysed by the National Kidney Foundation Kidney Disease Outcome Quality Initiative (NKF KDOQI), which confirmed the validity and quality of the selected references.

RESULTS

Aetiopathogenesis of left ventricle hypertrophy

The most important risk factors of left ventricle hypertrophy in haemodialysis patients are hypertension, arteriosclerosis, adult aortic stenosis, anaemia, increased blood flow through the vascular access for haemodialysis and increased volume of extracellular fluid [3, 4]. Pressure overloads of the left ventricle due to hypertension, aortic stenosis and arteriosclerosis of blood vessels can cause thickening of the left ventricle wall without the enlargement of the ventricle diameter (concentric left ventricle hypertrophy) [5, 6]. Volume overloads of the left ventricle due to increased sodium and water intake, anaemia and increased blood flow through the vascular access for haemodialysis (Q_{AV} ≥ 1000 ml/min) cause the ventricle wall to become thickened and cause an enlargement of ventricle diameter (eccentric left ventricle hypertrophy) [5, 6]. The development of left ventricle hypertrophy and fibrosis of the myocardial interstitium can also be affected by factors that do not depend on the *afterload* and *preload*, such as microinflammation, oxidative stress, the activation of the intracardial renin-angiotensin system-RAS, the vitamin D deficiency and uncontrolled secondary hyperparathyroidism, scheme 1 [7-10]. Left ventricle hypertrophy goes through two phases. Adaptive hypertrophy is actually the response to increased tension stress to the left ventricle wall and has a protective function. When volume and pressure overload the left ventricle to the point of cardiac muscle failure, adaptive hypertrophy becomes maladaptive left ventricle hypertrophy, with myocyte loss, heart failure and, eventually, death [11].

Diagnostics of left ventricular hypertrophy

Morphological and functional disorders of the left ventricle in haemodialysis patients include systolic disorder, concentric hypertrophy, eccentric hypertrophy, left ventricle dilation and diastolic dysfunction. The systolic function of the left ventricle is disturbed when echocardiography reveals that the fractional shortening of the left ventricle (FSLV) is ≤ 25% and that the ejection fraction of the left ventricle (EFLV) is ≤ 50% [12-14]. Concentric hypertrophy of the left ventricle is defined by a left ventricle mass index– (LVMi) > 131 g/m^2 in males and >100 g/m^2 in females and a relative wall thickness of the left ventricle (RWT) > 45% [12-14]. Eccentric hypertrophy of the left ventricle is characterised by an increased left ventricle mass index (LVMi > 131 g/m^2 in males and >100 g/m^2 in females) and an RWT ≤ 45% [12-14]. An echochardiographic estimation of the left ventricle function in diastole is based upon the measurement of the velocity of early (E) and late (A) components of blood flow through the mitral valve and their relative ratio E/A. There are three types of left ventricle diastolic dysfunction: relaxation disorder [VmaxE/VmaxA < 1,0; E wave deceleration time (DT_E) > 250 ms; and isovolumetric relaxation of the left ventricle (IVRT) > 100 ms]; pseudonormalisation and restriction disturbance [VmaxE/VmaxA > 1,6; DT_E < 150 ms; and IVRT < 60 ms] [15]. Cardiac Magnetic Resonance Imaging (CMRI) is the golden standard for remodelling of the left ventricle and for the estimation of myocardial interstitium fibrosis in haemodialysis patients [16].

Clinical importance of left ventricular hypertrophy

Left ventricle hypertrophy is accompanied by disordered diastolic function (50-60% of haemodialysis patients), by ventricle arrhythmias (dispersion interval (QTd) > 50 ms), by *de novo* ischemic heart disease (in patients with LVMi > 160 g/m^2) and by unfavourable outcomes in haemodialysis patients [17-19]. A high left ventricle mass index (LVMi > 120 g/m^2) and an LV mass/volume ratio (LVMi/iEDV) > 2,2 g/ml are predictors of a poor outcome in dialysis patients with a normal LV volume (iEDV ≤ 90 ml/m^2) and a normal systolic function (FS > 25%, EF > 50%) [20, 21].

Therapy of left ventricular hypertrophy

Well-timed risk factor detection and adequate therapy help regression of left ventricle hypertrophy in haemodialysis patients [22-25]. Results of large, well-controlled clinical trials stress that the management of anaemia and blood pressure control, the correction of metabolic disorders of calcium, phosphate, vitamin D and parathormone (parathyroid hormone), as well as the individualisation of treatment of haemodialysis as the most important factors in the successful management of left ventricle hypertrophy [22-25].

Anaemia is an important cause of left ventricle hypertrophy, and a decrease in haemoglobin of 10 g/l is

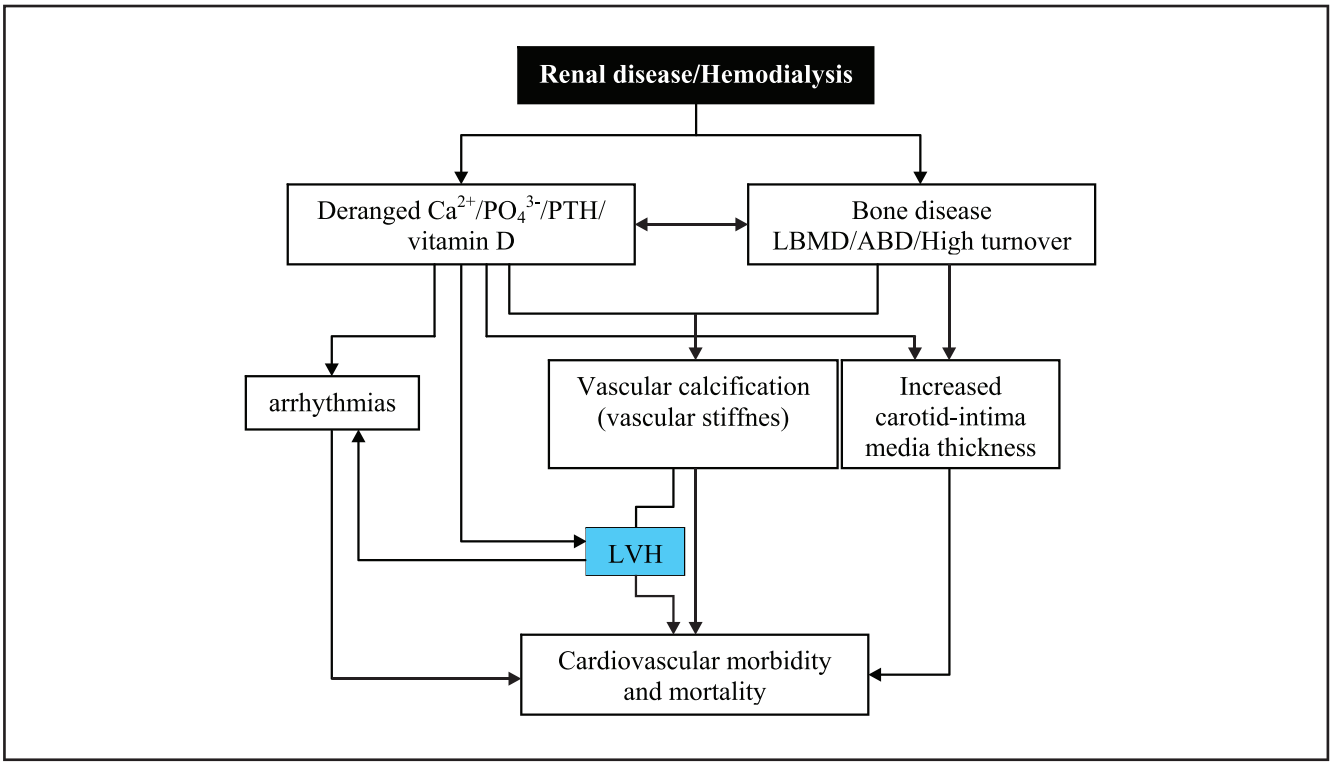

Shema 1. Impact of calcium and phosphate metabolism dosorder on progression of cardiovascular morbidity and mortality in hemodialysis patients

associated with an increase in the LVMi of 10 g/m^2 [25, 26]. Erythropoietin treatment and iron supplementation should maintain the haemoglobin levels at 110 - 120 g/l (Hct = 33 -36%) and feritin levels at 200-500 ng/ml [25, 26]. Hypertension is an important risk factor for the development of left ventricle hypertrophy, and an increase in the mean arterial blood pressure of 10 mmHg increases the left ventricle mass index by 7,2 g/m^2 [27]. In haemodialysis patients, before haemodialysis, the arterial blood pressure should be ≤ 140/90 mmHg and should be ≤ 130/80 mmHg afterwards. Angiotensin I convertase blockers, angiotensin II receptor blockers and ß-blockers should be used in the treatment of hypertension [27].

Arteriosclerosis increases peripheral vascular resistance, overloads the left ventricle because of increased blood pressure and acts as a stimulus for left ventricle remodelling [28]. The most important risk factors for the development of arteriosclerosis (media calcification) and for heart valve calcification in haemodialysis patients are hyperphosphatemia, increased solubility products and secondary hyperparathyroidism [29-31]. Calcification of the arterial medial wall, increased artery stiffness, heart valve calcification and decreased opening of the aortic valve leaflets leads to the development of left ventricle concentric hypertrophy, and an increased serum parathormone level also leads to a significant myocardial interstitial fibrosis (fibroblast proliferation, increased creation and deposition of extracellular matrix proteins in the myocardial interstitium) in haemodialysis patients [29-31]. Hygienic and diet regimens, phosphate binders, active vitamin D3 metabolites, and calcimimetics should maintain the phosphate concentration at < 1,6 mmol/l, the solubility product ([Ca^{2+}] x[$PO4^{3-}$]) at ≤ 4,4 mmol^2/l^2, the concentration of 25(OH) D_3 at > 30 ng/ml and the concentration of iPTH od at 100-300 pg/ml (iPTH < 500 pg/ml) [29-34].

Haemodialysis treatment significantly reduces left ventricle hypertrophy. Every-day short-term haemodialysis (6 times weekly, 3h) for 12 months decreases left ventricle hypertrophy by 30%, as compared to conventional haemodialysis (3 times weekly, 4h) [24]. Clinical trial results show that night-time haemodialysis (3 times weekly, 6-8h) during the six-month period significantly reduces left ventricle hypertrophy compared to conventional haemodialysis (3 times weekly, 4h) [25].

Recognising patients with an increased risk for the development of left ventricular hypertrophy and implementing adequate treatment to achieve target values of risk factors decreases cardiovascular morbidity and mortality and improves the quality of life in patients receiving regular haemodialysis treatments.

Acknowledgments: The authors would like to express their gratitude for Grant N0175014 of the Ministry of Science and Technological Development of The Republic of Serbia, which partially financed this study.

REFERENCES

1. Parfrey PS. Cardiac disease in dialysis patients: diagnosis, burden of disease, prognosis, risk factors and management. Nephrol Dial Transplant 2000; 15(Suppl 5): 5868.
2. Petrović D, Stojimirović B. Cardiovascular morbidity and mortality in hemodialysis patients - epidemiological analysis. Vojnosanit Pregl 2008; 65(12): 893-900.
3. Zoccali C, Mallamaci F, Tripepi G. Novel Cardiovascular Risk Factors in End-Stage Renal Disease. J Am Soc Nephrol 2004; 15(Suppl 1): 77-80.
4. Petrović D, Jagić N, Miloradović V, Stojimirović B. Non-tradicional risk factors for development of cardiovascular complications in haemodialysis patients. Ser J Exp Clin Res 2009; 10(3): 95-102.
5. London GM. Left ventricular alterations and end-stage renal disease. Nephrol Dial Transplant 2002; 17(Suppl 1): 29-36.
6. London GM. Cardiovascular Disease in Chronic Renal Failure: Patophysiologic Aspects. Semin Dial 2003; 16(2): 85-94.
7. Raggi P, Kleerekoper M. Contribution of Bone and Mineral Abnormalities to Cardiovascular Disease in Patients with Chronic Kidney Disease. Clin J Am Soc Nephrol 2008; 3(3): 836-43.
8. Valdivieslo JM, Ayus JC. Role of vitamin D receptor activators on cardiovascular risk. Kidney Int 2008; 74(Suppl 111): 44-9.
9. Eddington H, Klara PA. The association of chronic kidney disease - mineral bone disorder and cardiovascular risk. J Ren Car 2010; 36(Suppl 1): 61-7.
10. Cozzolino M, Ketteler M, Zehnder D. The vitamin D system: a crosstalk between the heart and kidney. Eur J Heart Fail 2010; 12(10): 1031-41.
11. Rigatto C, Parfrey PS. Uraemic Cardiomyopathy: an Overload Cardiomyopathy. J Clin Basic Cardiol 2001; 4(2): 93-5.
12. Parfrey PS, Collingwood P, Foley RN, Bahrle A. Left ventricular disorders detected by M-meode echocardiography in chronic uraemia. Nephrol Dial Transplant 1996; 11(7): 1328-31.
13. Middleton RJ, Parfrey PS, Foley RN. Left Ventricular Hypertrophy in the Renal Patient. J Am Soc Nephrol 2001; 12(5): 1079-84.
14. McIntyre C.W., John S.G., Jefferies H.J. Advances in the cardiovascular assessment of patients with chronic kidney disease. NDT Plus, 2008; 1(6): 383-91.
15. Cohen-Solal A. Left ventricular diastolic dysfunction: pathophysiology, diagnosis and treatment. Nephrol Dial Transplant 1998; 13(Suppl 4): 3-5.
16. Sood MM, Pauly RP, Rigatto C, Komenda P. Left ventricular dysfunction in the haemodialysis population. NDT Plus 2008; 1(4): 199-205.
17. Johnston N, Dargie H, Jardine A. Diagnosis and treatment of coronary artery disease in patients with chronic kidney disease. Heart 2008; 94(8): 1080-8.
18. Petrović D, Miloradović V, Poskurica M, Stojimirović B. Diagnostics and treatment of ischemic heart disease in hemodialysis patients. Vojnosanit Pregl 2009; 66(11): 897-903.
19. Voroneanu L, Covic A. Arrythmias in hemodialysis patients. J Nephrol 2009; 22(6): 716-25.
20. Foley RN, Parfrey PS, Harnett JD, Kent GM, Murray DC, Barre PE. The prognostic importance of left ventricular geometry in uremic cardiomyopathy. J Am Soc Nephrol 1995; 5(12): 2024-31.
21. Petrović D, Jagić N, Miloradović V, Stojimirović B. Left ventricular hypertrophy - risk factor for poor outcome in hemodialysis patients. Ser J Exp Clin Res 2008; 9(4): 129-35.
22. De Bie MK, van Dam B, Gaasbeek A, van Buren M, van Erven L, Bax JJ, et al. The current status of interventions aiming at reducing sudden cardiac death in dialysis patients. Eur Heart J 2009; 30(13): 1559-64.
23. Henrich WL. Optimal Cardiovascular Therapy for Patients with ESRD over the Next Several Years. Clin J Am Soc Nephrol 2009; 4(Suppl 1): 106-9.
24. Hampl H, Riedel E. Cardiac Disease in the Dialysis Patient: Good, Better, Best Clinical Practice. Blood Purif 2009; 27(1): 99-113.
25. Glassock RJ, Pecoits-Filho R, Barberato SH. Left Ventricular Mass in Chronic Kidney Disease and ERSD. Clin J Am Soc Nephrol 2009; 4(Suppl 1): 79-91.
26. Stojimirović B, Petrović D, Obrenović R. Left ventricular hypertrophy in patients on hemodialysis: importance of anaemia. Med Rev 2007; LX (Suppl 2): 155-9.
27. Lynn KL. Hypertension and Survival in Hemodialysis Patients. Semin Dial 2004; 17(4): 270-4.
28. London GM. Arterial function in renal failure. Nephrol Dial Transplant 1998; 13(Suppl 4): 125.
29. Petrović D, Stojimirović B. Secondary hiperparathyroidism - risk factor for development of cardiovascular complications in hemodialysis patients. Med Rev 2010; LXIII(9-10): (in press).
30. Petrović D, Obrenović R, Stojimirović B. Risk Factors for Aortic Valve Calcification in Patients on Regular Hemodialysis. Int J Artif Organs 2009; 32(3): 173-9.
31. Hörl WH. The clinical consequences of secondary hyperparathyroidism: focus on clinical outcomes. Nephrol Dial Transplant 2004; 19(Suppl 5): 2-8.
32. Messa P, Macario F, Yaqoob M, Bouman K, Braun J, von Albertini B, et al. The OPTIMA Study: Assessing a New Cinacalcet (Sensipar/Mimpara) Treatment Algorithm for Secondary Hyperparathyroidism. Clin J Am Soc Nephrol 2008; 3(1): 36-45.
33. Valdivieslo JM, Ayus JC. Role of vitamin D receptor activators on cardiovascular risk. Kidney Int 2008; 74(Suppl 111): 44-9.
34. Artaza JN, Mehrotra R, Norris KC. Vitamin D and the Cardiovascular System. Clin J Am Soc Nephrol 2009; 4(9): 1515-22.

THE RELATIONSHIP BETWEEN SPORTS ENGAGEMENT, BODY MASS INDEX AND PHYSICAL ABILITIES IN CHILDREN

Predrag Lazarevic[1], Vladimir Zivkovic[1], Milena Vuletic[1], Nevena Barudzic[1] and Dejan Cubrilo[1]
[1]Department for Physical Education, Faculty of Medicine, University of Kragujevac, Kragujevac

Received / Primljen: 21. 05. 2010. Accepted / Prihvaćen: 11. 04. 2011.

ABSTRACT

Hypokinesia, which is a consequence of modern technological development, is now one of the three biggest health risk factors. Whereas physical inactivity and obesity in adults is subject of concern, these factors in children presage an even greater public health problem because many health-related problems and life-threatening diseases begin in childhood and adolescence.

It has been noted that regular physical activity modulates vascular endothelial function via an effect on basal nitric oxide (NO) production, thus leading to a significant reduction in the incidence of cardiovascular disease (1). Exercise can also increase energy expenditure and can create a negative energy balance. Conversely, scientific data regarding the effect of school-based physical activity interventions on body mass index (BMI) in children are conflicting (2, 3). Moreover, there is insufficient clinically useful scientific data on BMI in children and its possible association with motor skills. With both sexes, motor abilities improve from physical development in adolescents, and regular sports training influences fitness and motor abilities.

The aim of our study was to evaluate the morphological status and physical abilities of 13-year-old children in order to investigate the relationship between sports engagement, BMI and physical abilities. The results of our study should give coaches important parameters in the selection of young athletes, as well as provide them with information that may be useful in training and programming assignments.

MATERIALS AND METHODS

The research was carried out with a group of 67 boys from an elementary school. The boys were 12-13 years old and had differing sports training experiences.

After an assessment of morphological characteristics (height, weight, BMI), the children were subjected to a battery of motor tests designed to test speed and coordination (Jumping and going through Swedish boxes, slalom with 3 balls, hand tapping, 50-m sprint, 30-m flying start sprint and 20-m slalom sprint (4)).

RESULTS AND DISCUSSION

The average BMI of the children who participated in the study was 19.2±3.4. After transforming BMI data to appropriate percentiles according to the formulas proposed by the National Center for Health Statistics of United States (5), we classified each subject into one of four groups: underweight (athletes vs. non-athletes: 7.7% vs. 17.8%), healthy weight (69.2% vs. 46.4%), overweight (12.8% vs. 21.4%) and obese (10.2% vs. 14.3%). Although BMI is thought to measure excess weight rather than excess body fat, if appropriate cut-off points are used, a high BMI level is a moderately sensitive and very specific indicator of excess adiposity among children (6).

Since hypokinesis in children and adolescents is thought to be a growing problem, especially in urban places, it is encouraging that 58.2% of the boys in the study stated that they participated in a sport activity. To determine if sport activity influences morphological status of young 13-year-old boys, we applied a contingency analysis (χ2-test) and found no significant difference between children who train for a sport and those that do not. These results are in agreement with many other studies that have found that, in contrast to biological growth, the absence of involvement in sports activities in children is not the main factor that influences their morphological status and physical fitness. Moreover, an analysis of morpho-functional skills of young

UDK 613.71-053.6 / Ser J Exp Clin Res 2011; 12 (1): 41-42

Correspondence: Predrag Lazarevic, Assistant trainee in Physical Education, Faculty of Medicine, University of Kragujevac
Svetozara Markovica 69, 34000 Kragujevac, Republic of Serbia, Tel. +381 64 877 66 68, E-mail: plazarevickg@sbb.rs

teens and premature soccer players (14 and 15 vs. 16 and 17 year olds) revealed that the aerobic capacity (VO_2 max) and BMI significantly changed with age, but not with the training experience of the examined athletes (7).

Regarding the influence of morphological status of 13-year-old boys on motor performance, the results of our study suggest that morphological status, estimated by BMI, is an important predictor of physical abilities in children. This finding is in agreement with the results of other studies (8). Discriminative analysis (Kruskal-Wallis test, Table 1) showed that subjects with different morphological status had significantly different performance in 5 out of the 6 tests performed, of which two were designed to test speed and three tested coordination. However, canonical discrimination, used to determine the influence of morphological status on latent motor function, showed significant differences only in coordination tests.

Regarding the influence of sports engagement on motor performance in our participants, a Man-Whitney test (Table 2) showed that, compared with those that did not train, boys who train for a sport had significantly better results only in 2 motor tests, which were confirmed by factor analysis to be valid tests of coordination. These results suggest that the morphological status of 13-year-old children better predicts coordination performance than speed performance.

The results of our study suggest that involvement of adolescents in sport activities has much less influence on motor abilities than that of natural biological growth and maturation. The age at which the boys in this study were tested falls within the first phase of adolescence, which is characterised by sudden and intermittent skeletal maturation without being followed by adequate skeletal muscle development. That is one of the reasons why boys of this age experience a fall in coordination performance. In other words, motor development in 13-year-old boys does not depend on training experience but instead relies on genetics and acceleration of growth.

It should be emphasised that the small number of participants in this study limited our ability to make any significant anthropological generalisations. However, the sample size did not affect the ability to address the main aim of this study, which was to assess the predictive value of morphological status and involvement in sports as parameters that affect motor performance.

Variable	Athletes	Non-athletes	Sig.
Jumping and going through Swedish boxes (sec)	15.85	16.58	.097
Hand tapping (taps)	69.28	64.07	.018*
Slalom with 3 balls (sec)	22.04	25.86	.004*
50-m sprint (sec)	9.24	9.49	.088
30-m flying start sprint (sec)	5.38	5.50	.065
20-m slalom sprint (sec)	4.76	4.88	.132

Table 2. Mean values of results that boys who train or do not train some sport achieved on motor tests.

REFERENCES

1. Green DJ, Maiorana A, O'Driscoll G, Taylor R. Effect of exercise training on endothelium-derived nitric oxide function in humans. J Physiol 2004; 561:1–25.
2. Lazaar N, Aucouturier J, Ratel S, Rance M, Meyer M, Duché P. Effect of physical activity intervention on body composition in young children: influence of body mass index status and gender. Acta Paediatr 2007; 96(9): 315-20.
3. Harris KC, Kuramoto LK, Schulzer M, Retallack JE. Effect of school-based physical activity interventions on body mass index in children: a meta-analysis. CMAJ 2009; 180(7):719-26.
4. Perić D. Operationalisation of research in sports and physical education. Beograd: Politop-p, 1994. (In Serbian)
5. National Center for Health Statistics of United States (2009): CDC Growth Charts. www. cdc.gov/childrens_BMI
6. Freedman DS, Ogden CL, Berenson GS, Horlick M. Body mass index and body fatness in childhood. Curr Opin Clin Nutr Metab Care 2005; 8(6): 618-23.
7. Čubrilo D: Systemic effects of redox balance disturbance caused by the intensive training of young soccer players, PhD dissertation, Medical faculty, University of Kragujevac, Serbia, 2009.
8. Manić G. Multivariant differencies of some biomechanical dimensions of elementary school children in relation to amount of fat tissue. Kinesiologica 2007; 1: 44-48. (in Croatian)

Table 1. Mean values of results that subjects with different morphological status achieved on motor tests.

Variable	Underweight	Healthy weight	Overweight	Obese	Sig.
Jumping and going through Swedish boxes (sec)	15.60	15.37	17.59	20.23	.000*
Hand tapping (taps)	60.00	69.00	73.09	73.75	.040*
Slalom with 3 balls(sec)	28.65	22.26	21.61	28.29	.004*
50-m sprint (sec)	9.90	9.15	9.47	10.28	.002*
30-m flying start sprint (sec)	5.82	5.37	5,53	6.01	.008*
20-m slalom sprint (sec)	5.03	4.77	4.97	5.05	.204

INSTRUCTION TO AUTHORS FOR MANUSCRIPT PREPARATION

Serbian Journal of Experimental and Clinical Research is a peer-reviewed, general biomedical journal. It publishes original basic and clinical research, clinical practice articles, critical reviews, case reports, evaluations of scientific methods, works dealing with ethical and social aspects of biomedicine as well as letters to the editor, reports of association activities, book reviews, news in biomedicine, and any other article and information concerned with practice and research in biomedicine, written in the English.

Original manuscripts will be accepted with the understanding that they are solely contributed to the Journal. The papers will be not accepted if they contain the material that has already been published or has been submitted or accepted for publication elsewhere, except of preliminary reports, such as an abstract, poster or press report presented at a professional or scientific meetings and not exceeding 400 words. Any previous publication in such form must be disclosed in a footnote. In rare exceptions a secondary publication will acceptable, but authors are required to contact Editor-in-chief before submission of such manuscript. the Journal is devoted to the Guidelines on Good Publication Practice as established by Committee on Publication Ethics-COPE (posted at www.publicationethics.org.uk).

Manuscripts are prepared in accordance with „Uniform Requirements for Manuscripts submitted to Biomedical Journals“ developed by the International Committee of Medical Journal Editors. Consult a current version of the instructions, which has been published in several journals (for example: Ann Intern Med 1997;126:36-47) and posted at www.icmje.org, and a recent issue of the Journal in preparing your manuscript. For articles of randomized controlled trials authors should refer to the „Consort statement“ (www.consort-statement.org). Manuscripts must be accompanied by a cover letter, signed by all authors, with a statement that the manuscript has been read and approved by them, and not published, submitted or accepted elsewhere. Manuscripts, which are accepted for publication in the Journal, become the property of the Journal, and may not be published anywhere else without written permission from the publisher.

Serbian Journal of Experimental and Clinical Research is owned and published by Medical Faculty University of Kragujevac. However, Editors have full academic freedom and authority for determining the content of the journal, according to their scientific, professional and ethical judgment. Editorial policy and decision making follow procedures which are endeavoring to ensure scientific credibility of published content, confidentiality and integrity of auth ors, reviewers, and review process, protection of patients' rights to privacy and disclosing of conflict of interests. For difficulties which might appear in the Journal content such as errors in published articles or scientific concerns about research findings, appropriate handling is provided. The requirements for the content, which appears on the Journal internet site or Supplements, are, in general, the same as for the master version. Advertising which appears in the Journal or its internet site is not allowed to influence editorial decisions.

Address manuscripts to:
Serbian Journal of Experimental and
Clinical Research
The Medical Faculty Kragujevac
P.O. Box 124, Svetozara Markovica 69
34000 Kragujevac, Serbia
Tel. +381 (0)34 30 68 00;
Tfx. +381 (0)34 30 68 00 ext. 112
E-mail: sjecr@medf.kg.ac.rs

Manuscript can also be submitted to web address of journal: www.medf.kg.ac.rs/journal

MANUSCRIPT

Original and two anonymous copies of a manuscript, typed double-spaced throughout (including references, tables, figure legends and footnotes) on A4 (21 cm x 29,7 cm) paper with wide margins, should be submitted for consideration for publication in Serbian Journal of Experimental and Clinical Research. Use Times New Roman font, 12 pt. Manuscript should be sent also on an IBM compatible

floppy disc (3.5"), written as Word file (version 2.0 or later), or via E-mail to the editor (see above for address) as file attachment. For papers that are accepted, Serbian Journal of Experimental and Clinical Research obligatory requires authors to provide an identical, electronic copy in appropriate textual and graphic format.

The manuscript of original, scinetific articles should be arranged as following: Title page, Abstract, Introduction, Patients and methods/Material and methods, Results, Discussion, Acknowledgements, References, Tables, Figure legends and Figures. The sections of other papers should be arranged according to the type of the article.

Each manuscript component (The Title page, etc.) should begins on a separate page. All pages should be numbered consecutively beginning with the title page.

All measurements, except blood pressure, should be reported in the System International (SI) units and, if necessary, in conventional units, too (in parentheses). Generic names should be used for drugs. Brand names may be inserted in parentheses.

Authors are advised to retain extra copies of the manuscript. Serbian Journal of Experimental and Clinical Research is not responsible for the loss of manuscripts in the mail.

TITLE PAGE

The Title page contains the title, full names of all the authors, names and full location of the department and institution where work was performed, abbreviations used, and the name of corresponding author.

The title of the article should be concise but informative, and include animal species if appropriate. A subtitle could be added if necessary.

A list of abbreviations used in the paper, if any, should be included. The abbreviations should be listed alphabetically, and followed by an explanation of what they stand for. In general, the use of abbreviations is discouraged unless they are essential for improving the readability of the text.

The name, telephone number, fax number, and exact postal address of the author to whom communications and reprints should be sent are typed et the end of the title page.

ABSTRACT

An abstract of less than 250 words should concisely state the objective, findings, and conclusions of the studies described in the manuscript. The abstract does not contain abbreviations, footnotes or references.

Below the abstract, 3 to 8 keywords or short phrases are provided for indexing purposes. The use of words from Medline thesaurus is recommended.

INTRODUCTION

The introduction is concise, and states the reason and specific purpose of the study.

PATIENTS AND METHODS/MATERIAL AND METHODS

The selection of patients or experimental animals, including controls, should be described. Patients' names and hospital numbers are not used.

Methods should be described in sufficient detail to permit evaluation and duplication of the work by other investigators.

When reporting experiments on human subjects, it should be indicated whether the procedures followed were in accordance with ethical standards of the Committee on human experimentation (or Ethics Committee) of the institution in which they were done and in accordance with the Helsinki Declaration. Hazardous procedures or chemicals, if used, should be described in details, including the safety precautions observed. When appropriate, a statement should be included verifying that the care of laboratory animals followed accepted standards.

Statistical methods used should be outlined.

RESULTS

Results should be clear and concise, and include a minimum number of tables and figures necessary for proper presentation.

DISCUSSION

An exhaustive review of literature is not necessary. The major findings should be discussed in relation to other published work. Attempts should be made to explain differences between the results of the present study and those of the others. The hypothesis and speculative statements should be clearly identified. The Discussion section should not be a restatement of results, and new results should not be introduced in the discussion.

ACKNOWLEDGMENTS

This section gives possibility to list all persons who contributed to the work or prepared the manuscript, but did not meet the criteria for authorship. Financial and material support, if existed, could be also emphasized in this section.

REFERENCES

References should be identified in the text by Arabic numerals in parentheses. They should be numbered consecutively, as they appeared in the text. Personal communications and unpublished observations should not be cited in the reference list, but may be mentioned in the text in parentheses. Abbreviations of journals should conform to those in Index Serbian Journal of Experimental and Clinical Research. The style and punctuation should conform to the Serbian Journal of Experimental and Clinical Research style requirements. The following are examples:

Article: (all authors are listed if there are six or fewer; otherwise only the first three are listed followed by "et al.")

12. Talley NJ, Zinsmeister AR, Schleck CD, Melton LJ. Dyspepsia and dyspeptic subgroups: a population-based study. Gastroenterology 1992; 102: 1259-68.

Book: 17. Sherlock S. Diseases of the liver and biliary system. 8th ed. Oxford: Blackwell Sc Publ, 1989.

Chapter or article in a book: 24. Trier JJ. Celiac sprue. In: Sleisenger MH, Fordtran JS, eds. Gastro-intestinal disease. 4th ed. Philadelphia: WB Saunders Co, 1989: 1134-52.

The authors are responsible for the exactness of reference data.

For other types of references, style and interpunction, the authors should refer to a recent issue of Serbian Journal of Experimental and Clinical Research or contact the editorial staff.

Non-English citation should be preferably translated to English language adding at the end in the brackets native langauage source, e.g. (in Serbian). Citation in old language recognised in medicine (eg. Latin, Greek) should be left in their own. For internet soruces add at the end in small bracckets ULR address and date of access, eg. (Accessed in Sep 2007 at www.medf.kg.ac.yu). If available, instead of ULR cite DOI code e.g. (doi: 10.1111/j.1442-2042 .2007.01834.x)

TABLES

Tables should be typed on separate sheets with table numbers (Arabic) and title above the table and explanatory notes, if any, below the table.

FIGURES AND FIGURE LEGENDS

All illustrations (photographs, graphs, diagrams) will be considered as figures, and numbered consecutively in Arabic numerals. The number of figures included should be the least required to convey the message of the paper, and no figure should duplicate the data presented in the tables or text. Figures should not have titles. Letters, numerals and symbols must be clear, in proportion to each other, and large enough to be readable when reduced for publication. Figures should be submitted as near to their printed size as possible. Figures are reproduced in one of the following width sizes: 8 cm, 12 cm or 17 cm, and with a maximal length of 20 cm. Legends for figures should be given on separate pages.

If magnification is significant (photomicrographs) it should be indicated by a calibration bar on the print, not by a magnification factor in the figure legend. The length of the bar should be indicated on the figure or in the figure legend.

Two complete sets of high quality unmounted glossy prints should be submitted in two separate envelopes, and shielded by an appropriate cardboard. The backs of single or grouped illustrations (plates) should bear the first authors last name, figure number, and an arrow indicating the top. This information should be penciled in lightly or placed on a typed self-adhesive label in order to prevent marking the front surface of the illustration.

Photographs of identifiable patients must be accompanied by written permission from the patient.

For figures published previously the original source should be acknowledged, and written permission from the copyright holder to reproduce it submitted.

Color prints are available by request at the authors expense.

LETTERS TO THE EDITOR

Both letters concerning and those not concerning the articles that have been published in Serbian Journal of Experimental and Clinical Research will be considered for publication. They may contain one table or figure and up to five references.

PROOFS

All manuscripts will be carefully revised by the publisher desk editor. Only in case of extensive corrections will the manuscript be returned to the authors for final approval. In order to speed up publication no proof will be sent to the authors, but will be read by the editor and the desk editor.

CIP – Каталогизација у публикацији
Народна библиотека Србије, Београд

61

SERBIAN Journal of Experimental and Clinical Research
editor - in - chief Slobodan
Janković. Vol. 9, no. 1 (2008) -
Kragujevac (Svetozara Markovića 69):
Medical faculty, 2008 - (Kragujevac: Medical faculty). - 29 cm

Je nastavak: Medicus (Kragujevac) = ISSN 1450 – 7994
ISSN 1820 – 8665 = Serbian Journal of
Experimental and Clinical Research
COBISS.SR-ID 149695244

Serbian Journal of Experimental and Clinical Research

2000

THE MEDICAL FACULTY KRAGUJEVAC
Svetozara Markovica 69, 34000 Kragujevac, SERBIA
P.O. Box 124
Tel. +381 (0)34 30 68 00 • Tfx. +381 (0)34 30 68 00 ext. 112
e-mail: sjecr@medf.kg.ac.rs

www.medf.kg.ac.rs